The effects of natural and anthropogenic disturbance in lotic ecosystems

by

Michael P. Beakes

B.Sc., Northern Arizona University, 2002

Thesis Submitted In Partial Fulfillment of the
Requirements for the Degree of
Doctor of Philosophy

in the
Department of Biological Sciences
Faculty of Science

SIMON FRASER UNIVERSITY

Fall 2014

Approval

Name: **Michael P. Beakes**

Degree: **Doctor of Philosophy**

Title of Thesis: ***The effects of natural and anthropogenic disturbance in lotic ecosystems***

Examining Committee: **Chair:** Dr. Gordon Rintoul
Associate Professor

Dr. Jonathan W. Moore
Senior Supervisor
Assistant Professor

Dr. Wendy J. Palen
Supervisor
Assistant Professor

Dr. Jeremy G. Venditti
Supervisor
Associate Professor
Department of Geography

Dr. John D. Reynolds
Internal Examiner
Professor

Dr. Colden V. Baxter
External Examiner
Associate Professor
Department of Biological Sciences
Idaho State University

Date Defended/Approved: September 3, 2014

Partial Copyright Licence

Ethics Statement

The author, whose name appears on the title page of this work, has obtained, for the research described in this work, either:

a. human research ethics approval from the Simon Fraser University Office of Research Ethics,

or

b. advance approval of the animal care protocol from the University Animal Care Committee of Simon Fraser University;

or has conducted the research

c. as a co-investigator, collaborator or research assistant in a research project approved in advance,

or

d. as a member of a course approved in advance for minimal risk human research, by the Office of Research Ethics.

A copy of the approval letter has been filed at the Theses Office of the University Library at the time of submission of this thesis or project.

The original application for approval and letter of approval are filed with the relevant offices. Inquiries may be directed to those authorities.

Simon Fraser University Library
Burnaby, British Columbia, Canada

update Spring 2010

Abstract

The prevalence of large-scale anthropogenic and natural disturbance has increased in recent decades around the world. For example, over 50% of the world's large rivers are currently dammed and the frequency of large wildfires has nearly quadrupled in western North America since the mid-1980s. Disturbances such as these are principal drivers of change in lotic ecosystems and we seek to improve our understanding of how they affect recipient ecosystems in the context of fisheries management and conservation.

My thesis research combines empirical studies and modeling to improve our ability to predict and measure the effects of several major types of natural and anthropogenic disturbance in lotic ecosystems. In Chapter 1 I improved the accuracy of hydrodynamic habitat models for juvenile salmon by up to 10% by applying Akaike information criterion and model averaging. In Chapters 2 and 3 I applied multiple regression and bioenergetic models to illustrate how wildfire, by burning riparian vegetation, can elevate stream temperatures by up to 0.6°C adding ~5 kJ of metabolic costs to salmonids. As well, I found concentrations of food web resources such as nitrate and fine particulate organic matter increased in burned compared to unburned regions by 244% and 44%, respectively, and I found significantly greater seasonal changes in terrestrial and aquatic invertebrate abundance than changes attributable to wildfire. Despite similar regional invertebrate prey abundance, Bayesian stable isotope mixing models revealed seasonal and regional differences in salmonid diets, with higher trophic level prey contributing more to diets in the burned compared to a reference region. Lastly, in Chapter 4 I found that forest harvest and rising air temperatures are warming waters in the Fraser River basin at 0.07°C per decade on average by applying Spatial Stream Network models.

In total, my thesis research builds on previous work and illuminates how disturbance can affect abiotic and biotic responses in lotic ecosystems at spatial scales ranging from less than 10 m^2 to over 200,000 km^2. Thus, results from my thesis research will aid fisheries management and conservation by improving our understanding of how natural and anthropogenic disturbance may alter streams and rivers in our future.

Keywords: River networks; climate change; riverscape; perturbation

To my grandfather Gerald Hosterman

Thank you for always being there for me, you have been a constant source of inspiration.

Acknowledgements

The body of work presented in this thesis represents the most challenging endeavour I have experienced in my burgeoning career. Without the support from a considerable number of individuals and organizations the completion of this work would not have been possible. I would first like to thank Wendy Palen and Jeremy Venditti for participating as members on my supervising committee. Their feedback and contributions to this work have helped expand and improve my understanding of ecological research and the physical processes of streams and rivers. I would like to especially thank my senior supervisor Jonathan Moore. Jon consistently provided support and advice on every aspect of my graduate research, and an infectious enthusiasm for ecological study for which I am very grateful.

My decision to pursue graduate school was strongly influenced by a few key people early in my career. I thank Sean Hayes, William Satterthwaite, and Andrew Shelton for their support and encouragement during my career leading up to graduate school and throughout my PhD. In particular I'd like to thank, Susan Sogard and Marc Mangel whose mentorship continues to make an impact on my work.

I received a lot of assistance from volunteers, technicians, research associates, and faculty throughout my PhD research. I thank Jesse Adams, Cristina Cois, Nicolas Retford, and Laura Twardochleb, for the time they invested assisting me with lab and field research in Santa Cruz, CA. I thank Steve Sharron, and Rachel Charish for their help in the lab and for their general support during my time at Simon Fraser University. I would also like to thank David Patterson, Lisa Thompson, and Jayme Hills with Fisheries and Oceans Canada and SFU's school of Resource and Environmental Management, in addition to Marvin Eng with the Forest Practices Board, Janie Dubman, Robin Munshaw, and Viorel Popescu from SFU's Palen lab for helping me acquire and interpret data upon which my fourth chapter was based.

I thank the organizations that supported and funded this work including the Liber Ero Foundation, the Public Interest Energy Research Program of the California Energy Commission through the Instream Flow Assessment Program at the University of

California, Davis contract number 019072–01, the National Science Foundation grant number DEB-1009018, and the Mitacs Accelerate internship program award reference number IT03381.

To my friends and colleagues in the Moore lab, Earth to Ocean Research group, and Simon Fraser University I owe a lot of gratitude. Many thanks to the past and current Moore lab members Anne-Marie Osterback and Corey Phillis, Corinna Favaro, Holly Nesbitt, Will Atlas, David Scott, Charmaine Carr-Harris, Rebecca Seifert, Kyle Chezik, Jen Gordon, and Sam Wilson for making our lab such a fun and positive aspect of my graduate experience. Of the many other people from Earth to Ocean and SFU that I am appreciative of, I recognize that Doug Braun, Sean Anderson, Sacha O'Regan, Jenny and Joel Harding, Chris Mull, Michelle Nelson, Brett Favaro, Sarah Thomsen, Julie Wray, Lindsey Button, Alison Collins, Melinda Fowler, and Justin Yeakel made a particularly positive impact on my time at SFU. And of course I would be remiss to exclude the Highland and Renaissance staff from my acknowledgements.

I cannot thank my extended family enough for everything they have done for me over the years. My aunts, uncles, and cousins from the Hosterman tree have all been incredibly supportive. My brothers Brad and Alex Beakes, and Marco Costales, as well as Fred Willetts provided a considerable amount of support in addition to many needed distractions during my visits home. I have no words to aptly express my gratitude for the unconditional love and encouragement I received from Christy Conner, my sister Sarah Costales, and mother Jane Beakes.

Without a doubt, I owe a world of gratitude to my partner Pascale Goertler. Pascale has been with me from the beginning to the end of my graduate program. During which we have shared the best and worst moments of my graduate experience and she has made all of them immeasurably better. Pascale has made my life and work better in everyway possible and I cannot thank her enough.

Table of Contents

List of Tables

List of Figures

List of Acronyms

AICc	Akaike Information Criteria
ANOVA	Analysis of Variance
AUC	Area Under a receiver operator Characteristic
CSI	Composit Siutability Index
DEM	Digital Elevation Model
ESA	Endangered Species Act
FLoWS	Functional Linkage of Water basins
FPOM	Fine Particulate Organic Matter
GAM	General Additive Model
GLM	Generalized Linear Model
GLMM	Generalized Linear Mixed Efffects Model
HDP	High-Density Polyethylene
IFIM	Instream Flow Incremental Methodology
LAR	Lower America River
LOOCV	Leave-One-Out Cross Validation
PCC	Percent Correctly Classified
PHABSIM	Physical Habitat Simulation
RCA	Reach Contributing Area
SSN	Spatial Stream Network
STARS	Spatial Tools for the Analysis of River Systems
WSEL	Water-Surface Elevation

Glossary

Anthropogenic	Originating in human activity
Cover	In Chapter 1, Cover refers to wood >7.5 cm diameter, vegetation >50 cm above ground, overhanging vegetation <50 cm from water's surface, boulders >17.5 cm diameter, undercut banks, and/or large bedrock crevasses.
Disturbance	Any discrete environmental fluctuation that disrupts ecosystem communities and populations, ecosystem resources, or the physical template upon which ecosystems are built.
Kappa statistic	Measures of all possible outcomes of presence or absence that are predicted correctly, after accounting for chance predictions.
Lotic	Flowing water.
Relative community homogeneity	A scalar between zero and one based on Shannon beta diversity, where zero indicates that the communities are distinct and one indicates that the communities are identical.
Sensitivity	In Chapter 1, sensitivity is the proportion of true positives correctly identified.
Substrate	In Chapter 1, substrate refers to the inorganic material composing a river bed.
Specificity	In Chapter 1, specificity is the proportion of true negatives correctly identified, where 1 - specificity is the proportion of false positives.

1. General Introduction

Disturbance is considered one of the dominant organizing forces in stream ecology (Resh et al. 1988). Broadly defined, disturbance constitutes a discrete environmental fluctuation that disrupts ecosystem communities and populations, ecosystem resources, or the physical template upon which ecosystems are built (Pickett and White 1985, Resh et al. 1988). There are myriad natural and anthropogenic sources of disturbance in lotic ecosystems such as flooding and drought (e.g., Townsend 1989, Gasith and Resh 1999, Lake 2000, Power et al. 2008), landslides and debris flows (e.g., (e.g., Lake 2000, Dunham et al. 2007), wildfire (e.g., Minshall et al. 1989, Gresswell 1999, Verkaik et al. 2013), dams and river regulation (e.g., Ward and Stanford 1995, Poff et al. 2007, Poff and Zimmerman 2010), along with many other forms. In response, lotic systems are shaped into a dynamic mosaic of abiotic and biotic conditions to which species, populations, and communities are locally adapted (Resh et al. 1988, Poff and Ward 1990, Allan 2004, Lytle and Poff 2004, Power et al. 2008). As such, a robust understanding of how disturbance affects lotic ecosystems is required for effective management and conservation (Resh et al. 1988, Fausch et al. 2002).

The effects of natural disturbance in lotic ecosystems can be observed across broad spatiotemporal scales (Resh et al. 1988, Poff and Ward 1990, Fausch et al. 2002, Miller et al. 2003). For example, annual floods can shape the physical features of streams and rivers such as riffles and pools (e.g., Montgomery and Buffington 1997), and drive behavioural responses or short-term fluctuations in organism abundance (e.g., McElravy et al. 1989, Power et al. 2008). Biological recovery from these low-magnitude and short-term perturbations is relatively rapid (Poff and Ward 1990). In contrast, during the Pleistocene ice age the Pacific Northwest was perturbed by a series of catastrophic ‘megafloods’ that followed broken ice dams (Waitt 1985, Smith 2006, Waples et al. 2008), some of which carried an amount of energy comparable to a hydrogen bomb exploding every 36 hours for 10 days (Allen 1984). Research suggests that these large-

scale disturbance events are responsible for shaping the ~670,000 km^2 Columbia River watershed (Allen 1984, Waitt 1985, Smith 2006) and for driving the evolutionary history of Pacific salmon (Waples et al. 2008). The contrast between natural annual flooding and the 'megafloods' of the Pleistocene help highlight our need to view disturbance at an various spatial and temporal scale in order to obtain a holistic understanding of the possible physical and biological responses (Wiens 1989).

The effects of anthropogenic disturbance on recipient ecosystems can be markedly different than that of natural disturbance. For example, natural disturbance such as wildfire and flooding drive spatial heterogeneity in streams and rivers (Resh et al. 1988, Miller et al. 2003, Allan 2004, Dunham et al. 2007, Verkaik et al. 2013a). Anthropogenic disturbance by contrast, can disrupt the geomorphic processes underpinning the physical complexity of rivers often resulting in homogenized and degraded habitat (Allan 2004). The construction of dams and regulation of rivers are some of the more common forms of anthropogenic disturbance that fundamentally alter the natural process by which streams and rivers maintain their heterogeneity (Poff et al. 1997, 2007, Lytle and Poff 2004). Currently, over 50% of the world's large rivers are dammed (Nilsson et al. 2005) resulting in a broad regional-scale homogenization of river processes on a global scale, thus prompting critical conservation concerns (Poff et al. 2007). As well, stream ecologists increasingly suggest that anthropogenic disturbance is one of the greatest threats to the ecological integrity of lotic ecosystems in our future (Allan et al. 1997, Townsend et al. 2003, Strayer et al. 2003, Allan 2004). As such, there is a growing need to better understand how anthropogenic disturbance affects recipient lotic ecosystems.

Managing and conserving perturbed ecosystems is challenging partly due to the diverse spatiotemporal scale and effect size of different disturbance types. The biological response to disturbance can be equally diverse and is often challenging to predict (e.g., Power et al. 2008). These challenges are exacerbated by the fact that streams and rivers are inherently difficult to study (Fausch et al. 2002), and because much of the previous research aimed at aiding managers has been focused on spatiotemporal scales that are inadequate for the management goals in question (Wiens 1989, Fausch et al. 2002). Thus, there is a need for additional research that may improve our understanding of how natural and anthropogenic disturbance affects ecosystems across multiple

temporal and spatial scales. Such an effort will aid the development of a more holistic management and conservation strategy that considers the positive and negative effects of disturbance (Hobbs and Huenneke 1992, Poff et al. 1997).

My PhD research focuses on the dynamics of large-scale natural and anthropogenic disturbance in lotic ecosystems. In total, my thesis research combines empirical research and modeling to examine multiple abiotic and biotic responses to disturbance in lotic ecosystems at spatial scales ranging from less than 10 m^2 to over 220,000 km^2. The overarching goal of my thesis research is to improve our ability to measure and predict the effects of disturbance on recipient ecosystems by applying quantitative tools such as information theory, model averaging, Bayesian stable isotope mixing models, and stream network models.

In my first chapter I address a need to improve existing hydrodynamic habitat models that are frequently used by resource managers to examine the effects of river regulation on salmon habitat. Specifically, I quantitatively compare two competing multivariate habitat models for juvenile Chinook salmon (*Oncorhynchus tshawytscha*) in a Central Valley California regulated river. The aim of this project was to provide resource managers with adequate information regarding the trade-offs between alternative habitat modeling methodologies. I built one habitat model using Akaike information criterion (AICc) and model averaging, and a second model using a standard method of aggregating univariate habitat models. Using a suite of model diagnostics I compared the ability of each model to predict juvenile salmon presence and absence. As well, across nine simulated river discharges I estimated the amount of useable habitat for my study system using both competing models, and I calculated the uncertainty around those estimates. The results from this chapter increased the amount of information available to resource managers, thus facilitating their evaluation of competing habitat models.

I examine the effects of wildfire in stream ecosystems in my second and third chapters, which is a prevalent form of natural disturbance in lotic ecosystems throughout regions with Mediterranean climates (Verkaik et al. 2013a). As well, the frequency of large wildfires has nearly quadrupled in western North America over the last few decades

(Westerling et al. 2006), thus highlighting our need to better understand how this form of disturbance effects recipient lotic ecosystems. In chapter two, I examined the short-term effects of a wildfire on temperatures and Steelhead/Rainbow Trout (*Oncorhynchus mykiss*) bioenergetics and distribution in a California coastal stream. Results from my second chapter demonstrate that wildfire can generate thermal heterogeneity in aquatic ecosystems and drive short-term increases in stream temperature, exacerbating bioenergetically stressful seasons for coldwater fishes (Beakes et al. 2014). My third chapter broadly examines stream food web responses to wildfire. Specifically, I measured seasonal changes in nitrate (μM NO_3-), suspended fine particulate organic matter (FPOM; $cg \cdot L^{-1}$), $\delta^{13}C$ and $\delta^{15}N$ stable isotopes, terrestrial and aquatic macroinvertebrate abundance and community composition, and Steelhead/Rainbow Trout (*Oncorhynchus mykiss*) inferred diet composition. Although I observed increased nutrient and FPOM concentrations in burned regions of the watershed relative to a reference region, results from my third chapter indicate that California stream food webs are driven primarily by seasonal climate forcing, and the effects of wildfire are minor by comparison.

In chapter four I apply a novel Spatial Stream Network (SSN) model to the Fraser River, one of North America's largest rivers without dams on its mainstem (Nilsson et al. 2005). The central aim of this chapter was to assess the effects of landscape change and climate on water temperatures in the Fraser River. Specifically, I fit a generalized linear mixed effects model to analyze the relative effects of summer month, mean monthly air temperature (°C), and upstream area logged or burned by wildfire (km^2) on water temperatures in the Fraser River. Results from my third chapter indicate that logging practices and warming air temperatures are contributing to a trend of warming waters throughout the Fraser River basin, thus aiding resource managers by identifying how landscape change and climate warming may alter the thermal future for the Fraser River. More generally, this study improves our understanding of how natural and anthropogenic landscape disturbance and climate warming may act in concert to warm freshwaters.

Collectively my thesis explores several predominant types of natural and anthropogenic disturbance. Generally, my research has shown that disturbance can drive spatial heterogeneity in abiotic and biotic responses such as water temperature and fish

distributions and that these responses can vary in magnitude across spatial and temporal scales. As a result, my thesis research has improved our understanding of how disturbance affects recipient lotic ecosystems, thus aiding the development of a holistic disturbance-based management and conservation framework.

2. Evaluating statistical approaches to quantifying juvenile Chinook salmon habitat in a regulated California river[1]

2.1. Abstract

Decisions on managed flow releases in regulated rivers should be informed by the best available science. To do this, resource managers require adequate information regarding the trade-offs between alternative methodologies. In this study, we quantitatively compare two competing multivariate habitat models for juvenile Chinook salmon (*Oncorhynchus tshawytscha*), a highly valued fish species under serious decline in a large extent of its range. We conducted large-scale snorkel surveys in the American River, California, to obtain a common dataset for model parameterization. We built one habitat model using Akaike information criterion analysis and model averaging, 'model G', and a second model by using a standard method of aggregating univariate habitat models, 'model A'. We calculated Cohen's kappa, percent correctly classified, sensitivity, specificity and the area under a receiver operator characteristic to compare the ability of each model to predict juvenile salmon presence and absence. We compared the predicted useable habitat of each model at nine simulated river discharges where usable habitat is equal to the product of a spatial area and the probability of habitat occupancy at that location. Generally, model G maintained greater predictive accuracy with a difference within 10% across the diagnostic statistics. Two key distinctions between models were that model G predicted 17.2% less useable habitat across simulated flows and had 5% fewer false positive classifications than model A. In contrast, model A had a

[1] A version of this chapter is published as Michael, P.B., Moore, J.W., Retford, N., Brown, R., Merz, J.E., and Sogard, S.M. 2014. Evaluating statistical approaches to quantifying juvenile Chinook salmon habitat in a regulated California river. River Research and Applications 30: 180-191.

tendency to over predict habitat occupancy and under predict model uncertainty. The largest discrepancy between model predictions occurred at the lowest flows simulated and in the habitats most likely to be occupied by juvenile salmon. This study supports the utility and quantitative framework of Akaike Information Criterion analysis and model averaging in developing habitat models.

2.2. Introduction

With over half of the earth's large river systems currently dammed (Nilsson et al. 2005), there is an increasing need for robust quantitative tools that can predict the impacts of flow regulation on riverine ecosystems (Petts 2009). Dams can allow water managers to control when and how much water flows downstream. As such, these quantitative tools must be able to provide resource managers with information that accurately reflects the trade-offs and their uncertainties between resource use and any potential ecological impacts of flow regulation. Understanding the ecological consequences of different flow releases can help balance the needs for energy generation, water storage, flood control, and downstream aquatic communities.

Over the last few decades, numerous competing techniques have been developed to aid managers in predicting how changes in river flow will modify inhabitable space for riverine species downstream of dams (Manel et al. 2001, Ahmadi-Nedushan et al. 2006, Mouton et al. 2010, Dunbar et al. 2012). These statistical techniques range considerably in complexity, but the common aim is to estimate how flow regulation alters physical characteristics of rivers (e.g. velocity and depth) and predict how those changes will impact individual species. For example, Bovee (1986) developed a statistical method where several habitat variables (e.g. depth, water velocity, cover or substrate) are parameterized independently and then combined as univariate model estimates into a composite index of habitat suitability (CSI). The CSI can be constructed by one of several available methods (e.g. geometric mean, arithmetic mean and product). The CSI approach has historically been integrated into a physical habitat simulation (PHABSIM), which is a fundamental component of the instream flow incremental methodology (IFIM). The IFIM and PHABSIM are used to inform management decisions in regulated river

systems, such as setting minimum flow standards and quantifying flow regulation impacts on aquatic habitats (Stalkner et al. 1995, Waddle 2001). The CSI approach is still integrated into IFIM and contemporary management decisions and is published in peer-reviewed literature (e.g., Ayllón et al. 2010, Boavida et al. 2010, Lee et al. 2010, Im et al. 2011). However, this method has several key assumptions that have been subject to considerable criticism over the last few decades. Specifically, the CSI approach requires assumptions that each parameter is selected independently by the target species (Bovee 1986), that each variable is equally important and that the covariance structure among variables is negligible (Mathur et al. 1985, Leclerc et al. 2003, Jowett and Davey 2007, Beecher et al. 2010). Furthermore, the CSI approach often ignores any uncertainty in model predictions (Burgman et al. 2001).

In contrast to the CSI approach, more complex techniques that allow numerous parameters to be estimated simultaneously have been developed in the past decade, such as generalized linear models (GLMs; Guisan et al. 2002). GLMs have only recently been applied in aquatic habitat modelling (Labonne et al. 2003, Ahmadi-Nedushan et al. 2006), but many of the statistical flaws and assumptions of the CSI approach are addressed with this technique; thus, our ability to describe ecological data has greatly improved (Guisan et al. 2002, Ahmadi-Nedushan et al. 2006). In addition, previous research has demonstrated that multivariate methods produce dissimilar predictions of usable habitat in comparison with a CSI method, and multivariate techniques provide a greater amount of information (Vismara et al. 2001). However, resource managers have been slow to adopt new methods, and multivariate techniques have received relatively little attention (Vismara et al. 2001, Dunbar et al. 2012).

The slow progression of new methods into the management community may be a result of inadequate information allowing resource managers to distinguish the trade-offs between alternative techniques. For example, Manel et al. (2001) reviewed 87 articles published in ecological literature between 1989 and1999 and reported that over 67% of the studies using presence–absence models failed to attempt any kind of model evaluation. In addition, there are relatively few published articles focused on aquatic habitat models that compare competing methodologies on a common data set (Ahmadi-Nedushan et al. 2006). As a consequence, there is a paucity of knowledge to make

informed decisions about methodologies for estimating how flow regulation alters aquatic habitat.

The aim of this study is to quantitatively compare two statistical methodologies and examine the potential role of Akaike information criterion (AICc) and model averaging (Akaike 1974, Burnham and Anderson 2002) in aquatic habitat modelling. This study builds on comprehensive reviews of the variety of methods available to resource managers by Manel et al. (2001), Ahmadi-Nedushan et al. (2006), Mouton et al. (2010) and Dunbar et al. (2012), and submits a novel application of AICc model averaging for estimating the impacts of flow regulation on habitat for the juvenile life stage of Chinook salmon (*Oncorhynchus tshawytscha*), a highly valued fish species under serious decline in a large extent of its range (Myers et al. 1998). We use AICc analysis and model averaging to construct a multivariate GLM and develop a second habitat model, following the CSI approach, comprised of aggregated univariate models. We compare the models with five diagnostic statistics deemed appropriate for gauging model performance during model development (Mouton et al. 2010). In addition, we include estimates of uncertainty around each model's predictions and extrapolate these predictions under several flow scenarios to gain perspective on the trade-offs between selecting one model over the other. We hypothesize that the AICc-averaged habitat model will have greater predictive accuracy and provide a more robust and conservative prediction of the relative impact of flow regulation on juvenile salmon habitat. Therefore, results from this study aim to advance an existing foundation for hydrodynamic habitat model development and application (Petts 2009).

2.3. Methods

2.3.1. Study system

This study was conducted in the Lower American River (LAR), which is primarily a snow-fed system, draining approximately 4900 km^2 of the Sierra Nevada Mountains in Northern California. Like other California Central Valley rivers, the American River has been highly modified from its historic state, including flow regulation and diversion, water

pollution, gold and gravel mining, hydropower and floodplain development, and the introduction of numerous non-native aquatic species (McEwan 2001, Williams 2001, Moyel 2002). Just downstream of the American River north and south fork confluences, Folsom Dam was completed in 1955, blocking upstream habitat for migratory fishes such as anadromous salmonids. The Bureau of Reclamation currently operates the dam for flood control, water storage and hydroelectric generation. The LAR is defined as the 37 km of unobstructed channel that flows downstream of Nimbus Dam, which is located approximately 11 km downstream from Folsom Dam. This portion of the river still provides spawning and rearing habitat for anadromous steelhead (*Oncorhynchus mykiss*) and Chinook salmon (Yoshiyama et al. 2001). American River fall-run Chinook salmon typically spawns from late September to December, with juvenile rearing from early January to June. Our study reach is approximately 800 m long and located within the Sacramento city limits, just downstream of the American River Parkway, Sunrise recreation area (Figure 2.1).

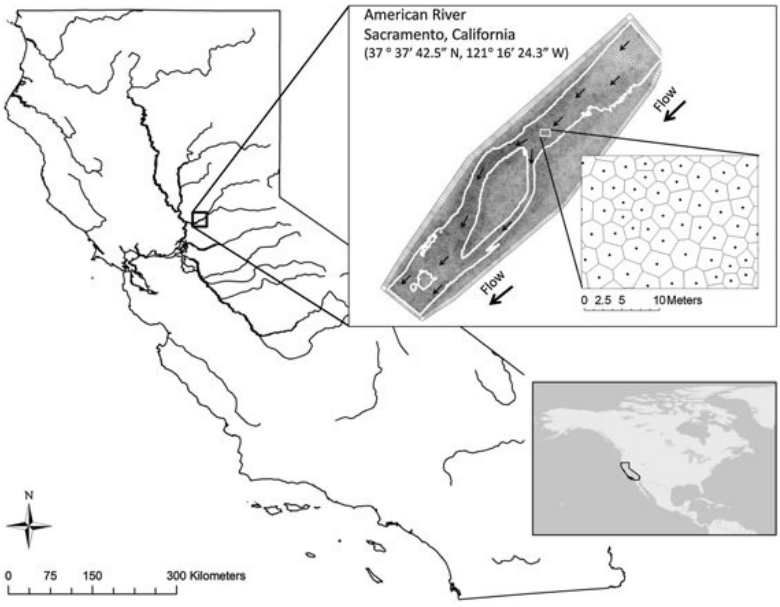

Figure 2.1. Map of study reach in the American River, California. Thiessen polygons (inset) encompassing the nodes generated in River 2D were used to estimate the area around each point for integration of the Hydrodynamic and habitat model estimates. Waters edge from the lowest (33.98 $m^3 \cdot s^{-1}$) discharge model outlined in white and the direction of flow indicated by bold black arrows.

2.3.2. Fish and habitat surveys

Following methods of Gard (2006), we attained our habitat occupancy data via large-scale snorkel surveys conducted from February to July (2009, 2010) across as many different accessible habitat types as feasible (e.g. riffles, runs and backwater habitat). We conducted the snorkel surveys during daylight along a linear transect from downstream to upstream and marked occupied locations of juvenile Chinook salmon (fork length >40 mm, <95 mm) with flagged weights. Fish sizes were visually estimated to the nearest 5 mm fork length. Regardless of the number of fish at occupied locations, each observation counted as a single statistical unit in our common dataset and analysis. When depth and velocity were too high to allow unaided upstream snorkelling, we used fixed ropes to facilitate our upstream movement. We then measured physical habitat characteristics (i.e. velocity, depth, cover and substrate) in flagged locations. Depth was measured as the distance from the water surface to the riverbed to the nearest centimetre, and velocity was measured to the nearest centimetre per second with a portable electromagnetic velocity flow meter (Marsh-McBirney, Flo-Mate) at 60% depth. Substrate diameter was visually estimated to the nearest centimetre except for particles less than 1 cm, which were classified as sand (0.25 cm) or fine sediment (0.025 cm). At regular intervals along each snorkel transect (10 or 20 m), we randomly selected unoccupied locations using a random number generator, excluding locations less than 1m from occupied locations, and measured the same suite of habitat characteristics as those measured in occupied locations. These data collection efforts thus resulted in a series of fish presence–absence data with associated habitat attributes.

We mapped dominant habitat cover into polygons using two categories (with and without cover) over the entire study reach. These cover types were similar to those described in Gard (2006). We identified locations with cover when they were within 50cm of large woody debris (>7.5 cm diameter), tall vegetation (>50 cm above ground), overhanging vegetation (<50 cm from water's surface), large boulders (>17.5 cm diameter), undercut banks, large bedrock crevasses or combinations of these cover types. Areas without cover included characteristics such as small vegetation, small substrate (<17.5 cm diameter) or filamentous algae. We used tools in ArcGIS (Version 9.3) to spatially join

cover attributes from delineated polygons to every node, or point, in the hydrodynamic model.

2.3.3. Competing habitat models

We analysed the binary occupied and unoccupied snorkel survey data via polynomial GLM with a logit link function (i.e., multiple logistic regression) in program R (R Development Core Team 2013), which estimates the probability of habitat occupancy as a function of the predictive habitat variables. Logistic regression has been used for similar modelling exercises in numerous studies and is arguably the most appropriate for presence–absence data (Ahmadi-Nedushan et al. 2006).

We used two competing methods to develop habitat models that predict the probability of habitat occupancy by our study species. In the first method, we estimated the probability of habitat occupancy for depth, velocity, substrate and cover independently of one another. We assumed that the logistic relationship for velocity, depth and substrate was parabolic and thus assigned a quadratic term to each variable (e.g. velocity+velocity^2). In addition, we tested all possible interactions among velocity, depth and cover, of which none were significant predictors of habitat occupancy ($p > 0.05$) and were subsequently excluded from further analysis. We selected statistically significant univariate habitat occupancy models and aggregated them by taking the geometric mean of the model predictions for each corresponding variable at a point in space. This method is comparable with the CSI approach, supported by the US Fish and Wildlife Service standards for habitat suitability index model development (USFWS 1981), recommended in contemporary habitat modelling software (e.g. River 2D) and applied in recent field studies (e.g., Ayllón et al. 2010). We estimated upper and lower confidence limits for this model by adding 1.96 standard errors, estimated with the 'predict' function in program R, to each point-specific probability of habitat occupancy. We refer to this model as 'model A' (for aggregated) hereafter.

We developed a second model with information theory via AICc and model averaging corrected for small sample sizes (Akaike 1974, Hurvich and Tsai 1989, Burnham and Anderson 2002). We compared the most complicated model with all possible model

combinations that did not include interaction terms to rank them in order of model parsimony. A difference greater than four AICc units between models can be interpreted as evidence for model superiority (Burnham and Anderson 2002). For each model and corresponding AICc score, we calculated an AICc weight, which is an estimate of the relative support for each model across all the models compared. The sum of all model weights equals 1; thus, an AICc weight of 0.25 is analogous to having 25% of the relative support across models. We averaged model coefficients across the 95% confidence model set (summed weight) because the AICc weight of the 'top' model was <0.9 (Grueber et al. 2011). Specifically, we averaged the parameter coefficients of the full model proportionally to the coefficients in the 95% confidence model set based on the AICc weight and relative support of each model. The main function of model averaging was to avoid losing information explained by any of the competing models. As such, the parameter coefficients of the averaged model represented a weighted average of the coefficients of all candidate models based on their relative support, or AICc weight (Burnham and Anderson 2002). By model averaging, we allowed for comparably supported models to influence the parameter coefficients of the global model and less supported models to have limited effects on the global model. We estimated upper and lower confidence limits for this model by adding 1.96 standard errors to each point-specific probability of habitat occupancy. We refer to the AICc averaged model as 'model G' (for global) hereafter.

2.3.4. 2D hydrodynamic model

We used a two-dimensional depth-averaged hydrodynamic model (River 2D), following methods described in Steffler and Blackburn (2002), to estimate point-specific values of depth and velocity at different flow rates within our study reach. River 2D is based on the St. Venant shallow water equations for shallow flows in natural streams, in conservation form (Steffler and Blackburn 2002). The key parameter inputs include a digital elevation model (DEM) of the study reach, estimates of riverbed roughness height and measured water surface elevations (WSELs) at the modelled discharge. The modelling process includes the development of a triangulated irregular network between points ('nodes') that are overlaid on top of the DEM at a user specified density. By spatial linear interpolation of the DEM, each node is assigned x, y and z coordinates and an estimate

of bed roughness height. The user inputs the WSEL at the upstream and downstream boundaries along with the corresponding discharge. The River 2D software then solves a hydraulic algorithm using Manning's N and the conservation of mass and momentum at each node. The end result is an estimate of velocity and depth, for a specified discharge, at each node in the study reach. For greater detail in the modelling procedure and model output, see Steffler and Blackburn (2002).

We constructed our study site DEM with topographic data that were previously collected on the LAR and enriched this data set with additional topographic surveys (2009, 2010). All additional topographic data were collected with a Topcon brand survey-grade RTK GPS in NAD (1983) State Plane, California Zone II, FIPS 0402 (Feet). We removed erroneous topographic points with spatial tools in ArcGIS (version 9.3). The average topographic survey density for the study reach was 0.13 points$\cdot m^{-2}$, and the hydrodynamic model node density was consistent between models and comparable with the topographic point density at 0.15 (nodes$\cdot m^{-2}$).

We mapped median riverbed substrate (D_{50}) over the entire study reach to characterize bed roughness in the 2D hydrodynamic model. We encompassed homogeneous regions of substrate with a large polygon, delineating the boundaries with the RTK GPS. In highly heterogeneous areas, we took point measurements and developed Thiessen polygons to encompass these points in ArcGIS. Using the equation from Thompson and Campbell (1979), we estimated bed roughness height (k_s) as $k_s = 4.5 \cdot D_{50}$. We used spatial join functions in ArcGIS to assign bed roughness height to each topographic point in the consolidated topography dataset.

We measured WSELs at four discharges (49.84, 55.39, 111.63 and 131.74 $m^3 \cdot s^{-1}$) and extrapolated WSELs for discharges of 33.98, 70.79, 87.78, 144.42 and 169.90 $m^3 \cdot s^{-1}$. We considered these flows to be within a conservative range of interpolation and extrapolation from our measured WSELs and discharges. These flows were representative of the mean daily flow frequency distribution post dam construction during salmonid rearing months, February to July. We then completed the modelling procedure in River 2D for each flow level.

We gauged the River 2D model performance on the basis of three criteria. First, we determined if a stable hydrodynamic solution was reached by evaluating the change in model variable estimates between the final model iterations. Specifically, the difference of the square root of sum of squares for all hydrodynamic model variables between the final model iterations needed to be less than 0.1% (Steffler and Blackburn 2002). Second, simulated outflow ($m^3 \cdot s^{-1}$) was within 1% of the measured inflow ($m^3 \cdot s^{-1}$) for all discharges modelled. The third criterion was the absence of supercritical flow, or low Froude (ratio of inertial force/ gravitation force) throughout the modelled reach; in natural systems, Froude numbers rarely exceed 1.0 (Grant 1997). The resulting hydrodynamic model was combined with each of the habitat models described previously to develop estimates of usable habitat at different discharges.

2.3.5. Model performance

To compare the performance of the competing habitat models (model A versus model G), we used program R (R Development Core Team 2013) and the 'PresenceAbsence' library (Freeman and Moisen 2008) to calculate optimized thresholds for models A and G. We set the threshold value where Kappa was maximized for both models and used this threshold value to estimate Kappa and three additional model performance statistics. Each statistic is a measure of the capacity to accurately discriminate the correct outcome of our habitat occupancy data, where probabilities that exceeded the threshold would be classified as occupied (positive) and those below the threshold would be classified as absent (negative). We evaluated model performance using Cohen's Kappa statistic, percent correctly classified (PCC), sensitivity, specificity and the area under a receiver operator characteristic (AUC). The Kappa statistic is a measure of all possible outcomes of presence or absence that are predicted correctly, after accounting for chance predictions; it is generally accepted as a conservative and standardized metric for comparing the predictive accuracy of binary models regardless of their statistical algorithm (Manel et al. 2001). PCC compares the proportion of outcomes correctly classified. In this application, sensitivity represents the proportion of true positives correctly identified, and specificity is the proportion of true negatives correctly identified, where 1 - specificity is the proportion of false positives. Kappa, PCC, sensitivity and specificity are all threshold dependent statistics, so we also included AUC

as a threshold independent statistic for model diagnostics. AUC is a measure of model accuracy across all potential thresholds in binary models. In our study, an AUC value of 1 is equivalent to perfect model agreement between observed and predicted habitat occupancy outcomes. An AUC value of 0.5 is approximately equal to random predictions of habitat occupancy.

2.3.6. Model extrapolation and usable habitat

To be useful in management, these models must be able to identify areas most likely to be occupied by a target species and to predict how the total area that is likely to be occupied will change as river flow is changed. To do this, we calculated the point-specific predictions from each habitat model and extrapolated those predictions over space for several flow scenarios. We constructed three quantitative comparisons between models. First, we plotted all point-specific probabilities of each model's predictions against one another to determine if there were systematic differences between competing models. Second, we calculated and plotted the absolute difference in point-specific model predictions for several flows to identify spatial disparities among flow scenarios. Third, we estimated the total usable habitat predicted by each model and included estimates of uncertainty around those predictions.

To extrapolate habitat model predictions across space, we first developed Thiessen polygons in ArcGIS for each node in all nine hydrodynamic models (one for each discharge level) to estimate an area around each node (Figure 2.1). We used the estimated velocity, depth and cover at each node across the study reach, for all nine simulated discharges, as independent parameter inputs for both habitat models mentioned previously and predicted a probability of habitat occupancy for each node. By multiplying this probability by the area encompassing each node, we calculated the usable habitat for each polygon and then summed the resulting values across the entire study reach to quantify the total usable habitat for each discharge. However, we restricted extrapolation to velocities <120 $cm \cdot s^{-1}$ and depths <113 cm to avoid extrapolating model predictions beyond the physical conditions observed in our habitat data. By multiplying the upper and lower confidence limits of each predicted probability by the area encompassing each node, we calculated the minimum and maximum

estimates of usable habitat for each polygon and again summed the resulting values across the entire study reach for each discharge to estimate uncertainty around usable habitat predictions. Our aim was to identify any systematic difference in model predictions across space and under different river flows, thereby providing a context for determining the trade-offs of using one model or the other in river management.

2.4. Results

2.4.1. Habitat occupancy

Our snorkel surveys covered a total area of approximately 182,000 m^2 along a total of approximately 22.5 river kilometres, and we observed a mean fish density of 0.005 juvenile Chinook$\cdot m^{-2}$. The mean stream temperature we observed during the dates of our snorkel surveys was 12.9 C (± 1.5°C S.D., United States Geologic Survey Station ID. 11446500, Fair Oaks Ave, California). We observed 88 habitat locations occupied by juvenile Chinook within our target size class and 391 unoccupied habitat locations. These data provided a common dataset for habitat model development and testing.

2.4.2. Model A

Independent factors of velocity, depth and cover were significant (Table 2.1, $p < 0.05$) predictors of habitat occupancy. There were no significant interactions between any variables, and they were excluded from further analysis. In addition, substrate was not significantly correlated with habitat occupancy (Table 2.1, $p > 0.05$) so it was excluded from model A. However, large substrate (>17.5 cm diameter) was included as a type of cover and thus included in the cover variable. The predicted optimal depth (33.8 cm) and velocity (36.7 cm$\cdot s^{-1}$) maintained a probability of habitat occupancy of 23.1% and 23.0%, respectively (Figure 2.2). In the absence of cover, the predicted probability of habitat occupancy was 16.9%, which increased to 27.7% in the presence of cover (Figure 2.1).

Table 2.1. Model A coefficients, standard errors and p-values for each independently fit polynomial logistic regression. In all analysis, 'Cover' is categorical and unitless. Specifically, 'Cover' is defined as the presence or absence of one or more cover types (e.g. large wood, overhanging vegetation). Except for cover, we assumed that the correlation between habitat occupancy and our predictor variables was non-linear and thus included a quadratic term with each parameter.

Parameter	Coefficient	S.E.	*p*
Intercept	-1.7393	0.2380	< 0.001
Velocity	0.0290	0.0143	0.043
Velocity^2	-0.0004	0.0002	0.020
Intercept	-2.1877	0.4523	< 0.001
Depth	0.0582	0.0254	0.022
Depth^2	-0.0009	0.0003	0.010
Intercept	-1.1098	0.3266	< 0.001
Substrate	-0.1133	0.0846	0.180
Substrate^2	0.0060	0.0046	0.187
Intercept	-1.5921	0.1311	< 0.001
Cover	0.6324	0.3066	0.039

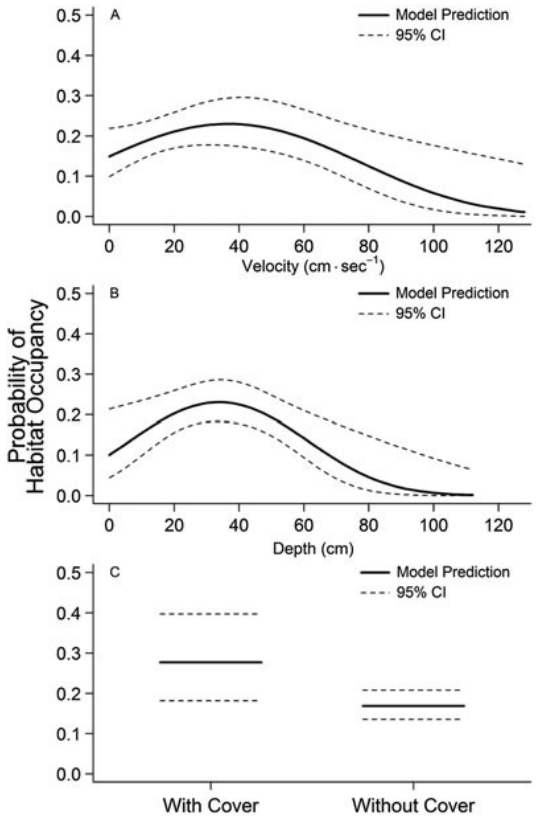

Figure 2.2. Univariate logistic regression (solid line) plotted as the predicted probability of habitat occupancy for (A) velocity, (B) depth and (C) cover. The fine dashed lines indicate the 95% confidence intervals (CI) of model predictions, estimated with the predict function in program R.

2.4.3. Model G

There were six candidate models that were comparably supported by AICc analysis (ΔAICc < 4). The top-supported model, with an AICc weight (w_i) of 0.34 or 34% of the relative support, was velocity+velocity^2+depth+depth^2+ cover (Table 2.2). All but one of the top six models (ΔAICc 4) were multivariate, with a collective 81% of the total support, indicating that a combination of predictor variables was far more supported than the univariate models. In total, multivariate models received 88% of the total support within the 95% candidate model set (Table 2.2).

Table 2.2. AICc 95% candidate model set and corresponding AICc score and AICc weight (W_i). A change greater than 4 AICc units (∆ AICc) is evidence of model superiority. The AICc weight is a proportional measure representing the relative support estimated with AIC analysis for each competing model.

Model Rank	Model Parameters	AICc	∆AICc	W_i
1	$V + V^2 + D + D^2 + C$	449.86	0.00	0.34
2	$D + D^2 + C$	450.64	0.78	0.23
3	$V + V^2 + D + D^2$	451.71	1.85	0.13
4	$D + D^2$	452.09	2.23	0.11
5	$V + V^2 + D + D^2 + S + S^2 + C$	453.45	3.59	0.06
6	$V + V^2 + C$	453.55	3.69	0.05
7	$D + D^2 + S + S^2 + C$	454.12	4.26	0.04
8	$V + V^2 + D + D^2 + S + S^2$	454.44	4.58	0.03

We adjusted the coefficient estimates in the global model for further analysis on the basis of the AICc weight of the 95% confidence model set (Table 2.3), thereby accounting for the relative support of each model.

Table 2.3. Model averaged coefficients and standard errors for model G. We cannot calculate a p-value for each of our parameters using model averaging and information theory so it is not provided. The coefficients are calculated as a weighted average of coefficients from each model in our candidate model set

Parameter	Averaged Coefficient	Standard Error
Intercept	-2.2724	0.4876
Velocity	0.0293	0.0157
$Velocity^2$	-0.0004	0.0002
Depth	0.0511	0.0268
$Depth^2$	-0.0008	0.0003
Substrate	-0.0727	0.0927
$Substrate^2$	0.0042	0.0049
Cover	0.6316	0.3263

Depth was the most strongly supported variable in AICc analysis, with relative variable support of 95%. Cover and velocity were also strongly supported variables at 72% and 62%, respectively. The inclusion of substrate as a predictor variable had the least support at 13%. The maximum predicted probability of habitat occupancy for model G was 34.9%, with velocity at 41.2 $cm \cdot s^{-1}$, with depth at 32.7 cm, with substrate at 20.32 cm and with cover present. The probability of habitat occupancy increased with increased substrate size. However, the probability of habitat occupancy changed by less than 2% at the smallest and largest substrate sizes in our model. The presence of cover

increased the probability of habitat occupancy by up to 9.5% when depth and velocity were at their optimal level (Figure 2.3). To illustrate the general correlation between the continuous variables in model G, we predicted the probability of habitat occupancy when depth was held constant at 2.5, 32.5 or 62.5 cm, substrate constant at 7.62 cm, with and without cover (Figure 2.3).

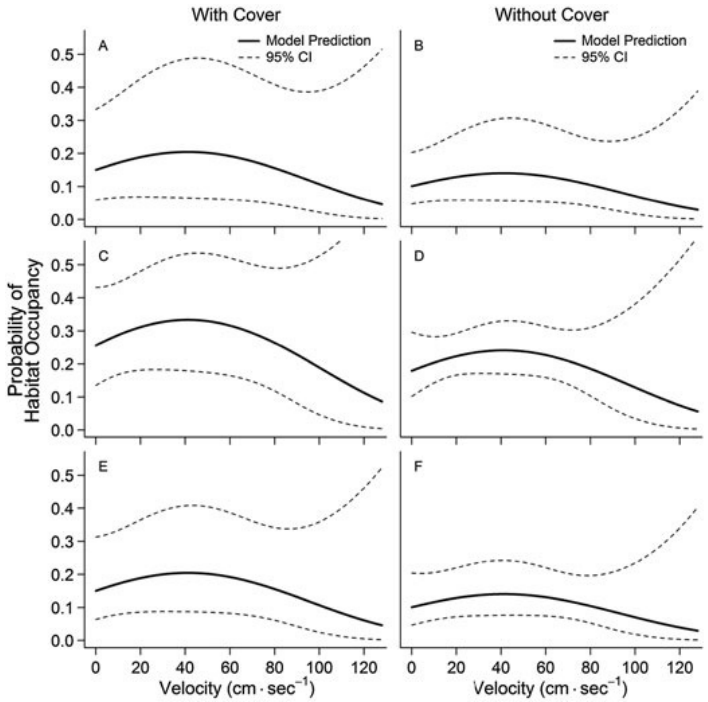

Figure 2.3. Multivariate logistic regression (solid line) plotted as the predicted probability of habitat occupancy for velocity (x axis), at depths of (A and B) 2.5 cm, (C and D) 32.5 cm and (E and F) 62.5 cm, (A, C and E) with cover and (B, D and F) without cover. Substrate size was held constant at 7.62 cm for (A–F) all model iterations. The fine dashed lines indicate the 95% confidence intervals (CI) of model predictions, estimated with the predict function in program R.

2.4.4. Model Performance

The optimum threshold values for models A and G were similar and estimated at 0.201 and 0.231, respectively. We estimated each performance statistic using the optimized thresholds and our presence and absence dataset. Model G had the highest Kappa statistic and correctly predicted 20.3% of all possible presence and absence data, adjusted for correct predictions by chance. In contrast, model A had a Kappa statistic of

18.9%. Model G also had a higher PCC statistic compared with model A at 75.2% and 72%, respectively. Model G predicted 37.5% of the true positives (sensitivity) correctly and 83.6% of the true negatives correctly (specificity), with a false positive classification of 16.4%. In contrast, model A predicted 43.2% proportion of the true positives (sensitivity) correctly and 78.5% of the true negatives correctly (specificity), with a false positive classification of 21.5%. The AUC value, a threshold independent statistic, for models G and A was 0.649 and 0.647, respectively, indicating that both models maintained fair predictive ability above random chance.

2.4.5. 2D hydrodynamic model

All hydrodynamic solutions reached a stable solution, indicating little change in the River 2D spatial algorithm solving for depth and velocity between solution iterations. The average end solution change was 0.18%, with minimum and maximum solution changes of 0.02% and 0.38%, respectively. The mean difference between the measured inflow and modelled outflows across the nine levels of discharge was 0.07%, with minimum and maximum differences of 0.03% and 0.10%, respectively. Within wetted regions, the average area with a Froude number ≥ 1, or supercritical flow, was 11.77 m^2 with minimum and maximum estimates of 0.00 and 26.00 m^2, respectively, or 0.00% and 0.04% of the wetted area. The model projections for velocity, depth and inundated area were qualitatively consistent with field observations and intuitive predictions, where all three variables increased positively with discharge. We could not obtain several modelled discharges to converge on a more stable solution and below our threshold of 0.001 even after following the prescribed QA/QC procedures in Steffler and Blackburn (2002). One potential, and likely, explanation is that one or more shallow nodes were oscillating between wet and dry status through different iterations of the hydrodynamic solution, thereby increasing the final solution change (Steffler and Blackburn 2002). We carefully examined the entire study reach for all modelled flows and could not find any sign of hydraulic anomalies (i.e. super critical flow and erroneous flow direction). The difference between measured inflow and modelled outflows was far below our threshold (< 1%), and at least 99.96% of the modelled space maintained physically natural velocities (Froude < 1.0). As such, we are confident that each discharge modelled was accurately estimating the depth and velocity across the study reach.

Modelled discharge altered total wetted area, where the total wetted area for flows of 33.98, 111.63 and 169.90 $m^3 \cdot s^{-1}$ was 63,501.5, 78,437.3 and 90,965.9 m^2, respectively. Increasing flow from 33.98 to 111.63 $m^3 \cdot s^{-1}$ resulted in a net increase of wetted area by 14,935 m^2 or 19.0%. Increasing flow from 111.63 to 169.90 $m^3 \cdot s^{-1}$ resulted in a net increase of wetted area of 12,528.6 m^2 or 13.8%. At higher flows, the wetted surface area increased by roughly 10.5% per additional cubic metre of water compared with the lower flows.

2.4.6. Comparing model predictions and calculating usable habitat

Over the three quantitative comparisons between competing models, we found clear systematic differences between model predictions. Model A generally estimated a higher probability of habitat occupancy for a point in space; however, the relationship between point-specific model predictions was non-linear and at the highest probabilities of habitat occupancy model G predicted higher probability (Figure 2.4). The greatest differences in model predictions occurred at intermediate and higher probabilities of habitat occupancy (Figure 2.4). In general, there was very little agreement between point-specific model predictions, and agreement only occurred where the probability of habitat occupancy was approximately 18%.

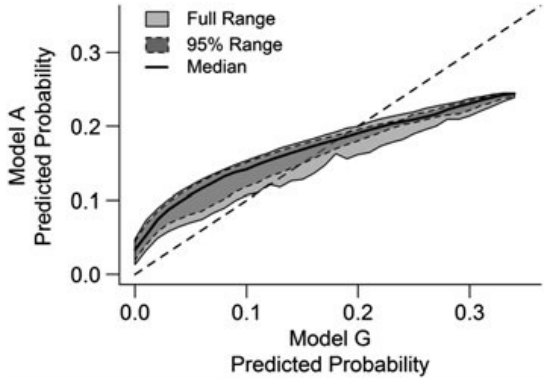

Figure 2.4. Point-specific estimates for model G (x axis) and model A (y axis) for all nine simulated flows. Model predictions are equal where they intersect with the dashed line.

To examine model comparisons in space, we calculated the difference between the point-specific predictions of each model for three of the nine flows we modelled (33.98,

111.63 and 169.90 $m^3 \cdot s^{-1}$). Disparities in model predictions covered the greatest area at the lowest flows we modelled (Figure 2.5) and decreased as flows increased; however, discrepancies in model predictions remained high in areas that were most likely to be occupied by juvenile Chinook (Figure 2.5). Specifically, model disagreement remained high in the stream margins and over the floodplain.

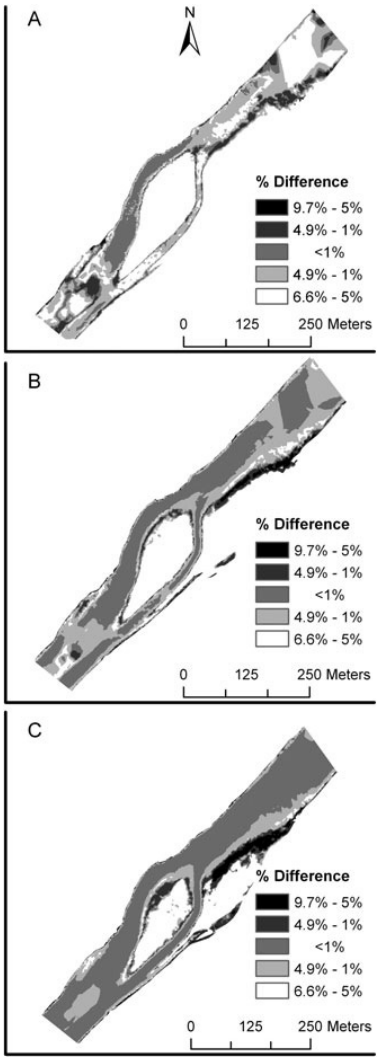

Figure 2.5. Estimated percent difference in model predictions plotted for the study reach at three simulated flows: (A) 33.98, (B) 111.63 and (C) 169.90 $m^3 \cdot s^{-1}$. Dark grey shades indicate space where model G estimated a higher probability of habitat occupancy than model A. Light grey shades indicate space where model A estimated a higher probability of habitat occupancy than model G.

We calculated total usable habitat across all nine flows simulated for models G and A (Figure 2.6). The relationship between usable habitat and discharge was non-linear differed between models. On average, model G predicted 17.25% less habitat than model A across the flows we simulated. Importantly, there was a high degree of uncertainty around the estimates of usable habitat, and model G had higher uncertainty than model A. At low flows, model G predicted 20.6% less usable habitat than model A; however, this difference decreased to 14.7% at higher flows. In addition, each model predicted a different change in habitat resulting from a change in flow indicating that extrapolation of either model over time would produce dissimilar habitat-flow, associations (Figure 2.6).

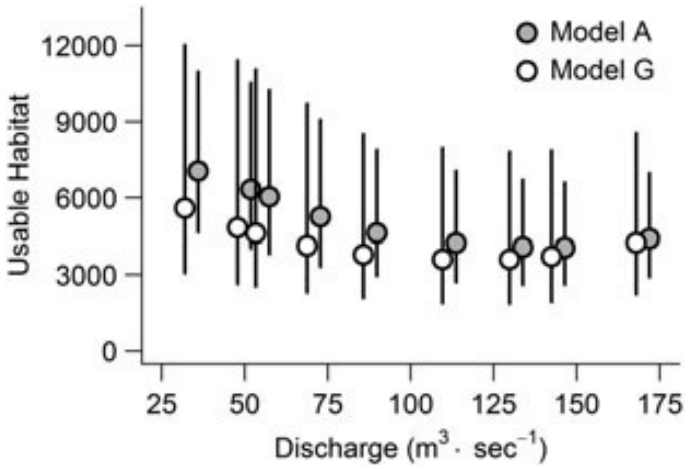

Figure 2.6. Estimated usable habitat based on predictions from competing hydrodynamic habitat models, A (grey circles) versus G (white circles). Error bars represent the minimum and maximum predicted usable habitat based on the upper and lower confidence limits of each respective model. X axis is slightly jittered (± 2 $m^3 \cdot s^{-1}$) to avoid overlap.

2.5. Discussion

The results of our diagnostic statistics indicate that model G correctly predicted a greater proportion of the outcomes in our habitat occupancy data compared with model A, commonly used in habitat modelling. However, the competing models were somewhat comparable in overall predictive accuracy and maintained slight to fair predictive capacities based on the Kappa statistic and AUC value. As well, the total usable habitat

estimated by each model was similar given the degree of uncertainty around the model predictions. Despite these similarities, there were several important differences.

First, the models differed in the proportion of false positives and false negatives. Model A had a higher proportion of correctly identified occupied locations but at the cost of an increased proportion of falsely identified unoccupied locations. As a result, model A had a greater tendency to overestimate habitat occupancy, whereas model G tended to underestimate occupancy. Second, the difference between model predictions was greatest at the lowest flows we modelled and in the physical locations most likely to be occupied by juvenile Chinook salmon. Third, the amount of uncertainty around model predictions was much greater for model G than that for model A.

The relative consequence of using the aggregated (i.e. CSI method; model A) versus the global model (i.e. GLM; model G) in a management scenario is largely dependent on the differences between the model predictions. For example, each model had a clear bias between under-predicting and over-predicting habitat occupancy. If the management goal is to minimize habitat lost by flow regulation, then we posit it is more important to design a habitat model that has the lowest false positive rate. In other words, the best predictive model is one that accurately identifies habitat that will not be occupied by the target species. In this modelling exercise, our results support the conclusion that model G more accurately identified unoccupied locations. In this context, resource managers would have a better estimate of flow regulation effects using model G. In addition, the greatest differences between model predictions occurred in the stream margins and floodplain, which are known to be important rearing habitats for juvenile salmon (Sommer et al. 2001, Beechie et al. 2005). As such, our results indicate that model G had a higher overall predictive ability and therefore provides resource managers with a better tool for predicting how flow regulation will impact those important habitats. In total, the overall accuracy between the models was similar; however, the global model (G) is better suited for management applications and predicting the impact of flow regulation on rearing habitat for juvenile salmon.

The disparity in the amount of uncertainty around model predictions is one of the most important differences between the competing models. As suggested in previous

research, by aggregating univariate models, the modeller must assume each parameter is independent, and thus, the error is also independent (Mathur et al. 1985, Leclerc et al. 2003, Jowett and Davey 2007, Beecher et al. 2010). As such, taking the geometric mean of multiple univariate model predictions does not correctly propagate the uncertainty between model parameters in the aggregated prediction. In this study, we posit that model A considerably underestimated the error around model predictions while simultaneously overestimating habitat occupancy. It is quite possible that this flaw would magnify when additional parameters are added and model complexity increases. For habitat models to be useful management tools to guide flow releases, it is imperative that they accurately reflect the uncertainty in parameter estimation. In doing so, resource managers would be better equipped to identify potential consequences arising from flow regulation within the full range of uncertainty in model predictions.

Some of the uncertainty in each model was due to low salmon densities and the high frequency of unoccupied habitat locations in our data. It is possible that the high proportion of unoccupied locations was a result of low salmon returns in the LAR during the period of time this study was conducted (Carlson and Satterthwaite 2011). The lower the salmon population, the more difficult it is to parameterize the types of models we used in this study. As numerous salmon populations are currently depressed (Nehlsen et al. 1991, Gustafson et al. 2007), this is a concern and possible problem for future modelling in other watersheds. Our results lend further support for a more conservative statistical approach that more accurately incorporates uncertainty, such as AICc model averaging.

There were several candidate multivariate models with similar AICc scores in this study, but generally, multivariate models far outperformed the univariate models in predicting our observed patterns of occupancy by juvenile salmon. These results indicate that habitat occupancy is controlled by a combination of variables. Here, our study is limited to several key physical habitat variables that have repeatedly been reported to affect densities of aquatic species, including Chinook salmon, specifically water depth (Geist et al. 2000, Kynard et al. 2000, Guay et al. 2000, Beecher et al. 2002), velocity (Peeters and Gardeniers 1998, Geist et al. 2000, Kynard et al. 2000, Mallet et al. 2000), substrate size (Knapp and Preisler 1999, Vadas and Orth 2001) and physical cover (Vadas and

Orth 2001, Gard 2006). However, we recognize there are a number of additional habitat characteristics that are hypothesized to be important for functional salmonid rearing habitat, such as prey availability, stream temperature and dissolved oxygen (Hill and Grossman 1993, Braaten et al. 1997, Malcolm et al. 2003, Hayes et al. 2007). Furthermore, it is likely that interactions between parameters (e.g. temperature and velocity) will strongly influence the probability of habitat occupancy. Within the AICc framework we have presented, additional parameters and interactions can be easily integrated into predictive models and their relative importance balanced by model averaging.

We propose that the use of AICc and model averaging may be a valuable tool in producing objective and robust models of physical habitat for juvenile Chinook salmon or other species. Our results support the use of multivariate models over a CSI-based method for predicting the effects of habitat variables on the probability of habitat occupancy. We encourage the use of Cohen's kappa and other diagnostic statistics in model comparison and fully considering the context and consequences of model selection. Future research and management practices should carefully examine the role of multivariate dynamics and consider the implications of excluding them. Fresh water is, and will increasingly be, a limited resource throughout many areas of the world (Richter et al. 2003, Poff et al. 2003). Wise management of aquatic resources within highly regulated river systems is required to support ecosystem services and maintain quality of life for the people relying on such services (Arthington et al. 2006). Therefore, the decision on how to best manage flow releases for downstream organisms is critical and needs to be informed by the best available science. This study illustrates the importance of analytic approaches in developing habitat models that support effective management of flow in regulated river systems.

3. Wildfire and the effects of shifting stream temperature on salmonids[2]

3.1. Abstract

The frequency and magnitude of wildfires in North America have increased by four-fold over the last two decades. However, the impacts of wildfires on the thermal environments of freshwaters, and potential effects on coldwater fishes are incompletely understood. We examined the short-term effects of a wildfire on temperatures and Steelhead/Rainbow Trout (*Oncorhynchus mykiss*) bioenergetics and distribution in a California coastal stream. One year after the wildfire, mean daily stream temperatures were elevated by up to 0.68°C in burned compared to unburned pools. Among burned pools, light flux explained over 85% of the variation in altered stream temperatures, and 76% of the variation in light flux was explained by an index of burn severity based on proximity of the pool to burned streamside. We estimated that salmonids of variable sizes inhabiting burned pools had to consume between 0.3–264.3 mg of additional prey over 48 days to offset the 0.01–6.04 kJ increase in metabolic demand during the first post-fire summer. However, stomach content analysis showed that fish in the burned region were consuming relatively little prey and significantly less than fish in the reference region. Presumably due to starvation, mortality, or emigration, we found a significant negative relationship between the change in total salmonid biomass over the post-fire summer and the average energy costs ($kJ \cdot g^{-1} \cdot day^{-1}$) within a burned pool. This study demonstrates that wildfire can generate thermal heterogeneity in aquatic

[2] A version of this chapter is published as Beakes, M.P., Moore, J.W., Hayes, S.A., and Sogard, S.M. 2014. Wildfire and the effects of shifting stream temperature on salmonids. Ecosphere 5(5):63. http://dx.doi.org/10.1890/ES13-00325.1

ecosystems and drive short-term increases in stream temperature, exacerbating bioenergetically stressful seasons for coldwater fishes.

3.2. Introduction

The frequency and duration of large wildfires in Western North America has increased by nearly four times over the last two decades (Westerling et al. 2006). This dramatic increase could be driven by altered land-use, changes in patterns of precipitation, and increases in temperature (Westerling et al. 2006). Under current IPCC climate scenarios, the frequency and duration of wildfires in North America is expected to continue increasing (Running 2006, Meehl et al. 2007). For example, wildfire burn areas are predicted to increase by an additional 78–118% over the next century in Canada (Flannigan et al. 2005); thus, we need to better understand how wildfire affects ecosystems and vulnerable species. In this warming world, how do wildfires contribute to warming temperatures for thermally sensitive species?

Wildfire can increase temperatures in aquatic ecosystems from 0° to 15°C on short and protracted time scales (Gresswell 1999, Isaak et al. 2010), via different putative mechanisms (Gresswell 1999, Dunham et al. 2007). For example, immediate temperature change in aquatic systems during a wildfire is controlled by convection, the fire's intensity, and the volume of water in the burned region (Rieman and Clayton 1997). The degree of protracted warming, in contrast, is hypothesized to depend on burn severity, stream channel reorganization, the volume of burned riparian vegetation, and the subsequent increase in solar radiation (Minshall et al. 1989, Rieman and Clayton 1997, Gresswell 1999, Dunham et al. 2007). However, the effects of wildfire across a burned landscape are often heterogeneous, leading to disparate local alterations in stream temperatures. For example, Dunham et al. (2007) analyzed a set of temperature data collected before and after wildfires in the Boise River Basin of central Idaho, USA and found that fire heterogeneously increased stream temperatures from 0.4° to 3.7°C. The authors hypothesized that the variation among sites was partly attributed to secondary disturbances such as channel reorganization and changes in channel morphology, as well as to spatial variability in burn severity and degree of recovery of

streamside vegetation (Dunham et al. 2007). Studies similar to Dunham et al. (2007) that have temperature data from both before and after a wildfire are uncommon. As such, our understanding of the short- and long-term effects of wildfire is based on limited information, especially regarding the conservation and management of thermally sensitive species (Minshall et al. 1989, Dunham et al. 2003).

Salmonids are ecologically important and thermally sensitive stream fishes (Baxter et al. 2004, Meissner and Muotka 2006, Isaak et al. 2010, Wenger et al. 2011). Populations of numerous salmonid species are declining throughout their historical range due partly to thermal exclusion from spawning and rearing habitat (Gustafson et al. 2007, Isaak et al. 2010, Wenger et al. 2011). Although wildfires usually do not cause direct mortality of salmonids, they can contribute significantly to warming waters well after the fire is over (Gresswell 1999, Dunham et al. 2007, Isaak et al. 2010). For example, Isaak et al. (2010) found that both large-scale climate forcing and wildfire were associated with warmer headwater streams in the Boise River basin Idaho, USA, and predicted that these temperature changes have resulted in the loss of 11–20% of spawning and rearing habitat for Bull Charr (*Salvelinus confluentus*) over the last two decades. In that study, wildfire contributed to approximately nine percent of the warming trend in burned regions (Isaak et al. 2010). Thus, climate warming and wildfire additively elevate temperatures in coldwater habitats, which will likely affect thermally sensitive species (Rieman et al. 2003, Isaak et al. 2010, Mahlum et al. 2011). Consequently, several species of trout and salmon in the USA are expected to lose between 11% and 77% of suitable coldwater habitat due to climatic warming by the 2080s; however, the role of wildfire in contributing to shifting thermal environments remains uncertain (Dunham et al. 2003, Isaak et al. 2010, Wenger et al. 2011).

Here we examine the short-term effects of wildfire on temperatures and Steelhead/Rainbow Trout (*Oncorhynchus mykiss*) bioenergetics and distribution in a California coastal stream. A wildfire in 2009 burned a major tributary of the Scott Creek watershed in central California that we were actively studying, thereby providing the opportunity to compare mean daily stream temperatures before, during, and after a wildfire at numerous locations in the burned region (Figure. 3.1). We asked three interrelated questions: How does wildfire alter stream temperatures? Does spatial

variation in fire intensity drive spatial heterogeneity in stream temperatures and fish bioenergetics? How do coldwater fishes respond to fire-mediated temperature changes? This case study provides a close look at the effects of wildfire on local temperature dynamics and illuminates linkages between disturbance and abiotic and biotic responses.

3.3. Materials and Methods

3.3.1. Study system

The Lockheed wildfire burned approximately 41% (32 km^2) of the Scott Creek watershed from August 12 to 23, 2009 (Figure. 3.1). Scott Creek is a precipitation-dominated central California coastal stream that drains 78 km^2 of the Santa Cruz Mountains into the Pacific Ocean and contains Endangered Species Act (ESA)–listed Steelhead/Rainbow Trout (*O. mykiss*, listed as threatened) and the southernmost population of Coho Salmon (*O. kisutch*, ESA listed as endangered). The drainage area, mean annual discharge, riparian vegetation, and fish communities of Scott Creek are similar to other small coastal streams in California (Sogard et al. 2012). We conducted our study over the summer, during which California coastal streams are considered stressful for salmonids due to low flow, low prey availability, and seasonally high water temperatures (Grantham et al. 2012, Sogard et al. 2012, Sloat and Osterback 2013). Previous studies have reported negative growth rates and low survival of young-of-year salmonids during California summers partly due to bioenergetic stress, highlighting that small temperature changes may have important consequences for growth and survival (Hayes et al. 2008, Sogard et al. 2009, Sloat and Osterback 2013). We focus on six stream pools within the burned area that we had been monitoring prior to the wildfire (Figure. 3.1B, Big Creek tributary; pool length 11.3 ± 1.4 m [mean ± SE]) and six pools that were at least 1 km from the wildfire burn perimeter (Figure. 3.1C, Upper Scott Creek; pool length 9.2 ± 1.8 m). Prior to the wildfire, the pools in the burned and reference regions had similar canopy cover and morphology, and they were located in tributaries with similar aspect and catchment areas (Figure. 3.1). Thus, this disturbance presented us with a natural

‘‘experiment’’ to examine the effects of wildfire on stream temperatures and salmonids in a representative California coastal stream.

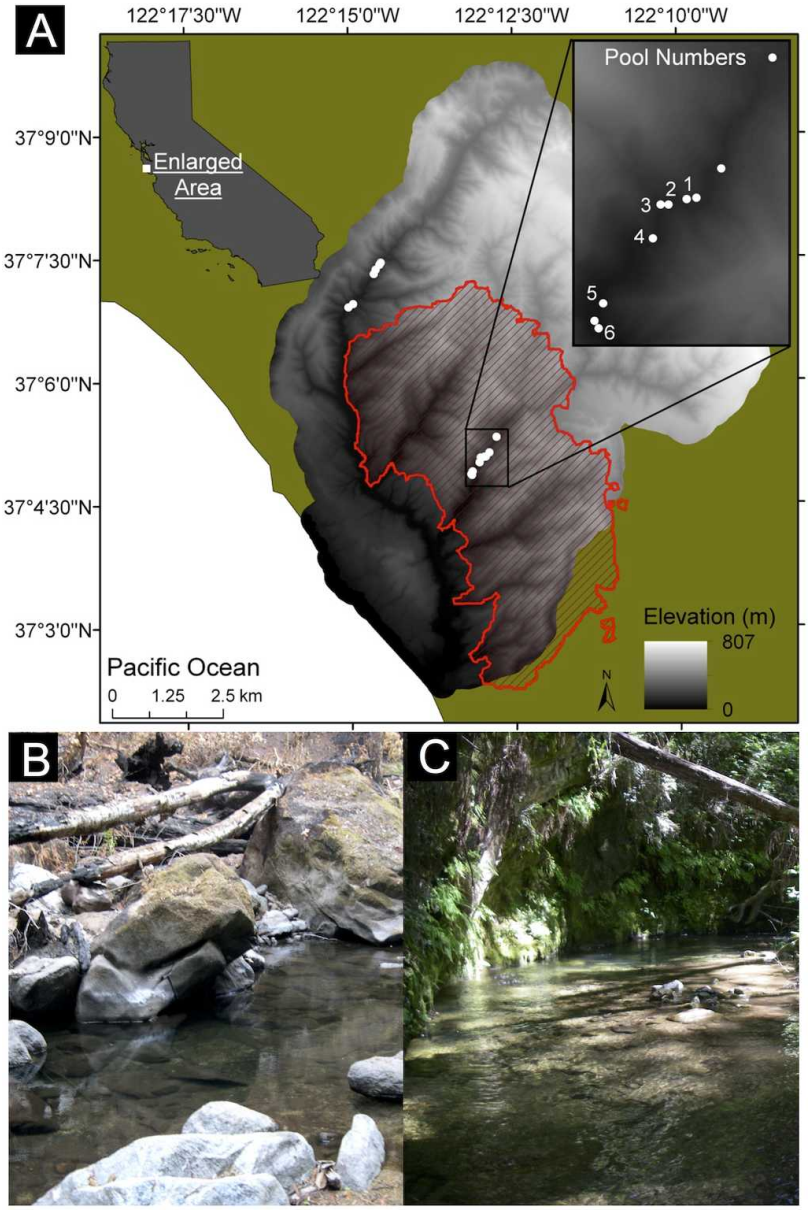

Figure 3.1. Map of Scott Creek, California, and study pools labeled 1–6 in the burned region and unlabeled reference pools located outside the indicated burn region (A). Unlabeled pools in the burned area were added in summer of 2010. The burn extent of the Lockheed wildfire (2009) is outlined in a red-hatched polygon. Also depicted are images of a (B) burned pool and (C) representative reference pool.

3.3.2. Wildfire and abiotic responses

We collected hourly temperature (°C) and light (lumen·m^{-2}) data before, during, and after the wildfire in burned and unburned pools with Onset corp. HOBO Pendant Temperature/Light Data Loggers. For analysis, we focus on three periods during the summer months, ‘‘pre-fire’’ (July 8–August 11, 2009), ‘‘during fire’’ (August 12–23, 2009), and ‘‘post-fire’’ (July 15–August 31, 2010). Within each time period we compared mean daily stream temperatures from each burned pool to the average of mean daily stream temperatures across all unburned pools. Hereafter, we refer to the unburned pools collectively as the ‘‘reference region’’. Using multiple linear regression in program R (R Development Core Team 2013), we regressed the daily temperatures in the burned region against the daily reference temperatures, with categorical factors for the discrete time periods (i.e., pre- vs. post-fire ‘‘Fire’’) and individual burned pools (‘‘Pool ID’’). In essence, this approach uses the reference region temperatures as a control. Using Akaike Information Criterion corrected for small sample sizes (AICc), we compared the performance of the most complex model, including all factors and interactions between them, to a candidate set of sub models (Table 3.1). We identified models of greater parsimony by assuming that a lower AICc score is indicative of a better balance between model fit and model complexity. We accepted a more complex model only if the AICc score was more than four units lower than a simpler model (Burnham and Anderson 2002) and used the most parsimonious model to estimate the degree of temperature change in burned pools relative to the reference region temperatures.

Table 3.1. The competing models, ranked in order of AICc, used for predicting pool-specific changes in temperature after the wildfire.

Model Rank	Model Parameters	df	AICc	∆ AICc
1	RT+ F + PID + F:RT + F:PID + RT:PID	15	-479.1	0
2	RT+ F + PID + F:PID	14	-478.2	0.9
3	RT+ F + PID + F:RT + F:PID + RT:R + RT:F:PID	25	-463.6	15.5
4	RT+ F + PID	9	-314.0	165.1
5	RT+ F	4	-254.4	224.7
6	RT+ F + RT:F	5	-254.2	224.9
7	RT+ PID	8	-81.5	397.6
8	RT	3	-47.0	432.1
9	Null	2	1005.2	1484.3

We compared changes in stream temperatures and light level to assess if changes in solar radiation were associated with changes in temperature, and we compared changes in light level with an index of burn severity to assess if the proximity of charring or burned vegetation to the stream was related to changes in solar radiation. Immediately after the wildfire (September 2009), we measured the minimum distance (meters, m) from the water's edge of each pool in the burned region to the nearest indication of charring or burned vegetation; as such, the proximity of burn evidence served as an index of burn severity. We used linear regression to estimate how much of the observed variation in temperature change was explained by light flux (the difference in median light level between the pre- and post-fire time periods), and how much of the observed variation in light flux was explained by our index of burn severity.

3.3.3. Salmonids and stream temperatures

In the summer after the wildfire we conducted single pass electrofishing in burned and reference pools during two periods (June 2010 and September 2010) to collect, measure, and tag salmonids. We added four pools to the original six burned pools (Figure. 3.1A inset) and two pools in the reference region to bolster our dataset. We blocked each pool with small mesh nets at the upstream and downstream ends, and electrofished upstream from the tail of each pool. All captured salmonids were lightly anesthetized (MS 222) and measured (fork-length, mm, and weight, g). Single-pass electrofishing can provide relatively accurate estimates of fish abundance when sampling short reaches on small streams (Sály et al. 2009), but due to unknown capture probabilities among sites and regions we could not precisely estimate pool-level or regional fish densities. Thus, we consider the difference in total salmonid biomass in each burned pool between sampling events as an index of change over the post-fire summer. We also evacuated the stomach contents of salmonids longer than 55 mm fork-length (FL) via gastric lavage to estimate prey consumption. Salmonids longer than 65 mm were tagged with full duplex Passive Integrated Transponder tags (Allflex corp.). Recaptures in September allowed us to estimate individual growth over the summer.

We used bioenergetics models to explore the energetic costs of fire to fish. With the algorithm and coefficients from Hanson et al. (1997), we estimated the specific rate of

respiration (R, kJ·g^{-1}·day^{-1}) for *O. mykiss*, where R is a function of the allometric mass function intercept (a = 0.00264, g·g^{-1}·d-^{1}), fish mass (W, g), the slope of the allometric mass function (b_1 = -0.217), a temperature dependent coefficient of consumption (b_2 = 0.06818), water temperature (T, °C), and an oxycalorific coefficient (13.56, kJ·g oxygen^{-1}) to convert from consumed oxygen to consumed energy (Hanson et al. 1997; Eq 3.1).

$$R = aW^{b_1} \times e^{b_2 T} \times 13.56$$

Using pool-specific estimates of temperature change from before and after the wildfire in the burned region, we calculated the change in energetic costs (kJ) for salmonids in each burned pool. Specifically, we calculated daily values of R (kJ·g^{-1}·day^{-1}) using mean daily stream temperatures from July 15 to August 31, 2010 for the mass of each fish observed during the June and September electrofishing samples. We multiplied R by each observed fish mass to estimate kJ·day^{-1} for each fish, and we summed the daily energy cost (kJ·day^{-1}) from July 15 to August 31, 2010 to estimate kJ expended by each fish over those 48 summer days. We subtracted the degree of pool-specific temperature change from July 15 to August 31, 2010 mean daily stream temperatures and repeated these bioenergetic calculations for each burned pool. We thus could back calculate the net change in energetic costs (kJ) for the fish we observed in the burned region. We calculated the kernel density (i.e., frequency distribution) of the net change in energetic costs to illustrate variability across individuals and pools; higher kernel density indicates more frequently observed energy costs. To contextualize our bioenergetic estimates, we calculated the minimum prey mass that must be consumed to offset increased energetic demands. We note that bioenergetics of salmonids depends on R and other factors such as population density, prey availability, and additional physiological functions. However, focusing on R avoids uncertain assumptions regarding fish activity levels, rates of prey consumption, and energy lost due to specific dynamic action, egestion, and excretion (Hanson et al. 1997). Our conservative analysis allows us to examine the minimum energy deficit fish accrued during the post-fire summer and provides insight into how much prey are needed to compensate for those costs. To examine the fish response to these energetic conditions, we used linear regression to estimate how much variation in the change in salmonid biomass between electrofishing surveys within each pool could be explained by the post-fire R for a salmonid of average mass.

3.4. Results

3.4.1. Wildfire and abiotic responses

Stream temperatures were variable during the wildfire and among years in both regions (Figure. 3.2). Prior to the wildfire, mean daily stream temperatures were 14.2°C ± 0.4°C (mean ± SD) and 14.9°C ± 0.9°C in the burned and reference regions respectively. The Lockheed wildfire increased stream temperatures in both regions during the wildfire, and reached a maximum of 16.5°C during the peak of the wildfire (Figure. 3.2A). Generally, stream temperatures were cooler in the burned (13.7°C ± 0.7°C) and reference (14.1°C ± 0.9°C) regions over the post-fire summer (Figure. 3.2B). However, the temperature difference between regions was narrower after the wildfire (Figure. 3.2).

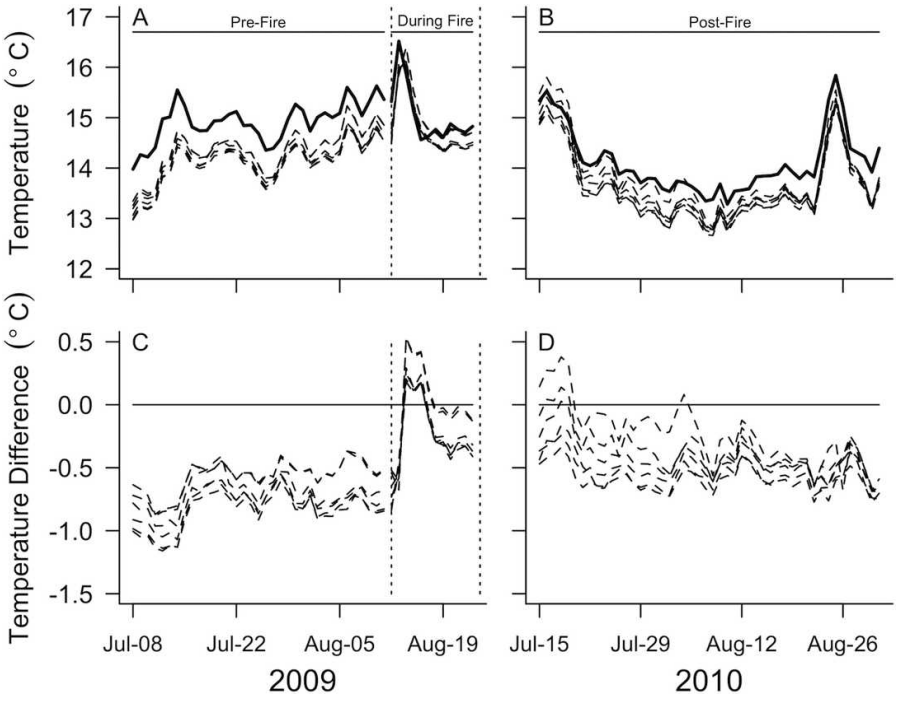

Figure 3.2. Pre-fire, during, and post-fire (A and B) mean daily stream temperatures for the reference region (solid line), and the burned pools (dashed lines) and (C and D) temperature difference between the burned pools and reference region. The date range and corresponding water temperatures during the Lockheed wildfire are bound by vertical dotted lines. The left panels (A and C) show the summer of the fire (2009), while the right panels (B and D) show the summer after the fire (2010).

Wildfire associated changes in mean daily stream temperatures in the burned region, relative to the reference region, were dissimilar during and after the fire (Figure. 3.2C, D). Compared to reference temperatures, mean daily stream temperatures among the burned pools increased relatively homogenously by 0.56°C ± 0.03°C (mean ± SE) during the fire (Figure. 3.2C). During the post-fire summer, the difference in temperature between burned and reference pools indicated an average increase of 0.34°C ± 0.09°C in the burned region mean daily stream temperatures; however, there was a significant difference among burned pools (Figure. 3.2D and 3.3A, Table 3.2). For example, mean daily stream temperatures showed a relative increase of 0.6°C ± 0.03°C in pool 2 compared to 0.04°C ± 0.05°C in pool 6 (Figure. 3.3A). Mean daily stream temperatures in the burned region were best explained by a multiple linear regression model that included the reference temperatures and factors for ''Time,'' ''Pool ID,'' and an interaction between ''Time'' and ''Pool ID'' (adjusted R^2 > 0.95; Table 3.2). All factors were significant in the model (P < 0.05; Table 3.2). The top ranked model included two additional interaction terms (Table 3.1), but was more complex and only slightly more supported (∆AICc < 1), with a negligible change in explained variance (∆ adjusted R^2 < 0.001); thus, we used the simpler model that excluded uninformative parameters (Arnold 2010). Lower ranked models were substantially less supported (∆AICc > 15) and were not considered in further analysis.

Table 3.2. Regression coefficients obtained from the most parsimonious linear regression fit to estimate stream temperature change.

Parameter	Coefficient	S.E.	*t*	*P*
Intercept	-1.37124	0.1755	-7.81	< 0.001
Reference Temp	1.08065	0.01233	87.61	< 0.001
Pre-Fire	-0.60075	0.03421	-17.56	< 0.001
Pool 1	-0.31614	0.03008	-10.51	< 0.001
Pool 3	-0.12946	0.03008	-4.30	< 0.001
Pool 4	-0.18643	0.03008	-6.20	< 0.001
Pool 5	-0.25026	0.03008	-8.32	< 0.001
Pool 6	-0.35941	0.03008	-11.95	< 0.001
Pre-Fire: Pool 1	0.26311	0.04632	5.68	< 0.001
Pre-Fire: Pool 3	0.19271	0.04632	4.16	< 0.001
Pre-Fire: Pool 4	0.11176	0.04632	2.41	0.0162
Pre-Fire: Pool 5	0.44549	0.04632	9.62	< 0.001
Pre-Fire: Pool 6	0.56038	0.04632	12.10	< 0.001

Note: All pool specific levels of significance are based on the model confidence intervals and fit relative to Pool 2.

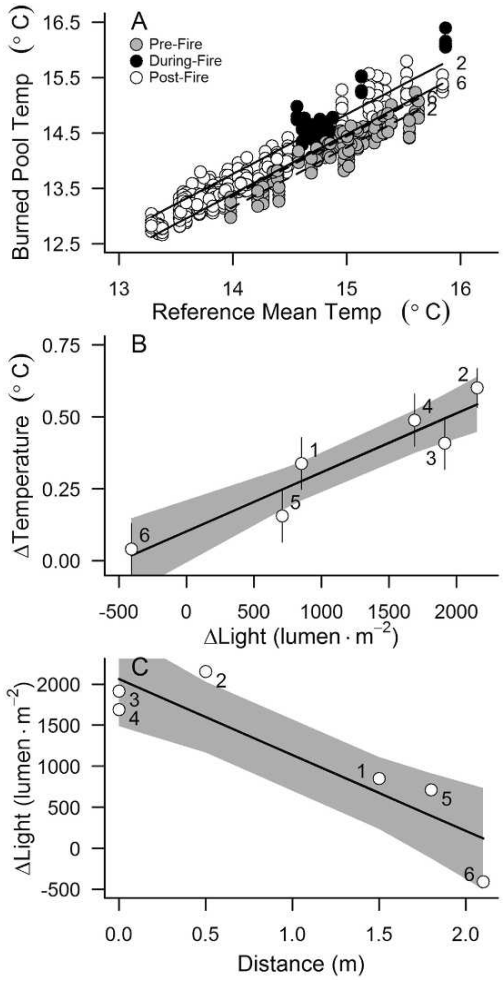

Figure 3.3. Relationship between reference and burned pool (A) mean daily stream temperatures from the pre- fire (grey circles, July 8–August 11, 2009), during-fire (black circles, August 12–23, 2009) and the post-fire (white circles, July 15–August 31, 2010) time periods. Linear model fits (lines) are shown for the most (2) and least (6) burned pools. (B) The relationship between change in light flux and the estimated change in temperature for each burned pool. The line indicates the best linear model fit. (C) The relationship between proximity to burned vegetation or earth and change in light flux for each burned pool. We bound (B and C) the 95% CI of linear model fit with grey polygons and estimated (B) D degrees with error bars. Pool numbers (1– 6) are next to each data point in the plot.

We observed increased instream light levels (lumen·m^{-2}) during the post-fire summer (Figure. 3.4). During the wildfire our temperature and light data loggers were buried

beneath debris, which likely impeded light penetration to the data loggers. As such, we could not accurately measure the change in light during the wildfire. Within a few months following the wildfire most of the instream debris was transported downstream. The summer following the wildfire we measured an increase in the median light levels in the burned region and in the reference region to a lesser degree (Figure. 3.4B). The observed increase in the reference region median light levels was likely driven by one pool, where a redwood tree (*Sequoia sempervirens*) fell and opened the canopy. The flux in median light levels between the pre- and post-fire summers among burned pools was variable, ranging from approximately -410 to 2,150 lumen·m^{-2}, and was associated with elevated mean daily stream temperatures (Figure. 4.3B). Specifically, we found a strong positive relationship between increased stream temperatures and light flux in burned pools (P < 0.01, adjusted R^2 = 0.86; Figure. 4.3B). We observed more burned vegetation and fallen trees around pools that had a larger positive flux in light and change in water temperature. As well, we found that the proximity of burned vegetation or earth to the water's edge in a burned pool was strongly and negatively related with light flux (P = 0.02, adjusted R^2 = 0.76; Figure. 4.3C).

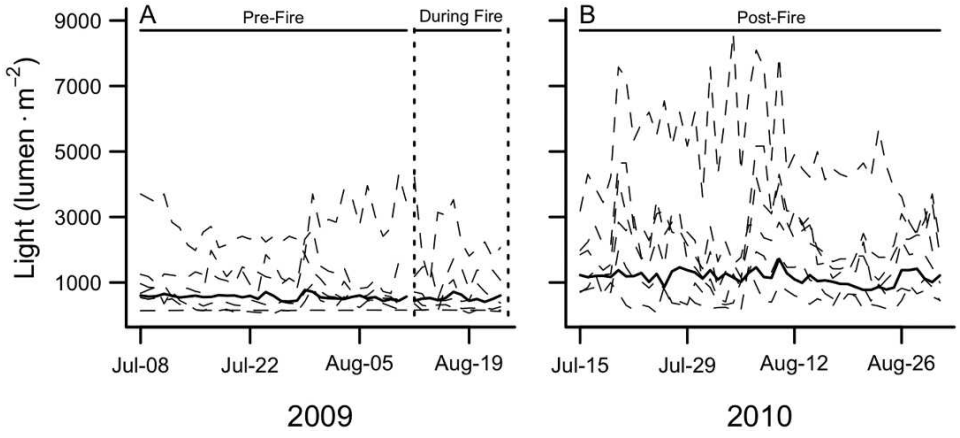

Figure 3.4. Pre-fire, during, and post-fire instream light levels for the reference region (solid line), and the burned pools (broken lines). The date range and corresponding water temperatures during the Lockheed wildfire are bound by vertical dotted lines. The left panel (A) depicts the summer of the fire (2009), while the right panel (B) shows the summer after the fire (2010).

3.4.2. Salmonids and stream temperature

The number and size of salmonids (*O. mykiss*) captured among regions in June and September varied (Table 3.3). In June 2010, we captured approximately 7% more fish in the burned region than in the reference region, and these fish were 15% longer and 46% heavier on average. In September 2010, the difference in the number of captured fish between regions increased to 58%. The increased difference between regions in September compared to June was due to a 28% increase and 14% decrease in captured fish in the burned and reference regions respectively. Although we captured more individuals in the burned region in September, the average length and mass of fish between regions was more similar in September compared to the average length and mass of fish in June (Table 3.3). We recaptured 8 of the 34-tagged fish from the burned region (mean individual mass change = -3.7% ± 8.8% [mean ± SD]; Table 3.3). The mass of 6 of these 8 recaptured fish decreased over the post-fire summer. In contrast to changes in individual fish mass, the mean fish mass in the burned region increased by approximately 14% between June and September. In the reference region, 2 of the 3 recaptured fish gained mass (mean individual mass change = 9.9% ± 13.1%; Table 3.3). Similarly, the mean fish mass in the reference region increased by approximately 56% between June and September.

The amount of prey found in *O. mykiss* stomachs differed between regions but not between survey months (Table 3.3). The average mass of stomach contents was influenced by individual *O. mykiss* with large prey items in their guts. For example, we found one fish in June with a 582 mg (dry mass) Pacific Giant Salamander (*Dicamptodon spp.*) in its stomach. After standardizing the mass of prey (mg) by fish mass (g), we found that both the mean and median amount of prey consumed per fish (prey (mg)·fish $(g)^{-1}$) were similar between June and September within each region (Table 3.3). We found that the amount of prey consumed per fish in the burned region was significantly less compared to fish from the reference region (log(prey (mg)·fish $(g)^{-1}$ + 1); GLM, $P = 0.011$; Figure. 3.5A).

Table 3.3. Summary statistics for salmonids captured during the electrofishing surveys in June and September 2010. Where applicable the mean (6 SD) across pools is reported.

	Burned Region		Reference Region	
Statistic	June	September	June	September
Fish Captured	47	60	44	38
Fork-Length (mm)	92.8 ± 39.9	99.6 ± 38.0	80.9 ± 34.0	97.6 ± 33.0
Mass (g)	13.6 ± 17.8	15.5 ± 19.5	9.3 ± 10.2	14.5 ± 17.0
Fish Tagged (N)	34	…	25	…
Recaptured Fish (N)	…	8	…	3
∆ Individual Mass (%)	…	-3.7 ± 8.8	…	9.9 ± 13.1
Mean Prey (mg)	30.4 ± 114.8	13.6 ± 24.1	43.6 ± 136.6	27.6 ± 38.8
Median Prey (mg)	6.7	4.6	10.6	13.1
Prey (mg) per Fish (g)	0.99 ± 1.74	1.01 ± 2.09	2.03 ± 4.53	1.66 ± 1.94

Note: Mean and median prey masses are dry weights of both terrestrial and aquatic sources found in the stomach contents.

On average, the post-fire energy cost (*R*) for salmonids was 2.34% higher than pre-fire energy cost in the burned pools relative to the reference pools. The maximum predicted change in energy costs was in pool 2 at 4.0% (CI, 4.67–3.71%) and the smallest was in pool 6, where confidence limits overlapped with 0. Pools with larger post-fire temperature differences had kernel density distributions that were shifted towards larger increases in energy costs (Figure. 3.5B). Given that fish of different sizes have different energetic expenditures, the observed size distribution of fish also influenced the distribution of predicted changes in energy costs. For example, energetic costs in pool 2 increased with fish size, estimated as an additional 0.19 kJ over the post-fire summer for a 1.1-g fish (5th percentile of fish size), 1.06 kJ for a 9.8-g fish (median fish mass), and 4.96 kJ for a 70.1-g fish (95th percentile of fish size). Due to variation in temperature change and fish size, the estimated energetic costs to individual fish among all the burned pools ranged between 0.01 and 6.04 kJ. As such, we estimated that fish in the burned region needed to consume approximately 0.3–264.3 mg (dry mass) of additional prey over 48 days to offset those added metabolic costs, with larger fish burning more energy than smaller fish in the same water temperature and thus requiring more prey. In terms of prey items, 0.3–264.3 mg of prey (dry mass) equates to approximately 10 – 2,250 average-sized mayflies (*Ephemeroptera spp*.; Cummins and Wuycheck 1971, Benke et al. 1999; M. Beakes, *unpublished data*).

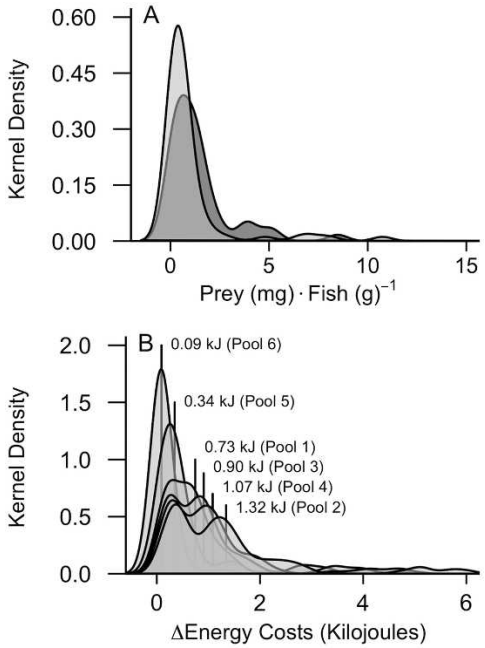

Figure 3.5. Kernel density distribution of (A) salmonid gut contents combined between sampling months for the reference region (dark grey polygon, n = 48) and the burned region (light grey polygon, n = 72). This distribution shows variability across individuals; higher kernel density indicates more frequently observed stomach content measurements. (B) Kernel density distribution of estimated post-fire Δ energy for each burned pool derived from R, the measured temperature change, and range of fish masses in the burned region. Thus, the observed size range of fish in the different pools drives the distribution in change in energy costs. Mean post-fire Δ energy for each burned pool is marked by vertical lines and text.

Within the burned region, total salmonid biomass change between June and September was negatively associated with increased post-fire summer energetic demands. Overall, we observed an increase in fish abundance and size between the electrofishing surveys in the burned region over the summer. However, specific pools had different patterns of change in total salmonid biomass, ranging from an increase of 78.7 g in pool 1, to a decrease of 41.9 g in pool 2 (Figure. 3.6). These post-fire changes in salmonid biomass were negatively correlated with the predicted metabolic cost of the pool (P = 0.034, adjusted R^2 = 0.43; Figure. 3.6). We removed a single outlier pool from this analysis that had high residual variance (Studentized residual = -3.1); deviation from the model fit in this pool was driven by a single *O. mykiss* that was not recaptured in the September electrofishing survey and was the largest fish we observed during the course of this study.

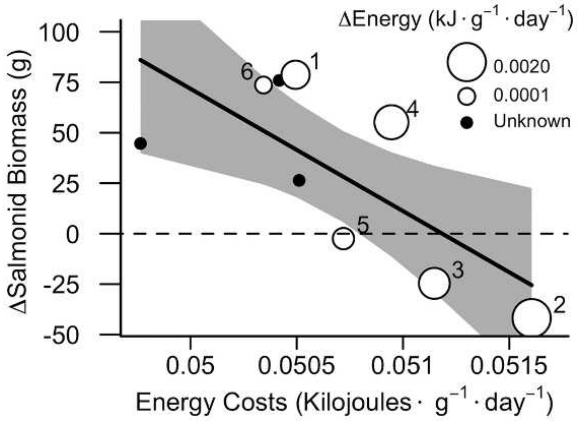

Figure 3.6. Relationship between estimated energy cost of the pool and the observed change in salmonid biomass. Linear model fit and 95% CI (grey polygon) between energetic costs R for an average size fish (14.66 g) and over-summer change in salmonid biomass. Pool numbers (1–6) are next to each respective data point. The predicted change in energy costs scales with the size of each point except for pools added in 2010 summer (black), for which we could not estimate pre-fire costs.

3.5. Discussion

In a central California coastal stream we found that wildfire altered stream temperatures, which in turn led to elevated energetic needs for thermally-sensitive *O. mykiss*. Daily stream temperatures were 0.6°C warmer on average one year after the fire in the most intensely burned pool, relative to unburned regions. While this does not sound like much change, it is worth noting that this is the equivalent of approximately two decades of directional climate warming (Stefan and Preud'homme 1993, Meehl et al. 2007). We estimated that these shifts in relative temperature also increased bioenergetic costs for coldwater salmonids, and over the post-fire summer we observed that total salmonid biomass decreased the most in pools that had the highest energetic costs. Together, these data suggest that fire, through removing riparian vegetation, leads to increased light, thereby warming temperatures, which in turn drives local decreases in bioenergetically stressed salmonids.

Our study illustrates how fine-scale heterogeneity in burn severity drives spatial variation in abiotic conditions. More severely burned pools had increased light, and this increased light was associated with relatively increased stream temperatures. Our results

corroborate observations from several other studies (e.g., Albin 1979, Amaranthus et al. 1989, Royer and Minshall 1997, Hitt 2003, Dunham et al. 2007). For example, Isaak et al. (2010) estimated that 50% of the stream temperature warming within burned regions in Idaho, USA, could be accounted for by increased solar radiation associated with canopy and vegetation loss. Often, burn severity is measured on a categorical scale (e.g., moderate, stand replacing, etc.), which necessitates spatial averaging of fire intensity and implies a homogenous effect of the wildfire over large spatial scales. For example, based on the US Forest Service Burned Area Reflectance Classification (BARC) we would conclude that most, if not all, of our burned pools fell under the category of ‘‘moderate’’ burn severity, rendering the analysis presented in this study impossible. By integrating local measures of distance to burn in our analysis we have provided new empirical measures for how heterogeneity in burn intensity can generate a heterogeneous thermal environment even at small spatial scales.

Our study illustrates how fire contributes to the temporal dynamics in stream abiotic conditions, over short time periods. The fire itself led to a short-term increase in temperature, and then the removal of riparian vegetation apparently led to increases in stream temperature that lasted for at least one year. Our evidence suggests that temperature is linked to light flux controlled by riparian vegetation. As streamside vegetation regenerates, stream temperatures will likely return to their pre-perturbed state, as suggested in previous research (Gresswell 1999, Dunham et al. 2007, Verkaik et al. 2013a).

We estimated that energy costs increased by up to 4.0% in some burned pools, equating up to 6.04 kJ of added energetic expense for the largest fish over the post-fire summer. To offset these costs, individual fish would have to increase their prey consumption rate, lose energy reserves, or seek less energetically costly habitat. In general, prey available in the drift appears limited in California coastal streams during the summer and fall partly due to low base flows (e.g., Sogard et al. 2012), and our diet data indicate that most fish in the burned region were eating relatively little compared to fish in the reference region.

Thermal heterogeneity caused by the wildfire was associated with shifts in *O. mykiss* biomass, perhaps due to individual mass loss, mortality, and potential emigration from

more energetically costly pools (Figure. 3.6). We suspect that insufficient prey consumption during the post-fire summer resulted in lost energy reserves for some fish. Negative summer growth estimates have previously been observed in this and other coastal California watersheds, reflecting overall poor growth conditions in the summer for age-1 and larger fish (Hayes et al. 2008, Sogard et al. 2009, Grantham et al. 2012). As such, this pattern of weight loss is not unique to the burned region of Scott Creek, but rather highlights that these populations must delicately balance energetic costs and energetic intake during the food-poor and warmer summer months. Some of the shifts in *O. mykiss* biomass we observed over the summer within burned pools and at the aggregate region scale may have also been influenced by movement. *O. mykiss* have been shown to move between habitats in search of more thermally suitable habitat on small spatial scales (Ebersole et al. 2001) or to habitats such as riffles where rates of prey delivery are greater (Smith and Li 1983). However, *O. mykiss* movement on large spatial scales can be limited in California coastal watersheds during the summer (Hayes et al. 2011). Resource limitation can lead to increased antagonistic behavior and territoriality (Grant and Kramer 1990, Keeley 2001, Harvey et al. 2005, Sloat and Osterback 2013), driving size-selective movement or mortality where smaller individuals perish or are forced to emigrate from resource limited habitats (e.g., Keeley 2001). Indeed, studies have shown that warm summer water temperatures can drive changes in the abundance and distribution of salmonids (Sestrich et al. 2011, Sloat and Osterback 2013). Although water temperatures throughout Scott Creek during and after the wildfire were well within the thermal limits of *O. mykiss*, our results do suggest that small-scale changes in temperature can influence these fish.

The effects of wildfire on water temperature and fish are likely seasonally dynamic. In contrast to the dry, food-poor summer months, food availability and growth of both age-1 and young-of-year California coastal salmonids generally increases in the winter and spring (Hayes et al. 2008, Sogard et al. 2009, 2012). Historically, however, winter/spring water temperatures in the upper watershed and in the burned region of Scott Creek fall several degrees below the optimal temperatures for *O. mykiss* food consumption and growth (Myrick and Cech 2000, Hayes et al. 2008, Sogard et al. 2012). If wildfire increases stream temperatures throughout the year, we hypothesize that wildfire may improve growth conditions in the food-rich winter and spring.

We focused on salmonids, their energetics, and their abiotic environment, but wildfire can also simultaneously affect other aspects of stream ecology. Generally, wildfire is considered to be among the most important forms of natural disturbance, with multiple direct and indirect affects on aquatic ecosystems (Gresswell 1999, Malison and Baxter 2010a, Verkaik et al. 2013a). For instance, wildfire can act as a fertilizing agent in aquatic ecosystems. By burning vegetation in the riparian zone and surrounding areas, wildfires can increase nutrient availability and light, which subsequently stimulates primary production (Minshall et al. 1989, Gresswell 1999, Dunham et al. 2003, Verkaik et al. 2013a). In some aquatic systems, wildfires lead to greater benthic invertebrate production (e.g., Malison and Baxter 2010). Alternatively, many studies report that benthic macroinvertebrate production remains unchanged or declines initially and returns to pre-fire levels within a few years post-fire (reviewed by Minshall 2003, Verkaik et al. 2013). The production of invertebrate prey naturally fluctuates seasonally in burned and unburned watersheds, although peak production may become asynchronous relative to neighboring unburned systems (Malison and Baxter 2010b). As such, the long-term effects of the Lockheed wildfire on stream temperatures and fish in Scott Creek will likely be dependent on within season changes to the prey base and water temperature.

Wildfire and climate warming can act in concert to warm waters. Small or isolated populations of coldwater species will be disproportionately affected by warming temperatures, especially those near the limits of their distribution (Isaak et al. 2010, Wenger et al. 2011). The net effect of wildfire on stream temperatures and fish will likely be spatially variable. Stream temperatures will increase more in areas of a watershed more intensely burned relative to those less intensely burned. As well, warming waters during food-poor seasons will carry greater bioenergetic costs, whereas warming during food-rich seasons may produce bioenergetically favorable conditions for accelerated growth. Our study illustrates how wildfire can drive short-term, highly localized increases in stream temperature with associated effects on the bioenergetics and distribution of salmonids. More generally, our study highlights the importance of considering the fine-scale impacts of large-scale disturbances on the thermal environments of aquatic ecosystems.

4. Seasonality, wildfire, and shifting food webs in a coastal stream[3]

4.1. Abstract

Wildfire has increased in duration and frequency by nearly four-fold in Western North America over the last two decades. Our appreciation of wildfire as a principal driver of change in recipient ecosystems has grown with our knowledge of the myriad effects wildfire has on terrestrial and aquatic systems. In this study, we examined stream ecosystem elements that are putatively linked with terrestrial ecosystems in burned and unburned reference regions of a California coastal watershed for one year following a wildfire. Specifically, we measured seasonal changes in nitrate (μM NO_3-), suspended fine particulate organic matter (FPOM; $cg \cdot L^{-1}$), $\delta^{13}C$ and $\delta^{15}N$ stable isotopes, invertebrate abundance and biomass, and Steelhead/Rainbow Trout (*Oncorhynchus mykiss*) inferred diet composition. In the burned region, we observed increased nitrate (244%) and fine particulate organic matter (44%) concentrations compared to the reference region, with these increases primarily associated with rainstorms. We also found enriched $\delta^{13}C$ and $\delta^{15}N$ levels in aquatic invertebrate and dissimilar seasonal isotope patterns in the burned region relative to the reference region. There were clear seasonal differences in terrestrial and aquatic invertebrate abundance and biomass but no differences between burned and reference regions. However, Bayesian stable isotope mixing models illuminated differences across seasons and between the burned and reference regions in inferred *O. mykiss* diets, with higher trophic level prey contributing more to diets in the burned compared to the reference region. This study suggests that fire can drive short-term changes stream food webs, but that the

[3] A version of this chapter is in preparation for publication with the following coauthors: Moore, J.W., Cois, C., Collins, A., Retford, N., Twardochleb, L., Hayes, S.A., and Sogard, S.M

magnitude of this type of disturbance may be relatively minor compared to the underlying seasonal changes.

4.2. Introduction

The frequency and duration of large wildfires in Western North America has increased by nearly four-fold over the last two decades (Westerling et al. 2006). Under current IPCC climate scenarios, the frequency and duration of wildfires in North America is expected to continue increasing (Running 2006, Meehl et al. 2007). For example, wildfire burn areas are predicted to increase by an additional 78% - 118% over the next century in Canada (Flannigan et al. 2005). Over the last four decades we have acquired considerable knowledge of the myriad effects wildfire has on terrestrial and aquatic systems (e.g., Attiwill 1994, Turner and Romme 1994, Gresswell 1999, Bisson et al. 2003, Dunham et al. 2007, Verkaik et al. 2013). As a result, wildfire is now recognized as a principal driver of change in stream and river ecosystems (Malison and Baxter 2010a).

Wildfire can alter key controls of ecosystems and food webs. By burning riparian vegetation and forests adjacent to lotic ecosystems, wildfire has been shown to increase the availability of light and nutrients (Gresswell 1999, Wan et al. 2001, Spencer et al. 2003, Verkaik et al. 2013a) which can limit primary production. In some cases, phosphate and nitrate concentrations have increased up to 60-fold above background levels during large wildfires (Spencer et al. 2003). The effects of wildfire can also alter the abundance or distribution of invertebrate and fish predators (Malison and Baxter 2010b, Sestrich et al. 2011, Beakes et al. 2014), of which some have the capacity to restructure stream and forest food webs through top-down forcing (e.g., Baxter et al. 2004). As well, recent research suggests that wildfire may alter terrestrial carbon and invertebrate prey subsides to streams (e.g., Jackson et al. 2012). However, relatively few studies have examined the effects of wildfire on terrestrial-aquatic linkages and subsidies (Bisson et al. 2003, Dwire and Kauffman 2003, Malison and Baxter 2010a).

The contribution of terrestrial resources to headwater streams is particularly prevalent as forests, riparian zones, and streams are tightly coupled (Vannote et al. 1980, Naiman and Henri 1997). In some cases, terrestrial nutrient and organic material inputs far

surpass instream production and availability (Fisher and Likens 1973, Boling et al. 1975, Polis et al. 1997). For example, Minshall (1967) found that 50-100% of herbivorous and omnivorous primary consumer diets in a small woodland creek were comprised of allocthonous organic material. Predatory stream fishes can also derive significant energy subsidies from terrestrial ecosystems, which can influence their growth and abundance (Nakano et al. 1999, Kawaguchi et al. 2003, Erős et al. 2012, Inoue et al. 2013). In some cases concerning trout and salmon, over 50% of the annual energy budget is obtained from seasonally available terrestrial arthropods (Wipfli 1997, Nakano and Murakami 2001, Kawaguchi and Nakano 2001, Baxter et al. 2005, Wipfli and Baxter 2010, Inoue et al. 2013). Thus, we might predict that fire can dramatically alter food webs in headwater streams by disturbing riparian ecosystems.

Perturbing forests and riparian zones can alter terrestrial resource subsidies in adjoining stream ecosystems. For example, wildfires can drive pulses of nutrients and organic matter into the streams of burned watersheds (Minshall et al. 1989, Gresswell 1999, Verkaik et al. 2013a). Inoue et al. (2013) found that terrestrial arthropod biomass available to Masu Salmon (*Oncorhynchus masou*) was 1.9-4.4 times higher in an intact forest compared to recently clear-cut sites in Shikoku, southwestern Japan. Similar effects were observed in watersheds naturally perturbed by wildfire, where Rainbow Trout (*Oncorhynchus mykiss*) stomach contents contained significantly greater proportions of aquatic prey sources and lower terrestrial sources on average in burned compared to unburned systems (Koetsier et al. 2007). However, it is important to note that the difference in terrestrial subsidies between the perturbed and intact forests reported in the studies above was mediated by underlying seasonal patterns of terrestrial subsidy availability (Nakano and Murakami 2001, Baxter et al. 2005).

Stream food webs can be structured by seasonal fluctuations in abiotic drivers, especially in the fire-prone landscapes of Mediterranean climate ecosystems (Gasith and Resh 1999, Power et al. 2008, Verkaik et al. 2013a). Streams in Mediterranean climates regularly experience both extreme flooding and droughts during the characteristically wet winters and dry summers (Gasith and Resh 1999). These seasonal disturbances can drive dramatic shifts in biological communities and food webs (McElravy et al. 1989, Power et al. 2008, 2013). For example, in California's South Fork

Eel River, bed-scouring winter floods can reduce the density of the river's dominant invertebrate grazer by up to two orders of magnitude resulting in large algal blooms the following summer (Power et al. 2008). As such, the biota and food webs that typify Mediterranean streams represent artifacts of historic disturbances. Thus, examining the effects of other perturbations such as wildfire relative to seasonal disturbances provides a context for comparing the magnitude of their effects and their relative importance as drivers of stream ecosystem change.

In this study we aimed to compare the relative influence of seasonality and wildfire on a Mediterranean climate stream food web. Specifically, we examined seasonal changes in nutrients, organic matter, $\delta^{13}C$ and $\delta^{15}N$ stable isotopes of primary and secondary consumers, invertebrate abundance, and Steelhead/Rainbow Trout (*Oncorhynchus mykiss*) diet composition in Scott Creek, a central California coastal watershed perturbed by wildfire. Using pre-fire data, and data collected in burned and unburned reference regions of the watershed over one post-fire year we ask, what is the relative influence of seasonality and wildfire on food webs and stream subsidies in Scott Creek? Specifically, our study was focused on four interrelated sets of response variables: 1) concentrations of nitrate and fine particulate organic matter, 2) the relative abundance and biomass of terrestrial and aquatic invertebrates, 3) isotopic signatures of sources and consumers, and 4) estimated contributions of terrestrial and aquatic prey sources to *O. mykiss* diets. This study provides insight into the effects of wildfire on basal resources, prey availability for fishes, and terrestrial subsidies in a California coastal stream.

4.3. Materials and Methods

4.3.1. Study system

The Lockheed wildfire burned approximately 41% (32 km^2) of the Scott Creek watershed from August 12 - 23, 2009 (Beakes et al. 2014; Figure 4.1). Scott Creek is a precipitation-dominated central California coastal stream that drains 78 km^2 of the Santa Cruz Mountains into the Pacific Ocean and contains Endangered Species Act–listed Steelhead/Rainbow Trout (listed as threatened) and the southernmost population of

Coho Salmon (*O. kisutch*, listed as endangered). The drainage area, mean annual discharge, riparian vegetation, and fish communities of Scott Creek are similar to other small coastal streams in California (Sogard et al. 2012). We focus on eleven stream pools within the burned area (Figure. 4.1, Big Creek tributary; mean pool length 10.4m ± 3.2m SD, depth 0.9m ± 0.3m SD) and eight stream pools located at least one kilometer outside the burn perimeter (Figure. 4.1, Upper Scott Creek; mean pool length 11.6m ± 5.1m SD, depth 0.7m ± 0.4m SD). Prior to the wildfire, the pools in the burned and reference regions had similar canopy cover and morphology, and they were located in tributaries with similar aspect and catchment areas (Beakes et al. 2014; Figure 4.1). Thus, the burn pattern provided a contrast within a watershed to examine the effects of wildfire on stream food webs and terrestrial subsidies in a representative California coastal stream.

The main contrasts of our study were the differences across season and across burned and reference regions. We collected data over 16 months from September 2009 to December 2010 starting immediately after the August 2009 wildfire. The frequency of sampling varied among nutrients, organic matter, $\delta^{13}C$ and $\delta^{15}N$ stable isotopes, and invertebrate abundance. We used pre-fire isotope data taken from *O. mykiss* tissues samples (2006) to examine pre-fire *O. mykiss* inferred diet composition. However, we did not have pre-fire isotope data for potential prey sources from the same year and season (2006, fall) so we used post-fire isotope data for prey sources taken from the reference region as a substitute. We assumed post-fire isotope signatures of prey sources in the reference region were similar to pre-fire isotope signatures of prey sources in the burned region. Differences across burned and reference regions were interpreted as potential effects of fire. We note that we have replication within each of these regions, however, without pre-fire data for both regions it is possible that the observed differences across regions were due to historic differences rather than the fire disturbance.

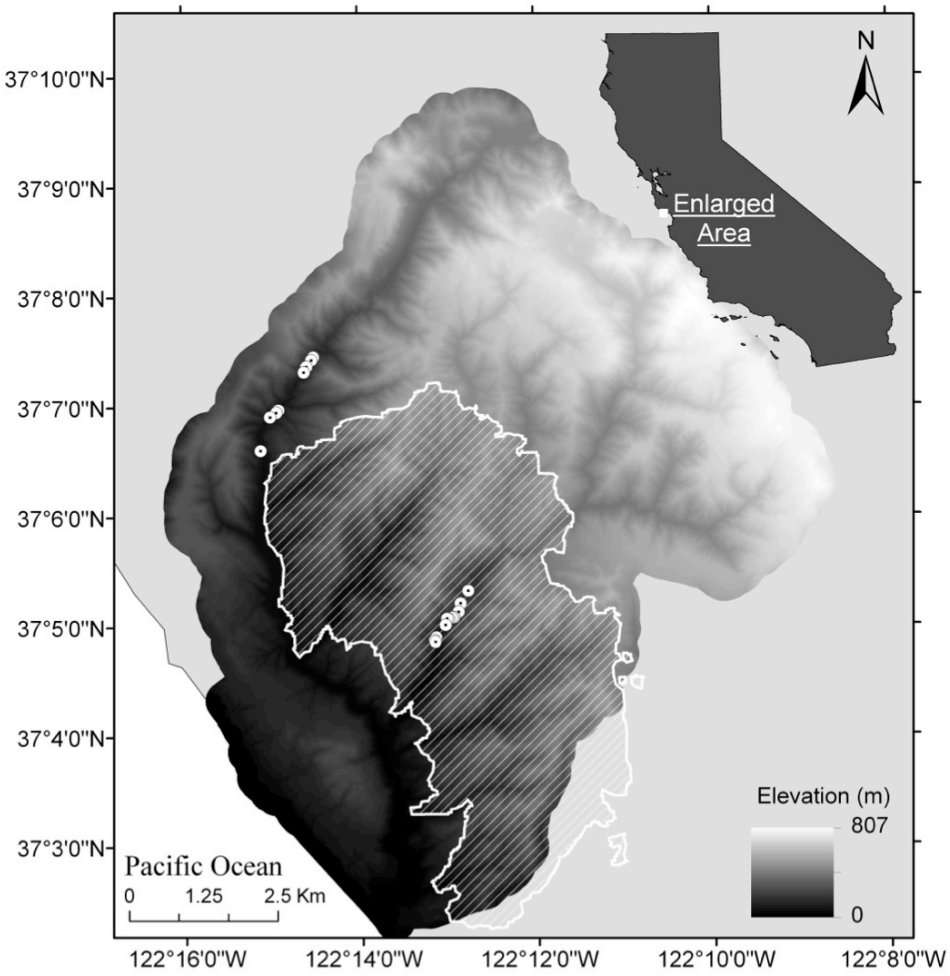

Figure 4.1. Map of Scott Creek, California, and study sites (white circles) in the burned and reference regions. The burn extent of the Lockheed wildfire (2009) is outlined in a white-hatched polygon.

4.3.2. Nitrate and suspended fine particulate organic matter

We sampled water in the burned and reference region to examine spatiotemporal trends in several key basal food web resources. Specifically, we analyzed water for concentrations of nitrate (μM NO_3-) every month from September 2009 to December 2010, and suspended FPOM ($cg \cdot L^{-1}$) from September 2009 to May 2010. In addition to monthly samples, water samples were collected before, during, and after rainstorms to capture changes due to run-off. We note that there are other important basal food web resources such as nitrite and phosphorous, and organic carbon from course and fine

particulate matter in the benthos. However, time and resource restrictions limited our study focus to nitrate and suspended FPOM, both of which are likely to respond to perturbations driven by wildfire (Gresswell 1999, Verkaik et al. 2013a).

For nitrate analysis, we collected duplicate 150 ml water samples on a monthly schedule from September 2009 through October 2010. Samples were collected at depths of approximately 30 cm from the surface in triple rinsed high-density polyethylene (HDP) jars and stored on ice for transportation from the field. In the laboratory, particulate matter was removed by pumping water through 47mm GF/F filters (Whatman; pore size = 0.7 μm) into a 500 ml Erlenmeyer flask that was triple rinsed between samples with deionized water. We transferred filtered water samples to acid-rinsed HDP jars and stored them at -20°C until processing. Samples were analyzed for nitrate using a QuickChem 8000 Flow Injection analyzer (Lachat Instruments).

We measured suspended FPOM ($cg \cdot L^{-1}$) in the burned and reference region on a monthly schedule from September 2009 to May 2010. Water samples (1-3 L) were collected in the same locations that water samples were taken for nitrate analysis. We filtered a known volume of water through burned (550°C) and pre-weighed 47mm GF/F filters (Whatman; pore size = 0.7 μm). We then dried the filters at 50°C, weighed them to the nearest microgram, and burned them a second time at 550°C to incinerate organic material. Burned samples were reweighed and organic mass was estimated as the difference between dried and ash-free dry mass. Data were log transformed (+1) prior to analysis to meet the assumptions of normality. Seasonal and regional differences in nitrate concentration and suspended FPOM were examined with a two-way analysis of variance (ANOVA) in program R (R Development Core Team 2013).

4.3.3. Terrestrial and aquatic invertebrate abundance and biomass

We collected terrestrial and aquatic macroinvertebrates over the first post-fire year in the burned and reference region to estimate seasonal changes in relative prey abundance and composition. Macroinvertebrate samples were collected at the pool level in each region in December 2009, February, May, July, and October 2010. We passively collected terrestrial macroinvertebrates infall using pan traps set streamside of each

pool. Each trap was made from clear 27 L storage containers (Sterilite corp.) with an approximate surface area of 0.24 m^2. Each trap was filled to approximately 25% with stream water and 2-3 drops of unscented biodegradable soap to break surface tension. Within each region, all traps were deployed and collected after 5 days of sampling on average (± 3 days SD). The contents of each trap were strained through a 500 µm mesh lined funnel into individual 90 ml polypropylene specimen containers (Starplex Scientific Inc.).

We collected aquatic macroinvertebrates at the head and tail of each pool using a Surber stream bottom sampler with a 0.31 m x 0.31 m quadrate frame and 500 µm mesh net. Substrate within the Surber quadrate was scrubbed by hand to dislodge macroinvertebrates. Once cleared of larger substrate, we thoroughly agitated bottom sediment within the Surber quadrate to stir-up the remaining benthic macroinvertebrates into the drift and Surber net. The net contents were spread onto a sorting tray, where we cleaned and removed small rocks and debris prior to straining the sample through a 500 µm mesh sieve and transferring it to individual 90 ml polypropylene specimen containers.

Terrestrial and aquatic invertebrate samples were stored in 75% ethanol prior to identification and processing. We counted all invertebrates in each sample and identified taxa to order, and individuals from *Arachnida* and *Annelida* to family. We measured the length of up to 20 individuals from each taxonomic group within a sample. Using the averaged length-mass relationships for taxa reported in Benke et al. (1999), length measurements were converted to estimates of dry mass; unmeasured individuals were assigned a pool/taxa-specific mean dry mass. We calculated daily terrestrial invertebrate biomass infall flux by dividing the estimated dry mass by the incubation time of each sample. Limited time and resources precluded the identification of invertebrates to a finer taxonomic resolution and measurement of more than 20 individuals of each taxonomic group within a sample. As such, our analyses related to differences in invertebrate abundance, biomass, and community composition in the burned and reference region are relatively course and should be interpreted with caution. Data were log transformed (+1) prior to analysis to meet the assumptions of normality. We analyzed seasonal and regional differences in invertebrate abundance with a two-way analysis of

variance (ANOVA). We compared the relative homogeneity of invertebrate communities between the burned and reference region based on Shannon beta diversity (Jost 2007) using the "vegetarian" package in program R (R Development Core Team 2013). In this analysis we estimated a scalar between zero and one of community similarity, where zero indicates that the invertebrate communities are distinct and one indicates that the communities are identical. We used bootstrapping to estimate uncertainty around relative community homogeneity calculations.

4.3.4. Stable isotope analysis

Stable isotope analyses have enabled ecologists to infer potential food web interactions within and between ecosystems (Martínez del Rio et al. 2009). For example, Bayesian stable isotope mixing models quantitatively assign the proportional contributions of several sources to consumers within a food web (Phillips and Gregg 2003, Moore and Semmens 2008). This class of stable isotope models has been used to examine food web interactions within and between terrestrial and aquatic ecosystems (e.g., Sanzone et al. 2003, Paetzold et al. 2005, Moore et al. 2012). However, mixing models partly depend on temporally accurate estimates of stable isotope signatures for sources and consumers (Woodland et al. 2012b, 2012a).

In this study, we used $\delta^{13}C$ and $\delta^{15}N$ stable isotopes to examine changes in isotopic signatures of terrestrial macroinvertebrates and aquatic macroinvertebrates in the burned and reference regions over time. Isotope samples of terrestrial macroinvertebrates were collected in September 2009, July and October 2010. Isotope samples of aquatic macroinvertebrates were collected in September 2009, March, July, and September 2010. We note that the collection of isotope samples immediately after the wildfire in 2009 was spatially and temporally restricted relative to later collection dates due to safety concerns in the burned region. In particular, the collection of terrestrial macroinvertebrate stable isotopes in September 2009 was limited to one sample within each the burned and reference region. These data were used as potential prey sources in a stable isotope mixing model for *O. mykiss* (see below). All samples used for isotope analysis were dried at 50°C prior to analysis. We haphazardly removed a subsample of terrestrial and aquatic macroinvertebrates from pan traps and Surber

samples taken over the first post-fire year from several pools in each region for isotope analysis. Aquatic invertebrates from the July and September 2010 samples were identified to the family level and analyzed at these taxonomic groupings. In addition, we partitioned invertebrates from the July and September 2010 samples into functional feeding groups based on their taxonomic grouping (Barbour et al. 1999, Tomanova et al. 2006, Thorp and Covich 2009) and examined changes in isotope signatures between the summer and fall one year after the fire. For samples from other months, small invertebrates were aggregated to meet a target sample weight of approximately 1 mg dry mass, and larger invertebrates were homogenized with a mortar and pestle, with ~1 mg withdrawn for isotope analysis.

We used $\delta^{13}C$ and $\delta^{15}N$ stable isotopes to examine changes in isotopic signatures of *O. mykiss* in the burned and reference regions over time. *O. mykiss* fin tissue samples were collected in September and October 2009 (after the August 12, 2009 wildfire), and in March, June, July, and September 2010. A small piece of fin tissue was removed from the upper lobe of caudal fins from *O. mykiss* greater than 35 mm fork length (FL). Fin tissue was stored in polyethylene vials and dried at 50°C prior to analysis. Samples that weighed less than 1mg (dry mass) were used whole; otherwise we took a subsample from each sample for analysis. These data illuminate shifts in isotope signatures of *O. mykiss* over time and also provide the isotopic signature of consumers for a Bayesian mixing model analysis.

Baseline pre-wildfire *O. mykiss* tissue samples were collected in fall 2006 in both the burned and reference regions. Tissue samples were taken from the left side above the lateral line and below the dorsal fin. Samples were freeze dried for 24 hours to rid samples of excess water and lipids extracted a Dionex ASE-200 Accelerated Solvent Extractor; lipids sequester lighter isotopes of carbon that potentially bias the isotopic signatures towards lower trophic levels. Samples were homogenized with a mortar and pestle and approximately 70 mg was used for isotope analysis. Baseline samples were analyzed at the University of California, Santa Cruz for $\delta^{13}C$ and $\delta^{15}N$ using a using Finnigan Delta Plus XT and 1108 Elemental Analyzer in which the eluted gas was analyzed to determine the isotopic ratios.

Post-fire invertebrate and *O. mykiss* tissue samples were sent to the Stable Isotope Facility at the University of California Davis, USA, where they were analyzed for $\delta^{13}C$ and $\delta^{15}N$ using a using a PDZ Europa ANCA-GSL elemental analyzer interfaced to a PDZ Europa 20-20 isotope ratio mass spectrometer (Sercon Ltd., Cheshire, UK). Samples were compared to at least two international standards including nylon, bovine liver, and USGS-41 glutamic acid and air to account for calibration, machine drift, and quality control. The facility reports measurement error of this analysis as having a long-term standard deviation of 0.2 ‰ $\delta^{13}C$ and 0.3 ‰ $\delta^{15}N$. Tissue with higher per mil of the heavier isotopes is considered enriched, while lower per mil is depleted. Invertebrate samples were stored in 75% ethanol, which is known to cause isotope fixation, so we subtracted a constant correction factor of 0.39 ‰ from $\delta^{15}N$ and 1.18 ‰ from $\delta^{13}C$ since we did not have information of C: N values prior to fixation (Ventura and Jeppesen 2009).

Isotope ratios are expressed in parts per thousand (0/00) from standard references, (Vienna Peedee belemnite for carbon39 and nitrogen from the atmosphere for nitrogen40) set at a value of 0 0/00 by the following convention delta notation (Eq 4.1):

$$\delta R = [(R_{sample})/(R_{standard}) - 1]\times 10^3$$

Where *R* is $^{13}C/^{12}C$ or $^{15}N/^{14}N$. R_{sample} is the ratio of heavy to light isotope in the sample and $R_{standard}$ is the ratio for the standard.

We used a two-way ANOVA to compare mean changes in seasonal $\delta^{13}C$ and $\delta^{15}N$ signatures of terrestrial and aquatic invertebrates among regions. Data were log transformed (+1) prior to analysis to meet the assumptions of normality. We used Tukey's Honestly Significant Difference (HSD) where multiple comparisons were made.

We used circular statistics to analyze directional changes in the stable isotope signatures of aquatic invertebrate functional feeding groups and *O. mykiss* between the summer and fall, 2010 (Zar 1999, Schmidt et al. 2007). This class of statistical analyses is generally used to examine circular data distributions such as compass directions or times of day. Here we calculated the change in mean $\delta^{15}N$ and $\delta^{13}C$ between the summer and fall 2010 of aquatic invertebrate functional feeding groups within each

region, and *O. mykiss* within each pool. The null expectation is that the direction of change is statistically uniform (i.e., all directions are equally probable) compared to the alternate hypothesis that change occurred in a consistent direction. We centered the summer isotope values on 0 and differenced the fall values to calculate circular vectors of change where $\delta^{15}N$ (y axis) and $\delta^{13}C$ (x axis) were either enriched or depleted from an origin of 0. We analyzed these data with Rayleigh's test, which examines the distribution of angular vectors (Zar 1999). With this test statistic we ask if the mean angle of isotopic change is homogeneous (Zar 1999). A significant result implies that the distribution of isotopic change between summer and fall is non-random among functional feeding groups or *O. mykiss* within different pools.

We used a Bayesian isotope mixing model (MixSIAR v1.2; Moore and Semmens 2008, Stock and Semmens 2013) to estimate the seasonal contribution of terrestrial and aquatic C and N sources to *O. mykiss* inferred diets and to estimate variation in inferred diet within each region and season at the individual and pool levels. In these analyses we assume there is no lag in time between the isotope signature of sources within time periods and isotope assimilation by consumers. We focused on isotope samples taken in the fall 2009 (September, October) following the wildfire and summer (June, July) and fall 2010 (September, October), one year after the fire. We also analyzed *O. mykiss* isotope samples from the burned region that were collected for an unrelated project in fall 2006. These pre-fire data provide insight into the contribution of terrestrial and aquatic C and N sources to *O. mykiss* inferred diets prior to the disturbance.

Source and consumer isotope samples were paired by region and time period for Bayesian mixing models when possible. We used aquatic and terrestrial macroinvertebrates and small *O. mykiss* (< 65 mm FL) as possible sources and considered all *O. mykiss* as consumers. We note that signal crayfish (*Pasifastacus leniusculus*) and Pacific giant salamanders (*Dicamptodontidae* spp.) were found in *O. mykiss* diet contents during this study (Beakes et al. 2014; M. Beakes, *unpublished data*), and that crayfish and giant salamanders have $\delta^{13}C$ and $\delta^{15}N$ isotopic signatures similar to the small *O. mykiss* in this study (Bondar et al. 2005, Sepulveda et al. 2012). However, we did not have the stable isotope data for these species and therefore cannot distinguish them from *O. mykiss* as potential sources in mixing model analysis. We

assumed a $\delta^{13}C$ trophic discrimination factor for *O. mykiss* of 1.9 ± 1.02 ‰ (average ± SD) and a $\delta^{15}N$ discrimination factor of 3.2 ± 0.4 ‰ (McCutchan et al. 2003). Pre-fire source isotope data were not available from fall 2006. As such, for pre-fire mixing model analysis we used the mean and SD of sources from the post-fire fall (2009) reference region samples. Due to limited data in fall 2009 for both terrestrial sources and prey fish sources (*O. mykiss* < 65 mm FL), we used SD of $\delta^{13}C$ and $\delta^{15}N$ from the 2010 fall reference region samples. For fall 2009 mixing model analysis, we paired source and consumer data within each region, again using SD values of terrestrial and fish prey $\delta^{13}C$ and $\delta^{15}N$ from the fall 2010 samples. For summer and fall 2010 mixing model analysis, we paired source and consumer data within the burned and reference regions.

We used a hierarchical model structure including both residual and process error terms, and coded individual fish and pools as random variables (Semmens et al. 2009, Parnell et al. 2010, 2013). MCMC sampling was conducted for each model using three 75,000 iteration chains in JAGS via R (R Development Core Team 2013) with a burn-in period of 25,000 iterations, retaining every 25th sample, to generate a posterior density composed of 6,000 draws. We ran Gelman-Rubin, Heidelberger-Welch, and Geweke diagnostics to ensure the MCMC chains converged on a posterior distribution for model parameters. We report the median parameter estimate with the credible interval. The credible interval represents the region of the posterior distribution that contains a specified percentage of the probability of the distribution (e.g., 75%) that is bounded by values of equal probability (Bolker 2008).

4.4. Results

4.4.1. Nitrate and suspended fine particulate organic matter

There were significantly higher levels of nitrate (μM NO_3-) in the burned region (ANOVA; $F_{1,46}$ = 7.65, P < 0.01; Figure 4.2A). The median concentration of nitrate was 244% higher in the burned region compared to the reference region over the first post-fire year. The median concentration of FPOM was 44% higher in the burned region relative to the reference region. However the difference in FPOM ($cg \cdot L^{-1}$) between the burned and

reference region was not significant (ANOVA; $F_{1,23} = 0.54$, $P > 0.05$; Figure. 4.2B). The larges differences in nitrate (µM NO_3-) and FPOM ($cg \cdot L^{-1}$) between the burned and reference region were measured in the samples collected during and after rainstorms, and presumably due to increased runoff.

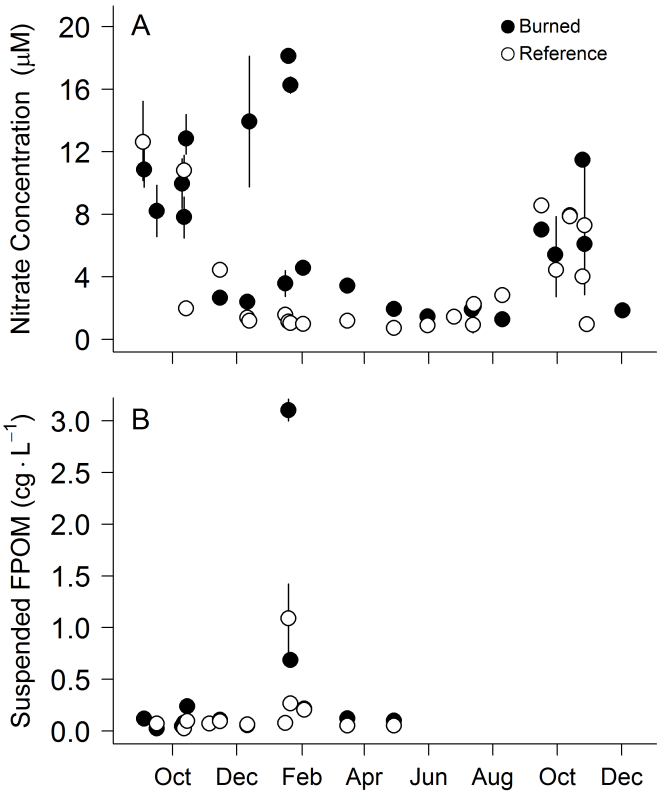

Figure 4.2. Change in nitrate concentration (A), and suspended fine particulate organic matter concentration (FPOM; B) over time following the 2009 Lockheed wildfire. Error bars encompass the range of observed values.

4.4.2. Terrestrial and aquatic invertebrate abundance and biomass

Terrestrial infall varied by season (Figure 4.3A), but the invertebrate community compositions were similar among seasons, burned and reference regions (Table 4.1). Within each region, the relative community homogeneity between sampling months was 0.85 (± 0.05 95% CI) in the burned region, and 0.71 (± 0.04 95% CI) in the reference region. The relative community homogeneity between regions was 0.91 (± 0.02 95%CI)

with all monthly samples combined. Over 91% of the terrestrial invertebrate abundance was composed of the *Arachnida* class, and *Coleoptera*, *Collembola*, *Diptera*, *Homoptera*, *Hymenoptera*, *Lepidoptera*, *Megaloptera*, and *Psocoptera* orders (Table 4.1). The overall flux of terrestrial biomass infall between the burned and reference regions was not significantly different (ANOVA; $F_{1,76} = 0.27$, $P > 0.05$). As well, we did not observe significant differences between regions in terrestrial biomass infall flux within sampling months (Tukey HSD; $P > 0.05$). Terrestrial infall ($mg \cdot m^{-2} \cdot d^{-1}$) did vary significantly among seasons in both regions (ANOVA; $F_{4,76} = 8.37$, $P < 0.001$; Figure 4.3A), such that the terrestrial in-fall generally increased from winter to fall and was highest in October (Figure 4.3A). We also found a significant interaction between sampling month and region (ANOVA; $F_{4,76} = 0.69$, $P = 0.053$), indicating that the effect of season on terrestrial in-fall flux differed significantly between regions. This result was partly driven by relatively larger seasonal changes in terrestrial in-fall in the burned region compared to the reference region (Figure 4.3A).

Aquatic macroinvertebrate abundance varied by season (Figure 4.3B), but the invertebrate communities were relatively homogeneous between sampling months and between regions (Table 4.2). Within each region, the relative community homogeneity between sampling months was 0.88 (± 0.01 95% CI) in the burned region, and 0.85 (± 0.02 95% CI) in the reference region. The relative community homogeneity between regions was 0.92 (± 0.01 95%CI) with all monthly samples combined. Over 88% of aquatic invertebrate abundance was composed of *Diptera*, *Ephemeroptera*, *Plecoptera*, and *Trichoptera* orders. We did not observe a significant difference in aquatic invertebrate biomass between the burned and reference regions overall (ANOVA; $F_{1,176} = 2.85$, $P > 0.05$). As well, we did not observe significant differences between regions in aquatic invertebrate biomass within sampling months (Tukey HSD; $P > 0.05$). Similar to terrestrial infall flux, we found a significant seasonal difference in aquatic invertebrate biomass (ANOVA; $F_{4,176} = 3.21$, $P < 0.05$; Figure 3B), such that aquatic invertebrate biomass was higher in the summer and fall (i.e., June and Oct) compared to the winter and spring (i.e., Dec, Feb, and May). The seasonal patterns in aquatic invertebrate biomass did not significantly differ between regions (ANOVA; interaction $F_{4,176} = 1.42$, $P > 0.05$).

Table 4.1: Summary table of dominant terrestrial invertebrates reported as $N \cdot m^{-2} \cdot d^{-1}$ at the pool level (mean ± SD) during each sampling event in the burned and reference region. Note: We mark samples with an * where the number of individuals collected was insufficient for calculating pool level variance (SD).

Taxa	2009		2010		
Region	December	February	May	July	October
Arachnida					
Burned	1.2 ± *	0.6 ± 0.2	2.0 ± 1.1	1.8 ± 0.7	2.2 ± 1.3
Reference	2.6 ± 3.3	1.8 ± 1.5	2.7 ± 1.5	2.8 ± 1.1	6.8 ± 9.9
Coleoptera					
Burned	1.0 ± 0.3	0.9 ± 0.6	7.3 ± 3.3	5.5 ± 4.1	7.0 ± 5.2
Reference	1.4 ± 0.6	1.5 ± 1.5	7.9 ± 4.9	3.4 ± 1.8	8.3 ± 5.2
Collembola					
Burned	0.6 ± *	0.8 ± 0.5	5.2 ± 3.3	3.2 ± 2.1	6.4 ± 3.1
Reference	1.2 ± 0.5	1.1 ± 0.5	2.1 ± 1.1	2.1 ± 0.8	2.8 ± 1.2
Diptera					
Burned	0.7 ± 0.3	0.5 ± 0.2	5.2 ± 1.8	5.0 ± 2.5	3.6 ± 2.2
Reference	2.1 ± 1.6	1.3 ± 1.2	4.8 ± 2.7	3.9 ± 2.0	8.3 ± 6.2
Homoptera					
Burned	0.6 ± *	0.6 ± 0.2	4.2 ± 4.6	4.4 ± 2.7	2.8 ± 1.7
Reference	0.9 ± 0.4	0.4 ± *	3.1 ± 2.0	3.0 ± 1.8	5.2 ± 4.0
Hymenoptera					
Burned	0.6 ± *	0.6 ± 0.2	2.5 ± 0.6	3.2 ± 3.0	4.9 ± 6.7
Reference	…	0.4 ± *	1.0 ± *	…	3.1 ± 1.7
Lepidoptera					
Burned	0.6 ± *	0.6 ± 0.2	4.4 ± 1.8	3.9 ± 2.5	3.5 ± 2.3
Reference	1.3 ± 0.5	0.9 ± 1.1	4.7 ± 3.1	1.4 ± *	6.8 ± 5.3
Megaloptera					
Burned	0.7 ± 0.3	0.5 ± 0.2	4.7 ± 1.7	3.3 ± 2.3	3.3 ± 2.3
Reference	1.4 ± 0.6	1.2 ± 1.4	4.5 ± 2.7	1.4 ± *	7.6 ± 5.4
Psocoptera					
Burned	1.8 ± 1.1	0.8 ± 0.7	16.1 ± 15.0	10.3 ± 7.0	10.4 ± 5.7
Reference	0.6 ± *	0.4 ± *	1.6 ± 0.6	2.3 ± 0.8	31.1 ± 18.7

Table 4.2: Summary table of dominant aquatic invertebrates reported as $N \cdot m^{-2}$ at the pool level (mean ± SD) during each sampling event in the burned and reference region.

Taxa	2009	2010			
Region	December	February	May	July	October
Diptera					
Burned	63.4 ± 115.5	101.6 ± 306.3	97.6 ± 116.8	90.6 ± 97.1	34.8 ± 26.2
Reference	44.9 ± 40.0	305.9 ± 841.2	49.2 ± 79.1	33.1 ± 19.4	56.3 ± 93.9
Chironomidae					
Burned	234.7 ± 541.6	52.2 ± 40.2	149.6 ± 185.5	194.3 ± 219.2	205.0 ± 268.6
Reference	176.1 ± 183.0	71.3 ± 58.1	89.1 ± 108.6	193.8 ± 298.5	491.8 ± 563.3
Ephemeroptera					
Burned	138.8 ± 143.8	128.0 ± 110.8	242.7 ± 170.1	381.4 ± 321.4	606.0 ± 877.7
Reference	240.7 ± 196.2	260.4 ± 213.8	255.0 ± 296.3	230.1 ± 222.9	875.9 ± 876.8
Plecoptera					
Burned	95.7 ± 89.8	21.5 ± 13.4	61.9 ± 72.7	234.9 ± 252.2	144.5 ± 205.1
Reference	104.6 ± 71.1	74.4 ± 56.4	55.8 ± 67.0	86.1 ± 85.0	40.0 ± 41.0
Trichoptera					
Burned	64.6 ± 66.5	46.9 ± 43.4	65.7 ± 79.7	74.8 ± 62.4	135.4 ± 180.9
Reference	92.4 ± 66.4	65.3 ± 77.1	118.4 ± 72.6	367.6 ± 556.4	329.4 ± 430.8

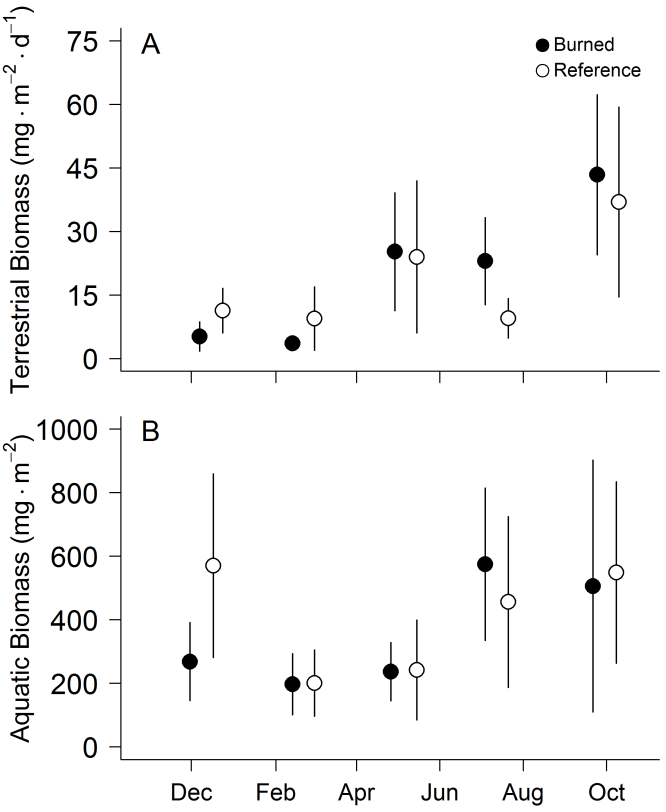

Figure 4.3. Change in the rate of terrestrial macroinvertebrate (A) in-fall (mg·m^{-2}·d^{-1}), and aquatic macroinvertebrate (B) density (mg·m^{-2}) measured following the 2009 Lockheed wildfire from December 2009 to October 2010. Error bars are approximated 95% CI of the mean (i.e., ± 1.96 SE).

4.4.3. Stable isotope analysis

The mean $\delta^{13}C$ and $\delta^{15}N$ signatures of terrestrial macroinvertebrates in the burned (Figure. 4.4A) and reference regions (Figure. 4.4B) were similar over the first post-fire year. We focus on the transition between summer and fall, 2010 due to limited sampling in fall, 2009 (aggregate sample, N = 1 per region). We found that terrestrial invertebrate $\delta^{13}C$ did not vary significantly by season (Two-way ANOVA; $F_{1,77} = 0.02$, $P < 0.05$), region (ANOVA; $F_{1,77} = 0.16$, $P < 0.05$), or by season within region (ANOVA; interaction $F_{1,77} = 0.63$, $P < 0.05$). Similarly, terrestrial invertebrate $\delta^{15}N$ did not significantly vary by season (ANOVA; $F_{1,77} = 2.79$, $P < 0.05$), region (ANOVA; $F_{1,77} = 0.05$, $P < 0.05$), or by season among regions (ANOVA; interaction $F_{1,77} = 1.30$, $P < 0.05$).

In contrast to terrestrial invertebrates, we found $\delta^{13}C$ of aquatic macroinvertebrates changed significantly among seasons (ANOVA; $F_{3,223} = 12.87$, $P < 0.001$), and between regions (ANOVA; interaction $F_{1,223} = 32.77$, $P < 0.001$). However, the seasonal differences in $\delta^{13}C$ did not significantly differ across regions (ANOVA; $F_{3,223} = 2.50$, $P > 0.05$). We observed similar patterns in benthic invertebrate $\delta^{15}N$ signatures among seasons (ANOVA; $F_{3,223} = 19.26$, $P < 0.001$), and regions (ANOVA; $F_{1,223} = 23.87$, $P < 0.001$). However, we also observed a significant season by region interaction (ANOVA; $F_{3,223} = 3.10$, $P < 0.05$) indicating that the $\delta^{15}N$ of aquatic invertebrates in different regions had different seasonal patterns (Figure. 4.4). We observed depleted $\delta^{13}C$ and $\delta^{15}N$ aquatic invertebrate signatures in the burned region compared to the reference region in fall 2009. Both burned region $\delta^{13}C$ and $\delta^{15}N$ were enriched the following spring, and again by summer 2010 before depletion from summer to fall 2010 (Figure. 4.4A). In contrast, we observed a cyclical seasonal pattern of isotopic depletion and enrichment that generally rotated around a mean $\delta^{13}C$ (-27.49 ± 1.65 ‰ SD) and $\delta^{15}N$ (2.10 ± 1.98 ‰ SD) in the reference region (Figure. 4.4B).

O. mykiss $\delta^{13}C$ and $\delta^{15}N$ displayed a cyclical seasonal pattern of depletion and enrichment in both the burned (Figure. 4.4A) and reference regions (Figure. 4.4B). On average however, *O. mykiss* in the burned region were significantly enriched in both $\delta^{13}C$ (ANOVA; $F_{1,219} = 5.06$, $P < 0.01$), and $\delta^{15}N$ (ANOVA; $F_{1,219} = 41.98$, $P < 0.001$). We found a significant seasonal difference in both $\delta^{13}C$ (ANOVA; $F_{3,219} = 14.80$, $P < 0.001$), and $\delta^{15}N$ (ANOVA; $F_{1,219} = 4.33$, $P < 0.01$) among regions. Generally, *O. mykiss* $\delta^{13}C$ was depleted in the summer relative to the fall and spring, whereas $\delta^{15}N$ was depleted in the spring relative to the summer and fall. The seasonal $\delta^{13}C$ shift between spring and summer, and summer and fall, was more pronounced in the reference region (Figure. 4.4), which likely drove the significant interaction between season and region (ANOVA; $F_{1,219} = 5.06$, $P < 0.01$).

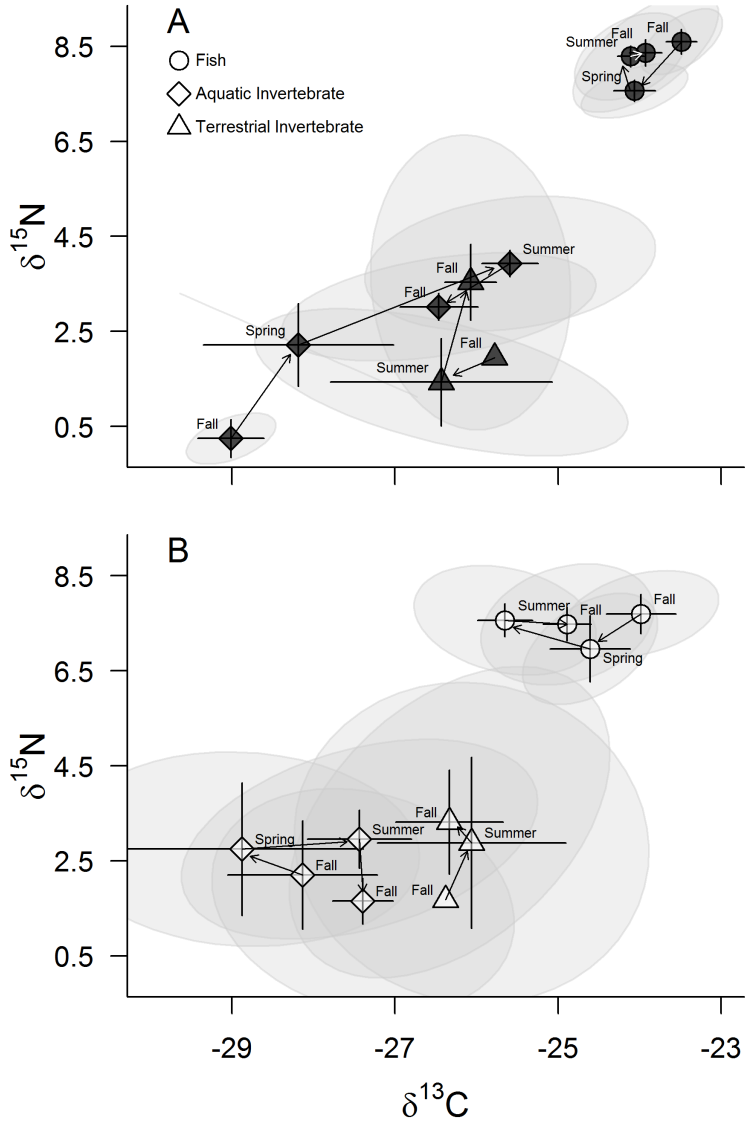

Figure 4.4. Plotted mean $\delta^{13}C$ and $\delta^{15}N$ values for terrestrial macroinvertebrates (triangles) collected in 2009 fall (September; N = 2), 2010 summer (July; N = 16), and fall (October; N = 65), aquatic macroinvertebrates (diamond) collected in 2009 fall (September; N = 7), 2010 spring (March; N = 7), summer (July; N = 105), and fall (September; N = 113), and O. mykiss (circles) collected in 2009 fall (September, October; N = 32), 2010 spring (March; N = 24), summer (June, July; N = 79), and fall (September; N = 83). The burned region (A) is represented with dark grey symbols and the reference region (B) by open symbols. Error bars on the x and y axis represent approximated 95% CI of the mean (i.e., ± 1.96 SE), and the ellipses encompass the 50% CI of the data range.

The shift in $\delta^{13}C$ and $\delta^{15}N$ values between summer and fall (2010) for aquatic invertebrate in the burned and reference region was different across functional feeding groups (Figure. 4.5A). Specifically, the shift in $\delta^{13}C$ and $\delta^{15}N$ of shredders, scrapers, collector-gatherers, collector-filterers, and predators was directionally cohesive (Rayleigh; Rbar = 0.93, $P < 0.01$), where $\delta^{13}C$ and $\delta^{15}N$ across functional feeding groups were depleted between the summer and fall in the burned region. In contrast, we found that the isotopic change between summer and fall of functional feeding groups in the reference region were statistically uniform (Rayleigh; Rbar = 0.50, $P > 0.05$), where $\delta^{15}N$ was depleted for most functional feeding groups in the reference region but $\delta^{13}C$ was depleted for some and enriched for others (Figure. 4.5A). We found that the summer-fall isotopic shift was similar for predators and collector-gatherers in both regions. The most notable regional difference was observed in scrapers and shredders (Figure. 4.5A).

Shifts in *O. mykiss* $\delta^{13}C$ and $\delta^{15}N$ between summer and fall, 2010 were statistically dissimilar at the pool level in the burned and reference regions (Figure. 4.5B). We observed unpredictable variation in isotopic change of *O. mykiss* in the burned region (Rayleigh; Rbar = 0.34, $P > 0.05$; Figure. 4.5B). In the reference region however, we observed a statistically cohesive shift in $\delta^{13}C$ and $\delta^{15}N$ between summer and fall 2010 (Rayleigh; Rbar = 0.84, $P < 0.01$; Figure. 4.5B). The isotope signatures of *O. mykiss* in the reference region were generally enriched in $\delta^{13}C$ between the summer and fall 2010 but both enriched and depleted $\delta^{15}N$ signatures in the fall (Figure. 4.5B).

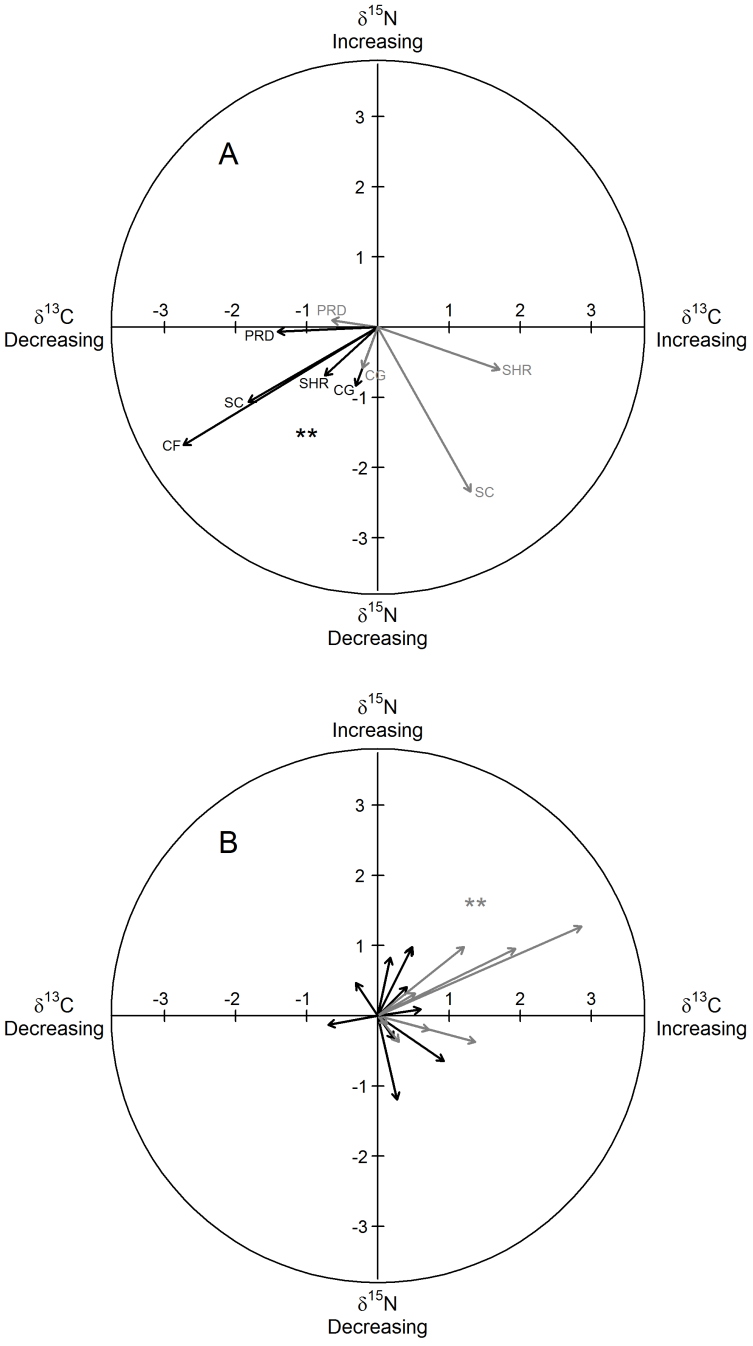

Figure 4.5. Polar plots for aquatic invertebrate functional feeding groups (A) and O. mykiss (B) in the burned (black vectors) and reference (light grey vectors). Changes in the isotope signatures between summer and fall for invertebrate functional feeding groups are at the region level compared to O. mykiss, which were calculated at the pool level.

Bayesian isotope mixing model analyses illuminated potential differences across the burned and reference regions in both the proportional contribution of prey sources, as well as variation in inferred diet at the individual and pool level (Figure. 4.6). In the burned region, the contribution of each prey source to inferred *O. mykiss* diets was relatively balanced pre-fire (fall 2006) compared to post-fire estimates (Figure. 4.6A). In the reference region, the pre-fire consumer isotope signatures (fall 2006) resided outside of the source mixing space, so we did not make a direct regional comparison for this time period. Across all sampling periods (i.e., fall 2006, fall 2009, summer and fall 2010), we found that inferred *O. mykiss* diets mostly composed of prey fish in both regions (Figure. 4.6A, B). In the burned region, the estimated contribution of prey fish to inferred *O. mykiss* diets increased by 77% after the fire (Figure. 4.6A). The estimated contribution of invertebrate prey sources to inferred O. mykiss diets increased in the summer 2010 in both regions but was still dominated by prey fish (Figure. 4.6A, B).

We observed different patterns of individual and pool level variation in inferred *O. mykiss* diets in the burned and reference regions over time (Figure. 4.6C, D). Across all sampling periods, individual level variation in inferred diets was similar between regions (Figure. 4.6C, D). Within sampling periods however, pool level variation in inferred diets was lower in the burned region compared to the reference until fall 2010 (Figure. 4.6C). In fall 2010 pool level variation in inferred diets increased considerably in the burned region relative to earlier estimates in both regions (Figure 4.6C). However, we note that these parameters had substantial variability associated with their estimation.

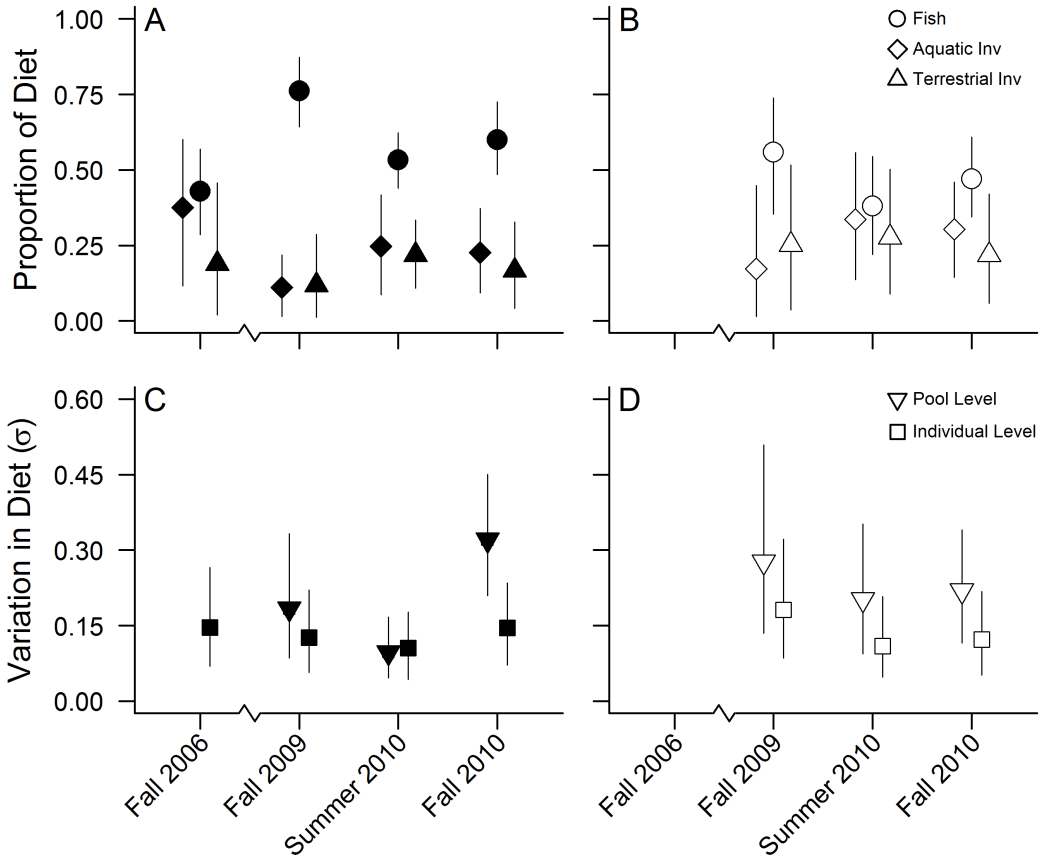

Figure 4.6. Plotted median estimates for the estimated proportion of terrestrial (triangle), aquatic (diamond) invertebrate, and fish (circle) to O. mykiss diets (A, B). Also plotted are median estimates of individual (inverted triangle) and pool level (square) variation in diet (C, D). The burned region (A, C) is depicted in black symbols and the reference region in open symbols (B, D). Error bars represent the 75% credible intervals of the posterior density. Fall 2006 samples were collected prior to the 2009 Lockheed wildfire.

4.5. Discussion

In a central California coastal stream we found evidence over the first year post-fire that wildfire can increase availability of basal food web resources, alter seasonal patterns of isotope signatures for aquatic invertebrates and fish, and possibly drive changes in the composition and spatial variation of inferred *O. mykiss* diets. After the wildfire, concentrations of nitrate and FPOM were elevated in the burned region relative to the

reference region throughout the year. In the burned region, we observed disparate seasonal dynamics of aquatic invertebrate and *O. mykiss* stable isotope signatures from those we observed in the reference region. The departure from the expected (i.e., reference region) summer isotope signature in the burned region appeared to be partly driven by specific aquatic invertebrate functional feeding groups. Whereas the departure from the expected summer isotope signature of *O. mykiss* in the burned region appeared to be driven by differences in the mean *O. mykiss* isotope signature across pools in the burned region compared to pools in the reference region. Although we found that seasonal terrestrial and aquatic prey abundances were comparable among the burned and reference regions, we found that prey fish had a greater contribution to *O. mykiss* inferred diets in the burned region relative to the reference region and pre-fire data.

Previous studies have shown that fire can induce nutrient pulses in burned regions through pyrolysis of organic material, increased mineralization, leaching, erosion and run-off in recently denuded landscapes (Minshall et al. 1997, Gresswell 1999, Wan et al. 2001, Verkaik et al. 2013a). Some of these processes also drive increases in FPOM concentration and dissolved organic carbon in burned watersheds (Gresswell 1999, Verkaik et al. 2013a, Ramchunder et al. 2013). In both cases, the delivery of these materials from the burned landscape to the stream was apparently influenced by local hydrology. We observed similar patterns in our study system, where the highest concentrations of nitrogen and FPOM were measured during winter storms, when runoff and water discharged were elevated. As such, it appears that wildfire is associated with pulses of increased terrestrial nutrient and organic material influx to aquatic systems, but their delivery is tightly coupled with seasonal climate and hydrology. Except for this storm period, FPOM showed little difference between the burned and reference regions.

Terrestrial and aquatic macroinvertebrate abundance and community composition in the burned and reference regions were similar over the first post-fire year. As well, we found that terrestrial and aquatic macroinvertebrate abundance in the burned and reference regions were similar to other nearby watersheds on the California coast (Rundio and Lindley 2008). Perhaps it should not be surprising that there were no large changes in invertebrate biomass associated with the Lockheed wildfire, since most of the burned region pools fell under the category of ‘moderate’ burn severity (Beakes et al. 2014), and

the effects of wildfire on invertebrate abundance are largely mediated by fire severity (Minshall 2003, Malison and Baxter 2010a, 2010b, Jackson et al. 2012). Previous research has shown that high severity wildfires can reduce the input of terrestrial invertebrates to streams (e.g., Jackson et al. 2012). Specifically, Jackson et al. (2012) found that terrestrial arthropod inputs to streams were more than two-fold higher in unburned stream reaches compared to reaches exposed to high-severity burns. However, they also found that low-severity burned reaches had reduced terrestrial arthropod inputs. The description from Jackson et al. (2012) of low-severity burns was similar to the burn severity we observed in our study system. We suspect that changes in the riparian and canopy vegetation structure associated with the Lockheed wildfire were insufficient to drive measurable changes in the terrestrial invertebrate inputs to streams. Relative to terrestrial invertebrates, aquatic invertebrates are generally considered robust to wildfire related disturbances (Gresswell 1999) particularly when the riparian canopy remains intact (Verkaik et al. 2013a). For example, in a review of stream benthic macroinvertebrate responses to wildfire Minshall (2003) reported that the direct effects of fire are "generally minor or indiscernible". As such, the similarity in aquatic invertebrate abundance among burned and reference reaches in this study is consistent with previous research. In total, the most notable changes in the availability of prey sources were observed on a seasonal basis (Figure. 4.3), where the abundance of both terrestrial and aquatic sources increased in the summer and fall relative to the winter and spring. As well, at the taxonomic resolution identified in this study the relative community homogeneity of both terrestrial and aquatic macroinvertebrates was more similar between regions than across seasons within either region. These results corroborate pervious research (Verkaik et al. 2013b) and reinforce the conclusion that the availability of invertebrate terrestrial and aquatic prey to drift-feeding fish such as *O. mykiss*, and the invertebrate community composition are principally governed by seasonal cycles. Thus, the short-term (1yr) effects of a moderate severity wildfire on terrestrial and aquatic macroinvertebrates abundance and community composition are relatively minor by comparison.

We observed strong seasonal patterns of stable isotopes in both benthic invertebrates and *O. mykiss* that appeared to be mediated by the wildfire. Seasonal cycles of $\delta^{13}C$ and $\delta^{15}N$ enrichment and depletion have been observed in multiple trophic positions in

streams (Woodland et al. 2012b, 2012a). There are a number of biotic and abiotic factors (e.g., diet, growth, temperature, water flow, nutrients, dissolved CO_2) that likely influence the mechanisms underpinning seasonal variation of $\delta^{13}C$ and $\delta^{15}N$ (Finlay 2004, Woodland et al. 2012a). The scope of this study was not designed to explicitly test hypotheses related to these underlying mechanisms. Our results corroborate this previous work (e.g., Woodland et al. 2012a) and provide new evidence that illustrates how wildfire is associated with altered $\delta^{13}C$ and $\delta^{15}N$ enrichment and depletion cycles in aquatic macroinvertebrates and *O. mykiss*. For example, we observed aquatic invertebrate $\delta^{13}C$ and $\delta^{15}N$ enrichment over the first post-fire year in the burned relative to the reference region (Figure. 4.4A). Analysis of these in isotopic shifts with circular statistics revealed that specific functional feeding groups (i.e., shredders and scrapers) were driving deviations of the burned region from the reference region isotope baseline. Similarly, Spencer et al. (2003) found that shredders and scrapers had enriched $\delta^{15}N$ signatures after the Red Bench wildfire in Montana. Lab experiments have shown that wildfire can enrich $\delta^{13}C$ and $\delta^{15}N$ through volatilization of lighter isotopes (Saito et al. 2000), and Spencer et al. (2003) suggested that increased assimilation of $\delta^{15}N$ enriched FPOM as a possible explanation for their observed increases in aquatic invertebrate $\delta^{15}N$. We suspect that similar mechanisms are driving the patterns observed in our study system.

At the top of the food web, we found that the $\delta^{13}C$ and $\delta^{15}N$ signatures of *O. mykiss* tissue in the burned region followed different seasonal patterns than fish from the reference region. Specifically, *O. mykiss* $\delta^{13}C$ in the burned region was less enriched in the transition from summer to fall compared to the reference region. Examining shifts in *O. mykiss* isotopic signatures at the pool level during this time period in the burned region revealed random shifts in *O. mykiss* $\delta^{13}C$ and $\delta^{15}N$. This pattern could possibly be due to increased diet heterogeneity at the pool level, which is supported by Bayesian stable isotope analysis that showed an increase in inferred diet variation in the burned region during this time period (Figure. 4.6C). These results indicate that *O. mykiss* diets among burned pools were more heterogeneous relative to the reference region and earlier post-fire time periods, which may partly explain the observed isotopic shifts.

Bayesian stable isotope analysis provided evidence that the composition and variation of *O. mykiss* diets varied over time and between the burned and reference region. *O. mykiss* were generally acquiring more of their carbon and nitrogen from invertebrate sources in the spring/summer and apparently from fish sources in the fall. Interestingly, we observed the pool-level variation in diet decline in the burned region relative to the reference region after the wildfire indicating a post-fire homogenization of *O. mykiss* diets. At the end of the first year we estimated that both individual and pool-level variation in diet were similar between the two regions. This result suggests that variation in diet associated with the wildfire was relatively short-term lasting less than a year. Overall, our analysis showed that *O. mykiss* consumers in the reference region and particularly in the burned region acquired a large percentage of their carbon and nitrogen from prey fish, which has been observed in other California systems (Finlay et al. 2002). We note, however, that signal crayfish (*Pasifastacus leniusculus*) and Pacific giant salamanders (*Dicamptodontidae* spp.) were also found in diet contents during this study (Beakes et al. 2014; M. Beakes, *unpublished data*) and their isotopic signatures are similar to the prey fish sources used in this analysis (e.g., Bondar et al. 2005, Sepulveda et al. 2012). As well, predatory terrestrial and aquatic macroinvertebrates are likely to have enriched nitrogen isotope signatures relative to other functional feeding groups (Lancaster and Waldron 2001, Collier et al. 2002), and isotopic signatures similar to the prey fish sources used in this analysis in some cases. Thus, any of these sources may contribute to *O. mykiss* diets but we could not distinguish their inferred contribution from that of prey fish.

While our analysis focused on fish isotopes and inferred diet changes, it is possible that other mechanisms contributed to the patterns we observed. Several studies found that nutritional stress and slow growth influences $\delta^{15}N$ fractionation, leading to $\delta^{15}N$ enrichment (Adams and Sterner 2000, Vanderklift and Ponsard 2003). In Scott Creek and other California watersheds, summer and fall are characterized by low flow, low food availability, and poor growth conditions for *O. mykiss* (Hayes et al. 2008, Sogard et al. 2009, Grantham et al. 2012, Beakes et al. 2014). Collectively, these conditions may have contributed to the enriched $\delta^{15}N$ of *O. mykiss* observed in Scott Creek. Thus, diet, nutritional constraints, and seasonal differences in growth may be influencing the isotopic composition of *O. mykiss* in this study.

Our study highlights the importance of considering seasonality when interpreting the effects of wildfire in stream food webs of Mediterranean climates. For example, the delivery of increased nutrients and FPOM in the burned region accompanied rainstorms associated with the typical wet winters of Mediterranean climates (Gasith and Resh 1999). In contrast, we observed little difference between the burned and reference region in nutrient or FPOM concentrations during the dry season. In addition, the abundance of terrestrial and aquatic macroinvertebrates in both burned and reference regions were primarily governed by seasonal cycles. We observed strong seasonal $\delta^{13}C$ and $\delta^{15}N$ enrichment and depletion cycles in the stable isotope signatures of aquatic invertebrates and *O. mykiss*, which may be partly driven by the cyclical nature of Mediterranean climates. Our study system appears to be relatively robust to wildfire related disturbance like other streams perturbed by wildfire in Mediterranean climates (Verkaik et al. 2013a, 2013b). In total, this study provides evidence that fire can drive short-term changes stream food web components, but that the magnitude of this type of disturbance may be relatively minor compared to the underlying seasonal changes.

5. Natural and anthropogenic disturbance and warming water temperatures in the Fraser River[4]

5.1. Abstract

Freshwaters have been warming throughout North America over the last few decades. Some of the variation in warming water temperatures can be explained by warming air temperatures, but the contribution of natural disturbance and land-use to this warming trend remains uncertain. In this study, I fit a novel geostatistical model to water temperatures in the Fraser River, one of the largest free-flowing rivers in the Pacific Northwest, to analyze the effects of summer month, mean monthly air temperature (°C), and upstream area logged (km^2) or burned by wildfire (km^2) on water temperatures. This model accounted for over 38% of the variation of Fraser River water temperatures, and I found that summer month, mean monthly air temperature, and the total area logged up stream significantly affected downstream water temperatures. Wildfire did not significantly affect stream temperature possibly due to small scale of this landscape disturbance relative to logging. On average, increasing air temperatures by 1°C and logging 1000 km^2 of forest upstream increased downstream water temperatures by 0.36°C and 0.1°C respectively. However, the degree of air temperature change throughout the Fraser River basin over the last 40 years was relatively small compared to the change in upstream area logged. As such, the warming waters of the Fraser River appear to be driven comparably by warming air temperatures and logging. This study highlights the need for considering the accumulative effects of land-use and climate on warming waters within a large river network. More generally, this study improves our understanding of how natural and anthropogenic landscape disturbance and climate warming may act in concert to warm freshwaters.

[4] A version of this chapter is in preparation for publication with the following coauthors: Moore, J.W., Braun, D., Thompson, L., and Patterson, D.

5.2. Introduction

Climate warming is currently raising freshwater temperatures throughout North American and the Pacific Northwest (Eaton and Scheller 1996, Schindler 2001, Mantua et al. 2010). In rivers throughout the United States for example, annual water temperatures have increased by approximately 0.1–0.8°C per decade over the last several decades (Kaushal et al. 2010). Increasing water temperatures are starting to negatively impact freshwater biodiversity and the services it provides. For example, Bull Tout (*Salvelinus confluentus*) have lost up to 20% of their habitat in the Boise River basin, Idaho, as a result of warming water (Isaak et al. 2010). For migratory fishes, warming temperatures may drive large-scale mortality events in abnormally hot years (Macdonald et al. 2010). Warming water temperatures can be driven by both climate as well as land-use change collectively degrading freshwater fisheries (Ficke et al. 2007). It is well established that warming air temperatures warm water temperatures (e.g., Stefan and Preud'homme 1993, Mohseni and Stefan 1999). However, there is a growing appreciation for the contribution of land-use change, such as urbanization, to the observed trends in warming waters (Nelson and Palmer 2007, Davis et al. 2013). Understanding the relative importance of land-use and climate on river temperatures may provide insight into management of watersheds faced with on-going climate change.

The Fraser River in British Columbia, Canada is a large watershed where warming water temperatures are negatively impacting biodiversity and ecosystem services. Some studies estimate the Fraser River has warmed approximately 1.5°C since the 1950's and up to 0.7°C over the last two decades (Hinch and Martins 2011, Martins et al. 2011) threatening the future of Fraser River salmon (Farrell et al. 2008, Eliason et al. 2011). In very warm years up to 90% of in-migrating sockeye salmon from some run-timing groups have died before spawning (Macdonald et al. 2010). Under moderate climate warming scenarios, Martins et al. (2011) report that the lower reaches of the Fraser River mainstem may warm by ~2°C by the end of the century (Morrison et al. 2002) resulting in up to a 16% decrease in the spawning migration survival of some Sockeye Salmon (*Oncorhynchus nerka*) populations. Fisheries managers close fisheries in these hot years in order to allow sufficient numbers of fish back to the spawning grounds (Macdonald et al. 2010). For example, in August of 2013 the Fraser River broke high

temperature records of daily maximum values for a record number of days leading to the closure of commercial, recreational, and First Nations fisheries targeting salmon. As such, the warming waters of the Fraser River are driving conservation concerns, economic costs, and a growing need to better understand the mechanisms underpinning this warming trend. While previous studies have attributed much of the observed warming trend in the Fraser River to altered discharge patterns and warming air temperatures (e.g., Morrison et al. 2002, Martins et al. 2011), altered land-use may also contribute to the warming trend.

Recent research has linked climate warming and natural landscape perturbations to rising temperatures in freshwaters (Isaak et al. 2010, Holsinger et al. 2014). For example, Isaak et al. (2010) found that solar radiation increases linked to wildfires in the Boise River basin accounted for ~9% percent of the basin-scale warming. Similarly, Holsinger et al. (2014) found that wildfires significantly contributed to the warming trend in Montana's East Fork Bitterroot River basin. However, in both of these studies the effects of fire on water temperatures were considerably smaller than the effects of increasing air temperature. As well, the effects of wildfire on water temperature have been tightly linked to wildfire severity, where larger and more intensely burned areas tend to exhibit greater changes in water temperatures (Minshall et al. 1997, Dunham et al. 2007, Mahlum et al. 2011, Sestrich et al. 2011, Beakes et al. 2014). As such, it is worth noting that the frequency and duration of large wildfires in Western North America has increased by nearly four times over the last two decades (Westerling et al. 2006). Thus, wildfire burn areas may be significantly adding to the current and future warming trends in freshwaters.

Anthropogenic perturbations of riverine landscapes from forestry practices can also contribute to warming waters (Burton and Likens 1973, Kiffney et al. 2003, Moore et al. 2005, Caissie 2006, Webb et al. 2008, Pollock et al. 2009, Janisch et al. 2012). For example, Janisch et al. (2012) have shown that forest harvesting via clear cutting can increase stream temperatures by as much as 1.5°C in adjacent streams. The degree of temperature change is possibly linked with proximity of clear cutting to the streamside, such that leaving larger the buffer zones between forest harvest and the streamside should result in smaller changes in stream temperature (Kiffney et al. 2003). For

example, Kiffney et al. (2003) found leaving a 30m buffer zone between logged forest and streams resulted in an insignificant change in stream temperature, whereas clear cutting down to a 10m buffer zone significantly increased stream temperatures. In contrast, some research suggests that clear cutting forest has no statistical effect on stream temperatures (e.g., Arthur et al. 1998), thus fuelling the ongoing debate regarding the potential thermal effects of forestry on streams (Beschta et al. 1987, Larson and Larson 1996, Beschta 1997, Moore et al. 2005, Webb et al. 2008). The impacts of logging on water temperatures, especially in larger river systems such as the Fraser River, remain unclear.

Novel spatial statistical applications have greatly improved our ability to understand the relationships linking climate warming and landscape perturbations to rising temperatures in freshwaters (e.g., Peterson and Ver Hoef 2010, Ver Hoef and Peterson 2010, Isaak et al. 2010). Specifically, Spatial Stream Network (SSN) models (Ver Hoef et al. 2012) have advanced conventional geostatistical models by integrating spatial autocorrelation that is tailored to the inherent nested dendritic structure and the directional connectivity of water flow in streams and rivers (Peterson and Ver Hoef 2010, Ver Hoef and Peterson 2010, Ver Hoef et al. 2012). As well, SSN models are designed to interface with specialized ArcGIS toolsets that allow the modeller to explicitly link landscape features to stream networks. As a result, SSN models provide a quantitatively robust framework for examining the effects of air temperatures and landscape-level factors (i.e., wildfire burned, or logged area) on stream temperatures.

This study seeks to examine the relative effect of natural and anthropogenic landscape disturbance and climate on water temperatures in the Fraser River. Specifically, I address three interrelated questions: How has wildfire and logging altered water temperatures? How have changes in summer air temperatures altered water temperatures in the Fraser River? And, what is the relative effect size of the perturbed landscape and climate on Fraser River water temperatures? I examined changes in land-use, air temperature, and water temperature throughout the Fraser River network over the last four decades. I developed a SSN model for the Fraser River using existing water temperature data, spatial data detailing the wildfire and logging history of the basin, and downscaled historical climate records. This study focuses on water

temperatures during the summer (i.e., June – September) at times that coincide with the return of Fraser Rivers' sockeye salmon (Gable and Cox-Rogers 1993). Results from this study will aid fisheries managers by clarifying of how landscape alterations and climate warming may shape the thermal future for the Fraser River. More generally, this study improves our understanding of how natural and anthropogenic perturbations of the landscape and climate warming may act in concert to warm freshwaters.

5.3. Methods

5.3.1. Study system

This study is focused on the Fraser River, one of North America's largest rives without dams on its mainstem (Nilsson et al. 2005). The Fraser River covers a broad geographic area in British Columbia, Canada and drains approximately 228,000 km^2 of the province at an average discharge of 3,474 $m^3 \cdot s^{-1}$ (Ministry of Environment 2008). At its headwaters near the British Columbia-Alberta border the Fraser River flows 1,375 km through steep mountainous terrain and approximately 400 km of bedrock canyons until it turns alluvial, wandering through 185 km of gravel- and sand-bedded reaches before discharging into the Strait of Georgia at Sand Heads (Venditti and Church *In Press*). The hydrology of the Fraser River is predominantly controlled by spring snowmelt that drives peak flows from late May into early July with a mean annual flood of 9,790 $m^3 \cdot s^{-1}$ (McLean et al. 1999). The flow regime of the Fraser River is still considered natural, however, the climate and landscape of the watershed have been changing over the last five decades. The Fraser River is home to all five species of Pacific salmon (*Oncorhynchus* spp.). These salmon runs are the largest in Canada and support commercial, recreational, and First Nations fisheries. Thus, it is important that we gain a better understanding of how changes in the landscape and climate are impacting this large free-flowing watershed.

The central aim of this study was to use a geostatistical model to examine the combined effects of climate and land-use change on rising water temperatures in the Fraser River. Specifically, I applied a SSN model to the Fraser River network and examine the effects

of air temperature (°C), upstream area logged (km^2), and upstream area burned by wildfire (km^2) on average water temperatures. Environment Canada and Fisheries and Oceans Canada provided water temperature data for the Fraser River. I extracted air temperature data from an open source designed for climate change studies and applications in British Columbia (Wang et al. 2012). And I acquired landscape data from British Columbia's government Geographic Data Discovery Service and Forest Lands and Natural Resource Operations. I focused on a 10 year window of disturbance to capture the immediate and some of the mid-term effects of logging and wildfire (Gresswell 1999, Moore et al. 2005, Caissie 2006, Verkaik et al. 2013a). Longer time windows were not considered for analyses because research suggests that stream and river water temperatures can often return to pre-fire and pre-harvest levels within 10 years (Moore et al. 2005, Dunham et al. 2007). Additional climate and landscape covariates were not included in the model to avoid over parameterization. However, I examined the residuals of the fit model relative to other possible covariates to ensure that important covariates weren't excluded. Specifically, I plotted the residuals from the model against the included covariates (e.g., air temperature, burned and logged area) and additional landscape and climate variables that were not included such as elevation, precipitation, latitude, and longitude. I fit a generalized additive model (GAM) to these data to facilitate identification of patters and non-linearity in the residual-covariate plots. Patterns or non-linearity in the residuals or GAM would indicate that an important covariate was left out of the model, or that the data used to fit the model needed to be transformed.

5.3.2. Water Temperatures

In this project, I developed a spatial statistical model for the Fraser River using temperature data from Environment Canada and Fisheries and Oceans. These temperature data contain records dating back to the late 1930's that were collected from numerous locations throughout the Fraser watershed (Figure 5.1A). Three periods of data were focused on that had strong spatial coverage. In addition, we focused on temperature data collected during the summer months (i.e., July – September) so that our results are focused on periods of time that coincide with the return of Fraser Rivers salmon. In total, our analysis included 15 years of mean monthly water temperatures

during July, August, and September in 2010-2006, 1995-1991, and 1970-1966. Hereafter we refer to these time periods as recent (2010-2006), middle (1995-1991), and historic (1970-1966). Each time period, site of data collection, and time period by site combination, was assigned a unique identifier. Temperature measures with the same time period by site combination were considered non-independent and I included a random factor in the analysis to account the repeated measures.

5.3.3. Climate in the Fraser River basin

We included measures of air temperature in our analysis to compare the effects of climate forcing on water temperature to those attributed to landscape change. I acquired fine resolution measures of mean monthly air temperature (°C) from ClimateBC/WNA (http://cfcg.forestry.ubc.ca/projects/climate-data/climatebcwna/), an open source program that is designed to provide high-resolution climate data for climate change studies and applications in British Columbia (Wang et al. 2012). In summary, the ClimateBC and Climate WNA programs downscale Parameter-elevation Regressions on Independent Slopes Model (PRISM; Daly et al. 2002) monthly climate data at a specified latitude, longitude, elevation, and year within a 2.5 x 2.5 arcmin grid (Mitchell and Jones 2005). For details regarding the interpolation and downscaling algorithms of historic climate data into point data please refer to Wang et al. (2006, 2012) and references therein. I extracted mean monthly estimates of air temperature (°C), and precipitation (mm) for July, Aug, and September during years in the recent, middle, and historic time periods for locations with water temperature records throughout the Fraser watershed based on their latitude, longitude, and elevation.

5.3.4. Wildfire and logging in the Fraser River basin

One of the focal goals of this study was to examine the relative influence of landscape change on water temperatures in the Fraser River. Specifically, what are the effects of wildfire and forest logging on water Fraser River water temperatures? Historical records of wildfire perimeters within the Fraser River watershed are available from British Columbia's government Geographic Data Discovery Service (https://apps.gov.bc.ca/pub/geometadata). These data are updated annually and

compiled from various sources. I attained historical records of forest logging throughout British Columbia from the Forest Practices Board based on the Vegetation Resources Inventory. These data are a product of British Columbia's Forest Lands and Natural Resource Operations (http://www.for.gov.bc.ca/hts/vri/) and are updated by BC's Reporting Silviculture Updates and Land status Tracking System (http://www.for.gov.bc.ca/his/results/).

5.3.5. Spatial Stream Network model object

Prior to statistical analysis, the Fraser watershed needed to be spatially organized as a landscape network in ArcGIS (version 10.2). A landscape network delineates a watershed into a series of discrete drainage areas, river reaches that hypothetically accumulate overland flow from those drainage areas, and linkages were river reaches coalesce (Figure 5.1B). I built the Fraser River landscape network in ArcGIS using the Functional Linkage of Water basins (FLoWS) toolbox (Theobald et al. 2006) oriented in Albers equal-area conic projection. I used tools within FLoWS to transform a multi-polyline shapefile representing rivers, fourth order and higher, into a continuous geometric network of nodes (point shapefile) and reaches (polyline shapefile). The nodes in a landscape network represent sources and outlets of flow, and the confluence of rivers; the reaches connect the nodes (Figure 5.1B inset). All nodes and reaches are assigned a unique identifier and the geometric connectivity of all nodes and reaches in the network is retained in a relationship table within the landscape network ESRI personal geodatabase (Theobald et al. 2006).

During the landscape network construction I performed a series of quality-control steps to ensure that the network was geometrically correct. For example, all stream reaches were visually examined to confirm that they were digitized in the downstream direction (Peterson 2013). I examined the network for topological errors such as converging stream nodes, where two reaches converge but do not 'flow' into a third reach (Theobald et al. 2006, Peterson 2013). As such, I confirmed that the connectivity of the landscape network was correct and that all source nodes flowed into a single outlet node that resided at the furthest downstream point on the network.

Each network reach had an associated reach contributing area (RCA) that allowed me to integrate wildfire burn and logged areas of the Fraser River into the landscape network (Figure 5.1B inset). RCAs are based on topography and represent the drainage area, or catchment area, that contributes overland flow to their associated network reach. I delineated the Fraser landscape network RCAs using a 100 m grid digital elevation model of the Fraser watershed, a 100 m grid raster of water bodies with a surface area greater than 2 km^2, and the 'Create Cost RCAs' tool in FLoWS (Theobald et al. 2006). This tool produces a network of non-overlapping RCA polygons that have a one-to-one relationship between reaches and RCAs, thus linking the surrounding landscape to the network reaches (Theobald et al. 2006, Peterson 2013). I quantified the RCA area (km^2) using the zonal statistics tools in the Spatial Analyst toolbox. In addition, I quantified the total area burned and logged (km^2) within each RCA over a 10-year period that preceded each year in the recent, middle, and historic time periods. For example, the 'burned area' for each RCA in 2008 was the accumulated burned area within a RCA between 2007 and 1998. Using the 'Accumulate Values Downstream' tool in FLoWS, I quantified the total upstream RCA, burned, and logged area (km^2) for each reach. As such, each reach in the landscape network contained measures of the spatial area from which it receives overland flow, in addition to measures of the accumulated upstream burned and logged area over a 10 year period for each year in the three focal time periods of this study.

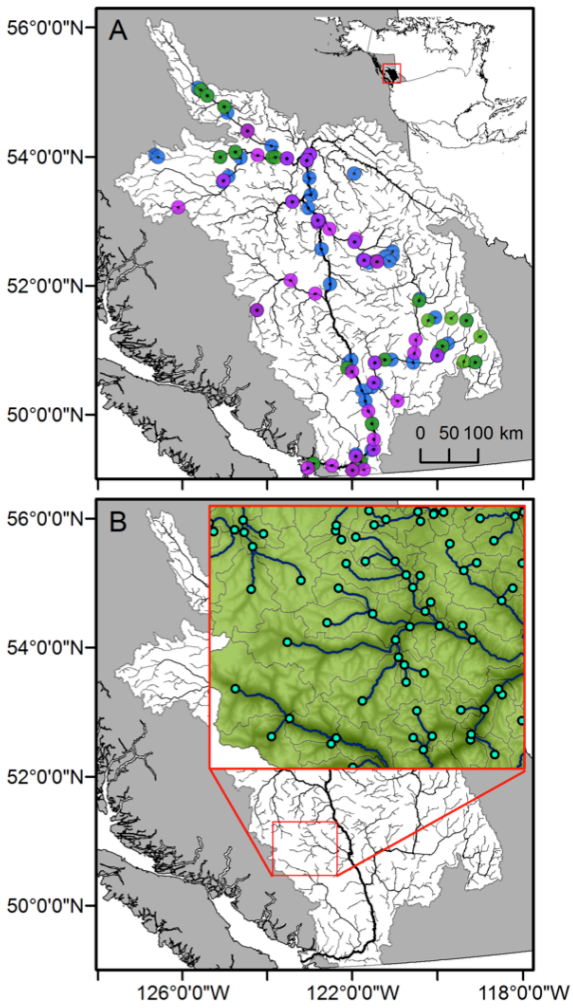

Figure 5.1. Map of the Fraser River in BC, Canada, and sites containing observed water temperature data (A) from the recent (purple), middle (blue), and historic (green) time periods. Points are slightly transparent to show overlap. An example of the SSN landscape network nodes (turquoise points, inset), reaches (blue lines, inset), and RCA polygons (grey outlined polygons, inset) are also plotted (B).

I used the geometric network of the Fraser River to generate a set of points for which I predicted water temperatures with the final SSN model. Specifically, I generated a point at the center of all reaches in the Fraser River geometric network. The resulting point shapefile contained 1551 'prediction points' stratified throughout the Fraser River network. At each of these locations I extracted climate data for July, August, and September for each year in the recent, middle, and historic time periods.

I appended point shapefiles of sites with observed water temperature and climate data and the 1551 additional prediction sites to the landscape network as the last step in construction. All sites were snapped to the landscape network based on their proximity to the nearest stream reach (Theobald et al. 2006). Measures of upstream RCA, burned, and logged area (km^2) were estimated for all sites based on the total upstream RCA, burned, and logged area (km^2) for the reach to which they were appended (Peterson 2013). Thus, all sites contained measures of mean monthly air temperature (°C), burned and logged area (km^2). In addition, all sites contained measures of additional covariates that were not included in the model such as mean monthly precipitation (mm), Elevation (m), latitude, and longitude. Sites containing observations of water temperature, sites for model predictions, the geometric landscape network, and the associated relationship tables were compiled and exported via Spatial Tools for the Analysis of River Systems (STARS) as a single spatial object for analysis in program R (Ver Hoef et al. 2012, Peterson 2013, R Development Core Team 2013).

5.3.6. Spatial Stream Network analysis

Using the SSN package in program R, I examined the relationship between water temperatures, climate, and the surrounding landscape of the Fraser River watershed. Specifically, I fit a generalized linear mixed effects model (GLMM) with spatial autocorrelation (Peterson and Ver Hoef 2010, Ver Hoef and Peterson 2010, Ver Hoef et al. 2012) to predict mean monthly water temperatures (°C) as a function of month (July, August, and September), upstream burned and logged area (km^2), and mean monthly air temperature (°C). In this model, I included a random effect to account for the repeated measurements of water temperature at the same site within a time period (i.e., time period by site combination). As well, I included a functional form of spatial autocorrelation that takes into account the connectivity of the river network and the direction of flow (i.e., exponential tail-down autocorrelation). This form of spatial autocorrelation is ideal for modeling temperatures in rivers because it can account for the difference in downstream flow connected and disconnected sites (Peterson and Ver Hoef 2010), such that sites that are connected by flow are spatially autocorrelated and sites that are disconnected are not. I used the upstream RCA area as a weighting scheme for the spatial autocorrelation function. This is an important component of the

autocorrelation function when calculating the net change in water temperature when stream reaches are linked. For instance, the temperature downstream of two linked stream reaches that have different RCA sizes will be more similar to the reach with the larger RCA because presumably there is more thermal inertia in reaches that have larger catchment areas. In addition, the spatial autocorrelation function uses a moving-average approach that determines how much downstream points on the network are spatially autocorrelated with all upstream points. The net amount of autocorrelation at a downstream point is a distance-based average of all upstream points. As such, temperatures at the most downstream reaches are partly a function of the temperatures at all upstream reaches.

I built two GLMM models to estimate the effect of air temperature, burned area, and logged area on water temperatures in the Fraser River. I used untransformed data in the first model, which provided coefficient estimates for the effect of air temperature, burned area, and logged area on water temperatures in the original units of measure (i.e., °C and km^2); significant effects of each factor were based on an alpha value of 0.05. In the second model I centered and scaled the air temperature, wildfire burn area, and logged area data by subtracting the mean of each variable and dividing by two standard deviations. Centering and scaling these data transformed the units from °C and km^2 to units of 2 SD, and thus the coefficient estimates and relative effect size of each parameter could be directly compared. For both models, I extracted and examined the residuals from the GLMM output to confirm that the models were fit appropriately.

Model validation is an important component of developing quantitative tools used for prediction. In many cases ecological models are developed but the derived model predictions are not validated (Manel et al. 2001). One of the strengths of the SSN package is that it contains several functions for estimating model diagnostics such as root-mean-square-prediction error (RMSPE) and leave-one-out cross validation (LOOCV; Ver Hoef et al. 2012). I estimated the RMSPE, the LOOCV, and the proportion of times the observed data were within the 95% prediction interval (cov.95) for the fit GLMM models. The results of these tests provide insight to the accuracy of the SSN model predictions.

I used the fit GLMM to examine how water temperatures have changed in the Fraser River overtime. Specifically, I predicted the water temperatures at 1551 locations stratified throughout the watershed for each year in the three focal time periods as a function of month (July, August, and September), upstream burned and logged area (km^2), and mean month air temperatures (°C). I averaged the predicted water temperatures within July, August, and September at each location over the five years in a time period to illustrate the mean spatiotemporal patterns in water temperature change throughout the Fraser River. In addition, I differenced the predicted water temperatures at each site across time periods within each month. By differencing these data I was able to illustrate the spatiotemporal changes in water temperatures over a 15, 25, and 40 year time period. For example, I differenced the predicted temperatures in July at all 1551 locations between 2010 and 1995 (i.e. 15yr period), 1995 and 1970 (i.e. 25yr period), and 2010 and 1970 (i.e., 40yr period). The reported temperature differences at 15, 25, and 40 years represent the average differences within time periods (e.g., recent and historic time periods).

5.4. Results

5.4.1. Water temperatures

Water temperatures in the Fraser River appear to have warmed over time. I compiled a dataset of 1,170 water temperature records collected from 141 locations (i.e., site by period combination; Figure 5.1A) after taking a subset of records from the time series that included data from summer months (i.e., July, August, and September) in each of our the focal time periods. The mean water temperature was 15.7°C ± 2.5°C SD (n=414, sites=37), 14.6°C ± 3.4°C SD (n=535, sites=75), and 14.9°C ± 2.5°C SD (n=236, sites=29) for the recent, middle, and historic time periods respectively. Generally, waters were warmest in August with a maximum measured temperature of 22.3, 21.3, and 21.2°C for the recent, middle, and historic time periods respectively. These data suggest that water temperatures are up to 5.2% warmer now than what was observed historically.

5.4.2. Climate in the Fraser River basin

Similar to water temperatures, mean summer air temperatures are 6.1% warmer throughout the Fraser watershed on average in the recent, and middle time periods compared to the historic time period. Using the data from ClimateBC/WNA, I calculated the mean summer air temperature for all sites throughout the Fraser watershed, including sites where water temperatures were predicted, as 13.9°C ± 3.2°C SD and 13.9°C ± 3.1°C SD for the recent and middle time periods respectively, compared to 13.3°C ± 3.2°C SD for the historic time period. Unlike air and water temperatures, average summer precipitation was only 2.2% greater during the recent and middle time periods compared to the historic time period.

5.4.3. Wildfire and logging in the Fraser River basin

The spatiotemporal disturbance history of wildfire and logging in the Fraser watershed was markedly different (Figure 5.2). The spatial distribution of burned area was relatively even throughout the watershed (Figure 5.2A) with a median fire size of 0.5 km^2 across the time series. However, the year-to-year variation in annual area burned was high relative to logging (Figure 5.2B, E) with some of the larger year-to-year differences in annual area burned approaching 2,580 km^2. Over time the annual area burned and the 10-year moving window of accumulated burned area appears to decline (Figure 5.2B, C). Specifically, the average 10yr accumulated burned area (km^2) decreased by 40% between the historic and recent time period.

Similar to wildfire burn area, the spatial distribution of logged area was relatively even throughout the watershed (Figure 5.2D). However, the median size of logged areas was 0.05 km^2 across the time series, which is an order of magnitude smaller than the median fire size. The year-to-year variation in annual logged area was much lower than that of wildfire burn area (Figure 5.2B, E), with 95% of the year-to-year differences in annual logged area less than 277 km^2. Over time the annual area logged and the 10-year moving window of accumulated logged area appears to increase (Figure 5.2E, F). Specifically, the average 10yr accumulated logged area (km^2) increased by over 360% between the historic and recent time period. The average 10yr accumulated logged area during the recent time period was 13,446.7 km^2 (Figure 5.2F). Thus despite the median

area logged equalling only 0.05 km^2, approximately 6% of the Fraser River watershed has recently been disturbed due to the accumulation of logging projects over space and time.

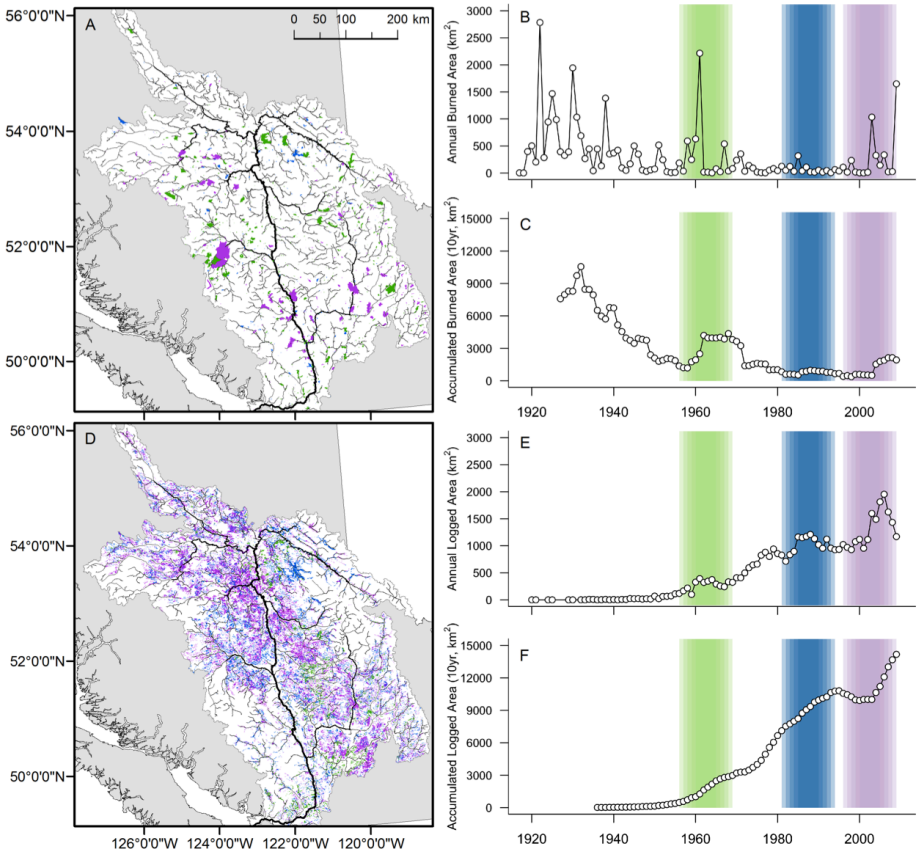

Figure 5.2. Map of the Fraser River and distribution of wildfires across space (A), annual burned area over time (B), and accumulated burn area over the previous 10 years (C). Also depicted is the distribution of logged areas in the Fraser River (D), as well as the annual logged area (E) and accumulated logged area over the previous 10 years (F). The three time periods included in the SSN model are color coded as purple (2010-2006), blue (1995-1991), and green (1970-1966).

5.4.4. Spatial Stream Network analysis

I found that water temperatures in the Fraser River were significantly different among the summer months (GLMM; $P < 0.001$) and significantly warmed by higher air temperatures (GLMM; $P < 0.001$) and larger upstream areas logged (GLMM; $P < 0.05$, Table 5.1,

Figure 5.3). Overall, the model accounted for approximately 39% of the observed variation in the water temperature data (GLMM; Generalized R^2 = 0.385). The coefficient estimates indicate that August is the warmest month, and both July and September are significantly colder (GLMM; $P < 0.001$). Within each month the average air temperature also significantly affected water temperatures (GLMM; $P < 0.001$), where warmer air temperatures were associated with warmer waters. Based on the model coefficients, for every 1°C increase in mean monthly air temperature Fraser River waters warmed by approximately 0.37°C on average (± 0.078°C 95% CI). In addition, the amount of upstream area logged was associated with significantly warmer water temperatures (GLMM; $P < 0.05$) but the amount of upstream burned area did not (GLMM; $P > 0.05$). Specifically, for every additional 1000 km^2 of upstream area logged within a 10 year time period, downstream Fraser River temperatures increase by approximately 0.10°C on average (± 0.097°C 95% CI). Given that approximately 13,500 km^2 of the Fraser River watershed has been logged over the last decade, as of 2010, I estimate that logging has warmed water temperatures by 1.35°C in the lower most reaches of the Fraser River mainstem. Based on the centered and scaled data, I estimated that the effect of air temperatures on Fraser River water temperatures was approximately 2.8 times the effect of upstream logged area (standardized coefficients of 2.05 vs. 0.74), and there was no statistical effect of upstream burned area with the coefficient confidence intervals broadly overlapping 0 (Figure 5.3).

Table 5.1. SSN GLMM parameter coefficient estimates.

Fixed Effects	Coef Estimate	SE	*t* value	*P*
Intercept	9.737	0.706	13.794	< 0.001
August	0.000	NA	NA	NA
July	-0.960	0.108	-8.870	< 0.001
September	-2.448	0.101	-24.212	< 0.001
Air Temp	0.369	3.970e-02	9.293	< 0.001
Logging	1.036e-04	4.936e-05	2.100	0.036
Wildfire	-8.610e-05	1.420e-04	-0.606	0.544
Random Effects				
Exp. Taildown parsill	4.383			
Exp. Taildown range	16,513.873			
Site.ID parsill	0.255			
Nugget parsill	1.960			

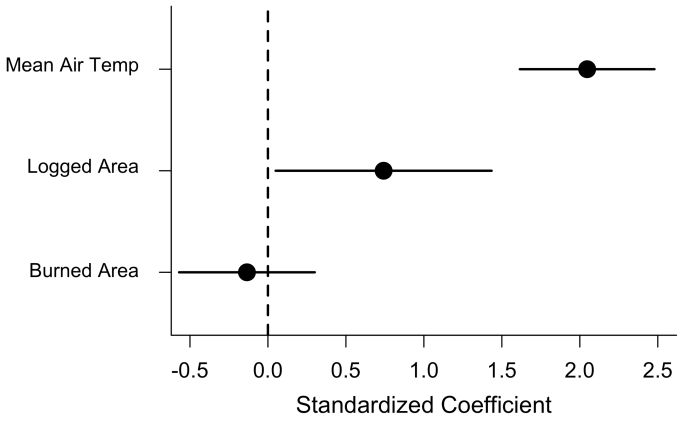

Figure 5.3. Standardized GLMM coefficients for average monthly air temperature (C°), upstream area logged (km^2), and upstream area burned by wildfire (km^2). Coefficients represent unites of 2 SD for each variable plotted, and error bars represent 95% coefficient CI.

5.4.5. SSN model cross validation and predictions

I calculated the RMSPE and completed LOOCV to examine the prediction accuracy of the fit GLMM. On average, the RMSPE was ± 1.48°C indicating a fair amount of uncertainty in model predictions. The relationship between predicted and observed values in the LOOCV computation indicate relatively good agreement between predicted and observed water temperatures (Figure 5.4; Generalized R^2 = 0.75). In addition, I calculated the cov.95, which was equal to 0.95 indicating that there is little bias and the prediction standard errors were estimated well (Ver Hoef et al. 2012).

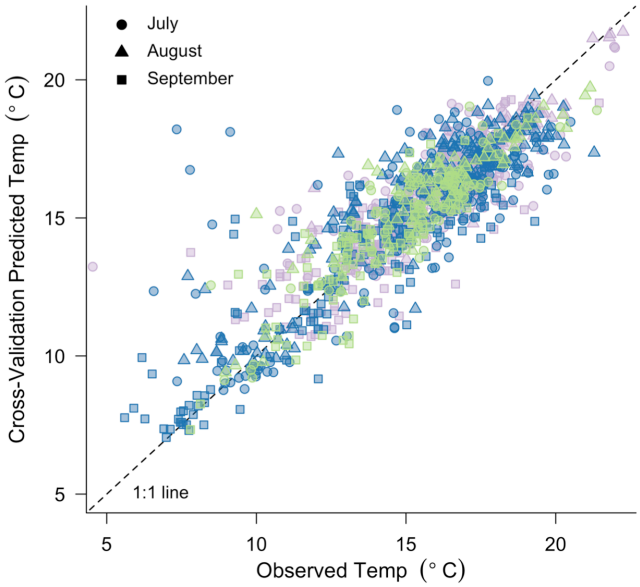

Figure 5.4. Observed Fraser River temperatures (°C) on the x-axis plotted against July (circle), August (triangle), and September (square) river temperatures (°C) predicted using LOOCV on the y-axis. The recent (purple), middle (blue), and historic (green) time periods are color-coded. Also plotted is a 1:1 dashed line.

To illustrate spatiotemporal trends in water temperatures throughout the Fraser River I used the fit GLMM model to predict temperatures for each year and month in the focal time periods. Across time periods, the warmest temperatures were predicted to occur in the lower mainstem Fraser River for all months, but and peaking in August (Figure 5.5). Overall, August was the warmest month for the Fraser River watershed with an average temperature of 16.1°C (± 2.78°C SD) and maximum temperature of 22.2°C. Waters were cooler on average in July and September with a mean temperature of 15.5°C (± 2.81°C SD) and 13.7°C (± 2.72°C SD) respectively.

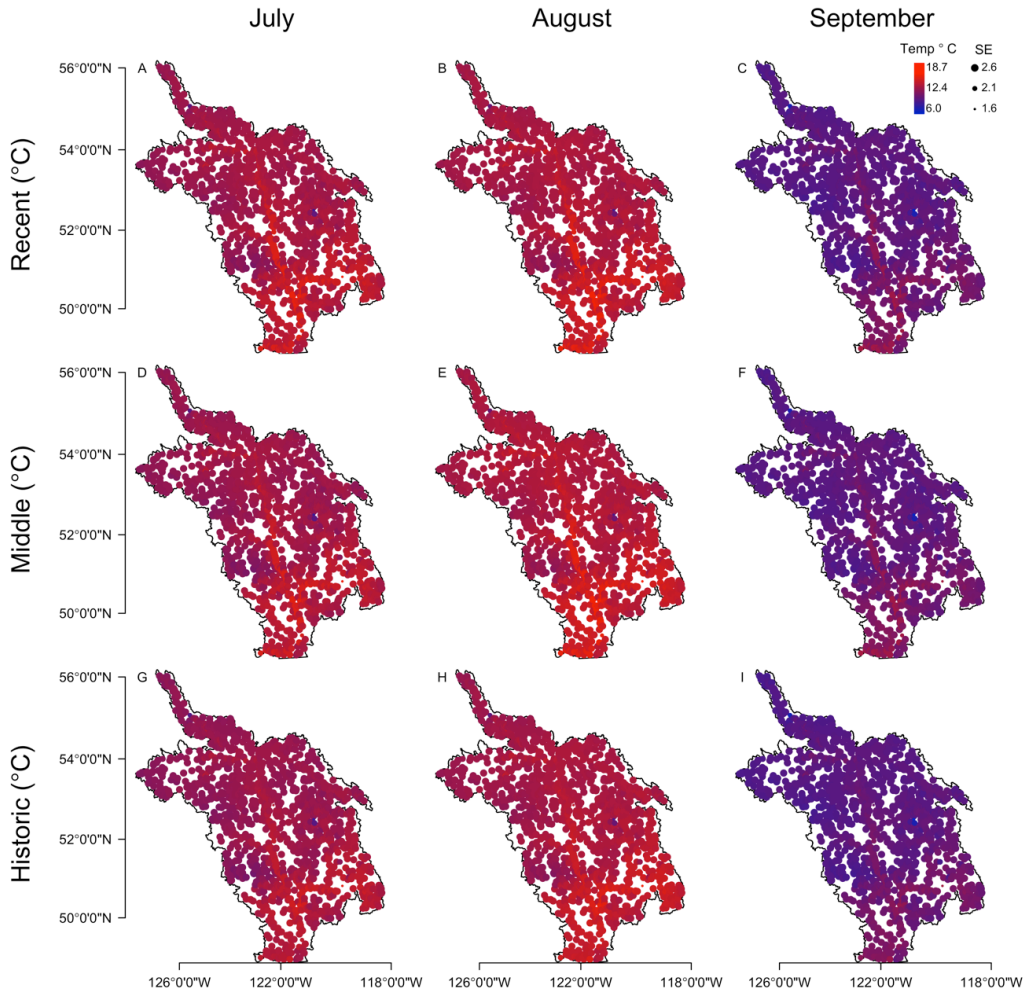

Figure 5.5. Predicted mean monthly water temperatures (°C) throughout the Fraser River. Predictions were based on a GLMM that included month, mean monthly air temperature (°C), upstream area logged or burned by wildfire (10yr accumulation, km^2). Predicted temperatures and SE are averaged for July, Aug, and Sept within each time period. Point color scales with temperature (°C) and the size of each point scales with the prediction standard error (SE).

I differenced the predicted water temperatures between years and time periods to illustrate spatiotemporal shifts in water temperatures throughout the Fraser River. Generally, water temperatures appear to be warming over time with the greatest changes occurring in the mainstem Fraser River and in July (Figure 5.7). There was visible spatial and temporal variation in the degree of temperature change throughout the Fraser River watershed (Figure 5.7). For example, July appears to have warmed to

most when comparing the recent to historic time periods, or recent to middle time periods (Figure 5.7A, D), whereas August appears to have warmed the most when comparing the middle to historic time periods (Figure 5.7E). Overall, summer water temperatures appear to be warming, and are 0.27°C (± 0.29°C SD) warmer on average in the recent compared to the historic time period. As such, waters are warming at approximately 0.07°C (± 0.07°C SD) per decade on average across the Fraser River basin.

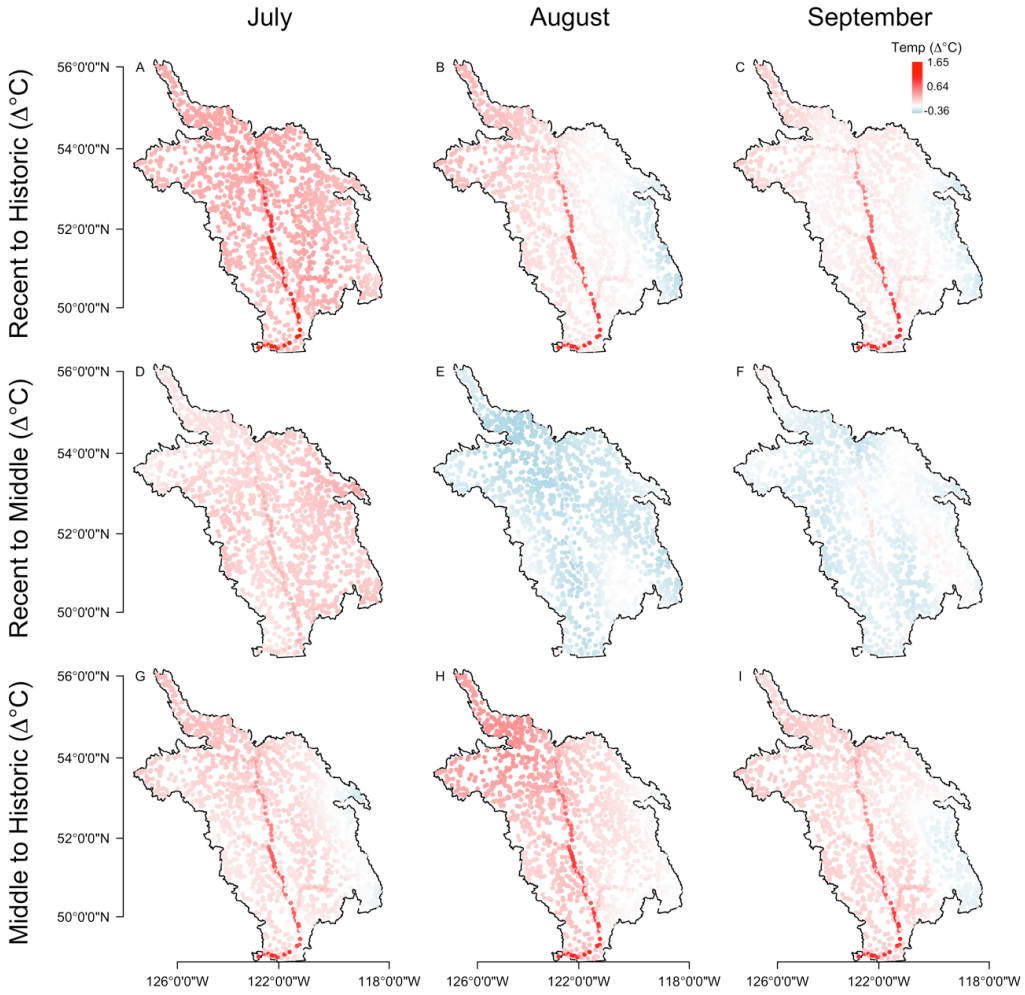

Figure 5.7. Average temperature difference (Δ°C) from the recent-historic (A-C), recent-middle (D-F), and middle-historic (G-I) time periods. Point colors scale with degree of temperature change (Δ°C), where white is equal to 0 difference or no data.

Some regions of the watershed are warming at a faster rate than others. The maximum predicted change in water temperature from the historic time period to the recent time period was 1.65°C in the lower mainstem of the Fraser River during July (X = 1289792, Y = 470577.3 Albers equal-area conic projection; Figure 5.7A). At this location in the lower mainstem of the Fraser River, the average change in air temperature (~Δ1.2°C) and the average change in the amount of upstream area logged (~Δ10,500 km^2) between the recent and historic time periods (Figure 5.8) may be warming water temperatures by ~0.4 °C and ~1.1 °C respectively. Thus logging appears to be driving most of the predicted water temperature change in the location where water temperatures have changed the most. Averaged across the watershed, air temperatures have risen by approximately 0.6°C between the recent and historic time periods, which equates to an approximate change in water temperature of 0.2°C (± 0.05°C 95% CI). Whereas the average change in upstream area logged was approximately 440 km^2 between the recent and historic time periods, which would drive an approximate increase in stream temperatures of 0.05°C (± 0.04°C 95% CI). Thus, while average changes in air temperature throughout the basin appear to be the dominant driver of increased water temperatures it is likely that logging is making a significant contribution to this warming trend (Figure 5.8).

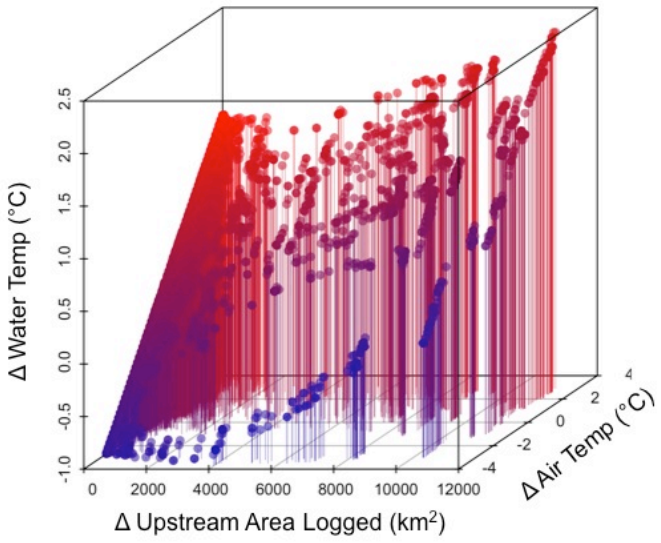

Figure 5.8. A 3-demensional plot of the predicted differences in water temperature (∆°C) y-axis, and observed differences in upstream area logged (∆ km^2) x-axis, and air temperature (∆°C) z-axis between the recent to historic time periods. Differences were calculated at 1551 locations during July, August, and September across all five years in each time period (n = 23,265). Point colors scale with the degree of air temperature change (∆°C).

5.5. Discussion

In this study I illustrate how climate and anthropogenic landscape perturbations can drive spatiotemporal variation in Fraser River water temperatures. Specifically, using a Spatial Stream Network model that accounts for repeated measures and spatial autocorrelation, I estimate that raising mean monthly air temperatures by 1°C and logging 1000 km^2 of forest will increase water temperatures downstream by approximately 0.37°C and 0.1°C, respectively, with no significant effect of wildfire on water temperatures. As a result, I found that waters are gradually warming in the Fraser River at a basin scale average of 0.07°C per decade, with disproportionately greater changes occurring in the lower reaches of the mainstem Fraser River. As such, this study provides insight into how natural and anthropogenic landscape disturbance and

climate warming may collectively contribute to the warming waters of the Fraser River in our future.

Air temperature is considered a very good predictor of water temperature (Stefan and Preud'homme 1993, Caissie 2006, Webb and Nobilis 2007, Webb et al. 2008, Kaushal et al. 2010). Some biological and water quality research of streams often use air temperature as a surrogate for water temperature because water temperature data are sometime scarce or are relatively difficult to obtain (Smith 1981, Stefan and Preud'homme 1993, Webb et al. 2008). As well, the majority of quantitative approaches to modeling water temperatures generally rely of air-water temperature relationships (Caissie 2006). As such, the strong positive air-water temperature relationship found in this study was not surprising, especially considering that the these relationships tend to strengthen when using monthly averages compared to shorter time scales (Stefan and Preud'homme 1993). However, the coefficient slope of the air-water temperature relationship estimated in this study was 0.369, which is approximately half as steep as coefficients estimated in other studies (e.g., Smith 1981, Stefan and Preud'homme 1993). I suspect this result is due to the relatively large size of rivers modeled in this study (i.e., > fourth order), and research has shown that increasing thermal capacity and discharge makes rivers and streams less sensitive to atmospheric influences (Smith and Lavis 1975, Ozaki et al. 2003, Webb et al. 2003, 2008). Despite the weakened air-water temperature association, I found that changing air temperature is the predominant factor driving basin-scale changes in water temperature in the Fraser River. As climate warming persists I expect that warming air temperatures will likely drive warming waters throughout the Fraser River. According to the ClimateBC and Climate WNA programs (Wang et al. 2006, 2012) and IPCC general circulation models, we might expect average air temperatures in the warmest month of the 2080's to be ~6°C warmer in the Fraser River basin compared to average air temperatures in the warmest months between 2006-2010. As a result, water temperatures in the Fraser will likely warm by over 2°C on average throughout the basin over the next century.

The logging practices in the Fraser River watershed appear to be associated with increased river temperatures. Previous research on small streams has shown that forest harvesting can can increase stream temperatures in adjacent streams (Burton and

Likens 1973, Kiffney et al. 2003, Janisch et al. 2012). Recently, studies have attempted to scale up these investigations and found a positive signal of warmer water temperatures in basins that were more heavily logged (Pollock et al. 2009). The association between logging and water temperature described in previous work and by the correlative analysis of this study may be explained by several potential mechanisms. For example, some studies suggest that clear-cutting forest can drive warming of shallow groundwater and subsequent heat advection to nearby streams (Hewlett and James 1982, Brosofske et al. 1997, Bourque and Pomeroy 2001, Alexander et al. 2003, Moore et al. 2005). However, the dominant thermal impact of forest harvest in streams and rivers appears to be linked to increased solar inputs and shortwave radiation (Johnson and Jones 2000, Moore et al. 2005, Caissie 2006). As such, shading provided by riparian vegetation, tall trees, and steep terrain may operate as a principal control on the amount of shortwave radiation that reaches streams and rivers, and thus likely constitutes an important control on stream temperatures (Allen 2008). Leaving buffer regions of riparian vegetation between the stream and forest harvest have been shown to significantly mitigate the thermal impacts of forest harvest (Kiffney et al. 2003). However, it is important to note that while buffer strips may mitigate for the thermal impacts of logging associated with solar radiation they may not be effective in mitigating for other possible mechanisms by which stream temperature is affected by logging (e.g., groundwater heating).

I found that the effects of wildfire on Fraser River water temperatures to be statistically negligible. Specifically, the amount of upstream area burned by wildfire did not significantly alter downstream water temperatures in the Fraser River. This result corroborates previous research that found the effects of wildfire diminished when they are examined at the river network scale (Isaak et al. 2010, Holsinger et al. 2014). As well, wildfire represented only one of multiple stressors on water temperatures in this study (Ormerod et al. 2010). Between 2006 and 2010, the average upstream area burned by wildfire over a 10yr period was ~2,300 km^2 or approximately 1% of the watershed. By comparison, between 2006 and 2010, the average upstream logged area over a 10yr period was approximately 6% of the Fraser River watershed, which is an area over twice the size of Delaware State, USA. As such, it is possible that the effects of the primary stressors (i.e., logging and climate warming) on Fraser River water

temperatures are strong enough to overshadow the effects of additional stressors such as wildfire (Fausch et al. 2010). In addition to the relatively small contribution of wildfire burn area to the amount of disturbed landscape throughout the Fraser River basin, over 78% of the historic wildfires in the basin were relatively small (< 2 km^2), and forest recovery from small and low severity wildfires can occur relatively rapidly over a period of years to decades (Dunham et al. 2007).

Changes to the hydrology of the Fraser River will likely impact water temperatures in the Fraser River. For example, the timing of freshet (i.e., spring runoff) has been shown to influence summer temperature regimes, where earlier onset of freshest results in warmer summer temperatures (Morrison et al. 2002, MacDonald et al. 2014). In the western United States and the Fraser River, the hydrology has been shifting such that freshet is occurring earlier in the year (Morrison et al. 2002, Stewart et al. 2004, Regonda and Rajagopalan 2005). These changes have been partly attributed to shifts from snow to rain dominated systems and early snow melt due to climate change (Hidalgo et al. 2009). Land-use has also been linked to shifts in the timing of freshet, such that clear-cutting is associated with increased rates of snow melt and earlier freshest (Schelker et al. 2013). Considering the magnitude of forest harvest in the Fraser River basin it is possible that both climate warming and land-use will likely influence the hydrology as well as the thermal regime of the Fraser River in the future.

Waters in the Fraser River during anomalously warm years surpass the thermal limits for in migrating salmon resulting in large-scale pre-spawn mortality (Foreman et al. 1997, Macdonald et al. 2010). Exposure of temperatures above 22°C for several days can result in acute infection or acute thermal shock and death (Servizi and Jensen 1977). Results from this study indicate that between 2006 and 2010 mean daily stream temperatures warmed as much as 22.2°C in August with daily maximum temperatures likely much higher. Indeed, the warming trends in the Fraser River pose serious conservation concerns for salmon returning during these warm months, such as the Summer Sockeye salmon run-timing group (Gable and Cox-Rogers 1993, Eliason et al. 2011).

This study has shown that rising air temperatures due to climate warming, and large-scale forest harvest are warming water temperatures in the Fraser River. The predicted rate of temperature change in the study was similar to those previously published (Foreman et al. 2001, Hinch and Martins 2011, Martins et al. 2011). However, this study explicitly links anthropogenic alterations of the landscape and climate to basin-scale changes in river temperatures. Analyses indicate that much of the warming throughout the basin is being driven by air temperature but that logging practices are significantly contributing to the warming trend. In British Columbia, Canada buffer zones along non-fish bearing streams are not currently required, nor are they required in fish bearing streams that have a bankfull width less than 1.5 m (Moore et al. 2005). These small streams are considered more vulnerable to the thermal effects of logging because they have a low thermal capacity relative to larger systems (Moore et al. 2005, Caissie 2006). As such, the most vulnerable streams are not protected from increased solar radiation associated with logging, which is the predominant factor driving summer stream temperature warming (Moore et al. 2005). As such, resource managers in British Columbia have the capacity to offset the trend of warming waters in the Fraser River by adopting forest management practices that minimize the thermal impacts of forest harvest (e.g., mandatory riparian buffer zones). In doing so, resource managers may possibly slow some of the deleterious impacts of climate warming. As well, research has shown that watersheds may recover from the thermal impacts of forest logging within 5 to 10 years after harvest (Moore et al. 2005). Thus, the positive effects of implementing protective forest management practices may manifest relatively rapidly. In total, results from this study will aid resource managers by clarifying of how landscape alterations and climate warming may shape the thermal future for the Fraser River. More generally, this study improves our understanding of how natural and anthropogenic landscape perturbations may act in concert with climate change to warm freshwaters.

6. General Discussion

In this thesis I explore the effects of several predominant forms of large-scale natural and anthropogenic disturbance in lotic ecosystems. My thesis examines how abiotic and biotic components of lotic ecosystems respond to wildfire, river regulation, forest logging, and climate warming at spatial scales ranging from less than 10 m^2 to over 220,000 km^2. By focusing on different disturbance types and by varying the spatial and temporal scope of my work, my thesis provides insight to basic stream ecology, and provides information at spatiotemporal scales conducive for aiding resource management (Wiens 1989, Fausch et al. 2002, Allan 2004).

6.1. Natural disturbance

Natural disturbance operates as a primary control on the distribution, abundance, and characteristics of organisms inhabiting lotic ecosystems (Resh et al. 1988, Poff and Ward 1990, Lytle 2002). This control arises partly from the effects disturbance has on the physical habitat template and resource availability in streams and rivers (Resh et al. 1988, Poff and Ward 1990, Poff et al. 1997). The types of disturbance that serve as controls and the frequency in which they occur (i.e., disturbance regime) are specific to geographic regions. For example, lotic ecosystems in Mediterranean regions are prone to frequent wildfires, winter flooding, and droughts that drive their structure and function (Gasith and Resh 1999, Verkaik et al. 2013a). As such, understanding the role of natural disturbance in lotic ecosystem necessitates studies focused within and across geographic regions.

Wildfire can help shape thermal heterogeneity in lotic ecosystems within Mediterranean regions (Chapter 2). Local-scale differences in fire severity will generate heterogeneous burn patterns in the removal of riparian vegetation leading to heterogeneous increases in light and stream temperatures. Local climate, and other common forms of disturbance in

Mediterranean regions, will likely mediate the biological response to wildfire driven thermal heterogeneity in lotic ecosystems. For example, hot, dry Mediterranean summers drive bioenergetically stressful conditions for thermally-sensitive fishes such as *O. mykiss* (Grantham et al. 2012, Sloat and Osterback 2013). I found that thermal heterogeneity caused by wildfire was associated with shifts in *O. mykiss* biomass, potentially due to emigration from more energetically costly pools (Chapter 2). Drought years with decreased flow and increased stream temperatures would likely exacerbate the biological response to warming waters associated with wildfire. In contrast, flood years may increase benthic invertebrate prey available to drift feeding fishes like *O. mykiss* via scour (Power et al. 2008, Sogard et al. 2012), in which case warming waters associated with wildfire would contribute to bioenergetically favorable conditions for accelerated growth. Thus, in Mediterranean regions the biological response to wildfire driven changes in stream temperature will likely be seasonally dynamic and exacerbated or attenuated by additional disturbance types such as winter floods or summer droughts.

Wildfire can alter the availability of nutrients and particulate organic matter in streams and rivers (Chapter 3). Fire has been shown to deliver pulses of nutrients and organic matter to streams in burned watersheds via pyrolysis of organic material, leaching, erosion and run-off (Minshall et al. 1997, Gresswell 1999, Wan et al. 2001, Verkaik et al. 2013a). For example, I observed a 244% increase in nitrate and a 44% increase in fine particulate organic matter in burned compared to unburned regions of Scott Creek following the Lockheed wildfire (Chapter 3). In Mediterranean systems such as Scott Creek, the natural seasonal patterns in precipitation and stream flow will mediate the timing of the delivery and the quantity of nutrients and organic matter derived from wildfire burn areas (Verkaik et al. 2013, Chapter 3). Whereas in snowpack dominated watersheds the delivery of nutrients and organic matter from burned landscapes tends to occur during the spring snowmelt and summer storms (e.g., Minshall 2001). Thus, the timing of nutrients and organic matter inputs is related to the region-specific seasonality and hydrology.

Lotic ecosystems in Mediterranean regions appear robust to wildfire related disturbance. For example, I found that the abundance and community composition of both terrestrial and aquatic macroinvertebrates were governed primarily by underlying seasonal cycles,

and the effects attributable to wildfire were relatively minor by comparison (Chapter 3). However, it is important to note that the wildfire that I examined in my thesis work was classified as relatively moderate in severity. Previous work has shown strong links between fire severity and ecosystem response (e.g., Malison and Baxter 2010b, Jackson et al. 2012). I suspect that larger and more severe wildfires are likely to contribute comparably to shaping food webs and the physical structure of streams in Mediterranean regions than flooding and drought, which are currently considered the primary controls (Gasith and Resh 1999, Power et al. 2008, Verkaik et al. 2013a).

6.2. Anthropogenic disturbance

In contrast to natural disturbance, anthropogenic disturbance can often lead to the homogenization of physical habitat and biological communities. In regulated rivers, dams and other impoundments have altered the duration, frequency and intensity of high flow events leading to channel simplification and the loss of important habitats such as sloughs, backwater areas and side channels (Ligon et al. 1995, Sear 1995, Poff et al. 1997). There is a growing concern that anthropogenic disturbance is a major threat to future lotic ecosystem integrity (Allan et al. 1997, Townsend et al. 2003, Strayer et al. 2003, Allan 2004). This concern is partly driven by the global-scale increase in anthropogenic disturbance, such as dam construction and river regulation (Nilsson et al. 2005, Poff et al. 2007). As well, habitat degradation from anthropogenic disturbance can propagate in all directions within river networks and sometimes great distances from the source of disturbance (Pringle 1997, Fausch et al. 2002).

The use of relatively new quantitative methods can greatly aid our ability to measure and predict the effects of anthropogenic disturbance. For example, hydrodynamic habitat models are a family quantitative tools that resource managers often used to estimate the effects of river regulation on salmon habitat (Ahmadi-Nedushan et al. 2006). Constructing these habitat models using AICc and modeling averaging will improve their predictive accuracy and more accurately reflect uncertainty in model predictions (Chapter 1). Therefore, integrating the use of AICc and model averaging into the current

hydrodynamic habitat-modelling framework will facilitate wise management of aquatic resources and the services that lotic ecosystems provide.

Recent advances in geostatistics have greatly improved our ability to quantify the effects of land-use change and anthropogenic disturbance in lotic ecosystems (Peterson and Ver Hoef 2010, Ver Hoef and Peterson 2010, Ver Hoef et al. 2012). For example, by applying Spatial Stream Network (SSN) models to water temperature data from the Fraser River I was able to quantify the combined effect of logging and rising air temperatures on warming water temperatures (Chapter 4). This study illuminated the importance of considering the accumulative impacts of multiple small-scale anthropogenic disturbances. For example, between 2000 and 2010 the median area of individual sites logged in the Fraser River basin was 0.04 km^2, which would have a negligible affect on water temperatures (Chapter 4). However, the accumulation of logged areas between 2000 and 2010 was approximately 14,200 km^2, which is an area over twice the size of Delaware State, USA. The accumulative impact of logging throughout the Fraser River basin is significantly contributing to the trend in warming water temperatures and the degradation of thermal habitat for Pacific salmon (Chapter 4).

6.3. Conservation and management implications

One of the key challenges we currently face is learning how acquire the goods and services we need from lotic ecosystems, while minimizing the anthropogenic threat to future ecological integrity. Previous research and results from my thesis lend support to three general considerations for the development of a holistic disturbance-based management and conservation framework (Hobbs and Huenneke 1992, Poff et al. 1997).

1. Natural disturbance is critical for healthy ecosystem function.

It is imperative that we integrate natural disturbance into management and conservation strategies. However, the contribution of natural disturbance to ecosystem health will likely vary by disturbance type, frequency of occurrence, and geographic region

(Chapter 2, 3). Thus, shifting to a disturbance-based management and conservation framework will need to be informed with regional studies focused on the region-specific role of natural disturbance in lotic ecosystems.

2. Impacts of anthropogenic disturbance to lotic ecosystems can be minimized.

The goods and services lotic ecosystems provide are a limited resource throughout many areas of the world (Richter et al. 2003, Poff et al. 2003). Management of these resources should be focused on minimizing deleterious impacts from anthropogenic disturbance in order to ensure their future availability. Effective management can be greatly aided by implementing improved quantitative tools that accurately estimate our impact on sensitive species and habitats, as well as accurately reflect the uncertainty around those estimates (Chapter 1).

3. Lotic ecosystems are nested hierarchical structures.

Streams and rivers are nested hierarchical structures, which allow the effects of disturbance to propagate throughout the network. Examining disturbance on a network scale will improve our understanding of how large-scale disturbance can propagate through lotic ecosystems, and how the accumulation of small-scale disturbances can drive large-scale changes (Chapter 4).

6.4. Conclusion

Noel Hynes and David Allan, aptly stated “in every respect the valley rules the stream (Hynes 1975)”, “but increasingly, human activities rule the valley (Allan 2004).” In part, Hynes was referring to fact that the valley provides the rocks that form the river channel and organic material that fuels the food web. The delivery and composition of these materials occurs through a complex suite of natural processes that include natural disturbance. On the other hand, Allan was acknowledging that human actions are fundamentally altering the natural process that maintain the form and function of streams and rivers, and that the frequency and spatial extent of these actions are increasing. I believe both Noel Hynes and David Allan’s statements touch on the central points of my thesis. Natural disturbance is an intrinsic and natural process critical for maintaining

healthy function in streams and rivers. To that end, the way humans interact with the landscape will have long-lasting and far-reaching implications for lotic ecosystems. And therein lies our responsibility as participants in the 'ecological theatre' (Hutchinson 1965). We have the privilege of deciding what role we want to play in shaping the streams and rivers of our future.

References

Adams, T. S., and R. W. Sterner. 2000. The effect of dietary nitrogen content on trophic level 15N enrichment. Limnology and Oceanography 45:601–607.

Ahmadi-Nedushan, B., A. St-Hilaire, M. Bérubé, É. Robichaud, N. Thiémonge, and B. Bobée. 2006. A review of statistical methods for the evaluation of aquatic habitat suitability for instream flow assessment. River Research and Applications 22:503–523.

Akaike, H. 1974. A new look at the statistical model identification. IEEE Transactions on Automatic Control 19:716–723.

Albin, D. P. 1979. Fire and stream ecology in some Yellowstone tributaries. California Fish and Game 64:216–238.

Alexander, M. D., K. T. B. MacQuarrie, D. Caissie, and K. D. Butler. 2003. The thermal regime of shallow groundwater and a small Atlantic salmon stream bordering a clearcut with a forested streamside buffer. Pages GCL 343–1–10 Annual Conference of the Canadian Society for Civil Engineering, Moncton, New Brunswick. Canadian Society for Civil Engineering. Montreal, Quebec, Canada.

Allan, J. D. 2004. Landscapes and riverscapes: the influence of land use on stream ecosystems. Annual Review of Ecology and Systematics 35:257–284.

Allan, J. D., D. L. Erickson, and J. Fay. 1997. The influence of catchment land use on stream integrity across multiple spatial scales. Freshwater Biology 37:149–161.

Allen, D. M. 2008. Development and application of a process-based, basin-scale stream temperature model. University of California, Berkeley.

Allen, J. E. 1984. Geology of the gorge. Pages 20–30 *in* M. S. Spranger, editor. The Columbia Gorge, a unique American treasure. Washington State University Cooperative Extension and Washington Sea Gran Program.

Amaranthus, M., H. Jubas, and D. Arthur. 2000. Stream shading, summer streamflow, and maximum water temperature following intense wildfire in headwater streams. In: Berg, Neil H., tech. coord. Proceedings of the Symposium on Fire and Watershed Management: October 26-28, 1988, Sacramento, California. General Technical Report GTR-PSW-109. Berkeley, CA. Pages 75-78.

Arnold, T. W. 2010. Uninformative parameters and model selection using Akaike's information criterion. Journal of Wildlife Management 74:1175–1178.

Arthington, A. H., S. E. Bunn, N. L. Poff, and R. J. Naiman. 2006. The challenge of providing environmental flow rules to sustain river ecosystems. Ecological Applications 16:1311–1318.

Arthur, M. A., G. B. Coltharp, and D. L. Brown. 1998. Effects of best management practices on forest streamwater quality in Eastern Kentucky. Journal of the American Water Resources Association 34:481–495.

Attiwill, P. M. 1994. The disturbance of forest ecosystems: the ecological basis for conservative management. Forest Ecology and Management 63:247–300.

Ayllón, D., A. Almodóvar, G. G. Nicola, and B. Elvira. 2010. Modelling Brown Trout spatial requirements through physical habitat simulations. River Research and Applications 26:1090–1102.

Barbour, M. T., J. Gerritsen, B. D. Snyder, and J. B. Stribling. 1999. Rapid bioassessment protocols for use in streams and wadeable rivers: periphyton, benthic macroinvertebrates, and fish. Second edition. EPA 841-B-99-002. U.S. Environmental Protection Agency; Office of Water; Washington, D.C.

Baxter, C. V, K. D. Fausch, M. Murakami, and P. L. Chapman. 2004. Fish invasion restructures stream and forest food webs by interrupting reciprocal prey subsidies. Ecology 85:2656–2663.

Baxter, C. V., K. D. Fausch, and S. W. Carl. 2005. Tangled webs: reciprocal flows of invertebrate prey link streams and riparian zones. Freshwater Biology 50:201–220.

Beakes, M. P., J. W. Moore, S. A. Hayes, and S. M. Sogard. 2014. Wildfire and the effects of shifting stream temperature on salmonids. Ecosphere 5:63.

Beecher, H. A., B. A. Caldwell, and S. B. Demond. 2002. Evaluation of depth and velocity preferences of juvenile Coho salmon in Washington streams. North American Journal of Fisheries Management 22:785–795.

Beecher, H. a., B. a. Caldwell, S. B. DeMond, D. Seiler, and S. N. Boessow. 2010. An empirical assessment of PHABSIM using long-term monitoring of Coho Salmon smolt production in Bingham Creek, Washington. North American Journal of Fisheries Management 30:1529–1543.

Beechie, T. J., M. Liermann, E. M. Beamer, and R. Henderson. 2005. A classification of habitat types in a large river and their use by juvenile salmonids. Transactions of the American Fisheries Society 134:717–729.

Benke, A. C., A. D. Huryn, L. A. Smock, and J. B. Wallace. 1999. Length-mass relationships for freshwater macroinvertebrates in North America with particular reference to the Southeastern United States. Journal of the North American Benthological Society 18:308–343.

Beschta, R. L. 1997. Riparian shade and stream temperature: an alternative perspective. Rangelands 19:25–28.

Beschta, R. L., R. E. Bilby, G. W. Brown, L. B. Holtby, and T. D. Hofstra. 1987. Stream temperature and aquatic habitat; fisheries and forestry interactions. Pages 191–232 *in* E. O. Salo and T. W. Cundy, editors. Streamside management forestry and fishery interactions. University of Washington, Institute of Forest Resources, Contribution No 57, Seattle, WA.

Bisson, P. a., B. E. Rieman, C. Luce, P. F. Hessburg, D. C. Lee, J. L. Kershner, G. H. Reeves, and R. E. Gresswell. 2003. Fire and aquatic ecosystems of the western USA: current knowledge and key questions. Forest Ecology and Management 178:213–229.

Boavida, I., J. M. Santos, R. V. Cortes, a. N. Pinheiro, and M. T. Ferreira. 2010. Assessment of instream structures for habitat improvement for two critically endangered fish species. Aquatic Ecology 45:113–124.

Boling, R. H., E. D. Goodman, J. A. Van Sickle, J. O. Zimmer, K. W. Cummings, R. C. Petersen, and S. R. Reice. 1975. Toward a model of detritus processing in a woodland stream. Ecology 56:141–151.

Bolker, B. M. 2008. Ecological Models and Data in R. First edition. Princeton University Press, 41 William Street, Princeton, New Jersey 08540.

Bondar, C. A., K. Bottriell, K. Zeron, and J. S. Richardson. 2005. Does trophic position of the omnivorous signal crayfish (*Pacifastacus leniusculus*) in a stream food web vary with life history stage or density? Canadian Journal of Fisheries and Aquatic Sciences 62:2632–2639.

Bourque, C. P.-A., and J. H. Pomeroy. 2001. Effects of forest harvesting on summer stream temperatures in New Brunswick, Canada: an inter-catchment, multiple-year comparison. Hydrology and Earth System Sciences 5:599–614.

Bovee, K. D. 1986. Development and evaluation of habitat suitability criteria for use in the instream flow incremental methodology. U.S. Fish and Wildlife Service Biological Report:1–235.

Braaten, P. J., P. D. Dey, and T. C. Annear. 1997. Development and evaluation of bioenergetic-based habitat suitability criteria for trout. Regulated Rivers: Research & Management 13:345–356.

Brosofske, K. D., J. Chen, R. J. Naiman, and J. F. Franklin. 1997. Harvesting effects on microclimatic gradients from small streams to uplands in western Washington. Ecological Applications 7:1188–1200.

Burgman, M. A., D. R. Breininger, B. W. Duncan, and S. Ferson. 2001. Setting reliability bounds on habitat suitability indices. Ecological Applications 11:70–78.

Burnham, K. P., and D. R. Anderson. 2002. Model selection and multimodel inference: a practical-theoretic approach. 2nd edition. Springer-Verlag, New York.

Burton, T. M., and G. E. Likens. 1973. The effect of strip-cutting on stream temperatures in the Hubbard Brook experimental forest, New Hampshire. BioScience 23:433–435.

Caissie, D. 2006. The thermal regime of rivers: a review. Freshwater Biology 51:1389–1406.

Carlson, S. M., and W. H. Satterthwaite. 2011. Weakened portfolio effect in a collapsed salmon population complex. Canadian Journal of Fisheries and Aquatic Sciences 68:1579–1589.

Collier, K. J., S. Bury, and M. Gibbs. 2002. A stable isotope study of linkages between stream and terrestrial food webs through spider predation. Freshwater Biology 47:1651–1659.

Cummins, K. W., and J. C. Wuycheck. 1971. Caloric equivalents for investigations in ecological energetics. International Association of Theoretical and Applied Limnology 18:1–158.

Daly, C., W. P. Gibson, G. H. Taylor, G. L. Johnson, and P. Pasteris. 2002. A knowledge-based approach to the statistical mapping of climate. Climate Research 22:99–113.

Davis, J. M., C. V. Baxter, E. J. Rosi-Marshall, J. L. Pierce, and B. T. Crosby. 2013. Anticipating stream ecosystem responses to climate change: toward predictions that incorporate effects via land–water linkages. Ecosystems 16:909–922.

Dunbar, M. J., K. Alfredsen, and a. Harby. 2012. Hydraulic-habitat modelling for setting environmental river flow needs for salmonids. Fisheries Management and Ecology 19:500–517.

Dunham, J. B., A. E. Rosenberger, C. H. Luce, and B. E. Rieman. 2007. Influences of wildfire and channel reorganization on spatial and temporal variation in stream temperature and the distribution of fish and amphibians. Ecosystems 10:335–346.

Dunham, J. B., M. K. Young, R. E. Gresswell, and B. E. Rieman. 2003. Effects of fire on fish populations: landscape perspectives on persistence of native fishes and nonnative fish invasions. Forest Ecology and Management 178:183–196.

Dwire, K. a., and J. B. Kauffman. 2003. Fire and riparian ecosystems in landscapes of the western USA. Forest Ecology and Management 178:61–74.

Eaton, J. G., and R. M. Scheller. 1996. Effects of climate warming on fish thermal habitat in streams of the United States. Limnology and Oceanography 41:1109–1115.

Ebersole, J. L., W. J. Liss, and C. A. Frissell. 2001. Relationship between stream temperature, thermal refugia and rainbow trout *Oncorhynchus mykiss* abundance in arid-land streams in the northwestern United States. Ecology of Freshwater Fish 10:1–10.

Eliason, E. J., T. D. Clark, M. J. Hague, L. M. Hanson, Z. S. Gallagher, K. M. Jeffries, M. K. Gale, D. A. Patterson, S. G. Hinch, and A. P. Farrell. 2011. Differences in thermal tolerance among sockeye salmon populations. Science 332:109–12.

Erős, T., P. Gustafsson, L. a Greenberg, and E. Bergman. 2012. Forest-stream linkages: effects of terrestrial invertebrate input and light on diet and growth of brown trout (*Salmo trutta*) in a boreal forest stream. PLoS ONE 7:e36462.

Farrell, A. P., S. G. Hinch, S. J. Cooke, D. A. Patterson, G. T. Crossin, M. Lapointe, and M. T. Mathes. 2008. Pacific salmon in hot water: applying aerobic scope models and biotelemetry to predict the success of spawning migrations. Physiological and Biochemical Zoology 81:697–708.

Fausch, K. D., C. V. Baxter, and M. Murakami. 2010. Multiple stressors in north temperate streams: lessons from linked forest-stream ecosystems in northern Japan. Freshwater Biology 55:120–134.

Fausch, K. D., C. E. Torgersen, C. V Baxter, and H. W. Li. 2002. Landscapes to riverscapes: bridging the gap between research and conservation of stream fishes. BioScience 52:483–498.

Ficke, A. D., C. a. Myrick, and L. J. Hansen. 2007. Potential impacts of global climate change on freshwater fisheries. Reviews in Fish Biology and Fisheries 17:581–613.

Finlay, J. C. 2004. Patterns and controls of lotic algal stable carbon isotope ratios. Limnology and Oceanography 49:850–861.

Finlay, J. C., S. Khandwala, and M. E. Power. 2002. Spatial scales of carbon flow in a river food web. Ecology 83:1845–1859.

Fisher, S. G., and G. E. Likens. 1973. Energy flow in Bear Brook, New Hampshire: an integrative approach to stream ecosystem metabolism. Ecological Monographs 43:421–439.

Flannigan, M. D., K. A. Logan, B. D. Amiro, W. R. Skinner, and B. J. Stocks. 2005. Future area burned in Canada. Climatic Change 72:1–16.

Foreman, M. G. G., C. B. James, M. C. Quick, P. Hollemans, and E. Wiebe. 1997. Flow and temperature models for the Fraser and Thompson Rivers. Atmosphere-Ocean 35:109–134.

Foreman, M. G. G., D. K. Lee, J. Morrison, S. Macdonald, D. Barnes, and I. V Williams. 2001. Simulations and retrospective analyses of Fraser watershed flows and temperatures. Atmosphere-Ocean 39:89–105.

Freeman, E. A., and G. Moisen. 2008. PresenceAbsence: an R package for presence absence analysis. Journal of Statistical Software 23:1–31.

Gable, J., and S. Cox-Rogers. 1993. Stock identification of Fraser River Sockeye Salmon: methodology and management applications. Pacific Salmon Commission Tech. Rept. 5: Page 36. Vancouver, BC.

Gard, M. 2006. Modeling changes in salmon spawning and rearing habitat associated with river channel restoration. International Journal of River Basin Management 4:201–211.

Gasith, A., and V. H. Resh. 1999. Streams in Mediterranean climate regions: abiotic influences and biotic responses to predictable seasonal events. Annual Review of Ecology and Systematics 30:51–81.

Geist, D. R., J. Jones, C. J. Murray, and D. D. Dauble. 2000. Suitability criteria analyzed at the spatial scale of redd clusters improved estimates of fall chinook salmon (*Oncorhynchus tshawytscha*) spawning habitat use in the Hanford Reach, Columbia River. Canadian Journal of Fisheries and Aquatic Sciences 57:1636–1646.

Grant, G. E. 1997. Critical flow constrains flow hydraulics in mobile-bed streams: a new hypothesis. Water Resources Research 33:349–358.

Grant, J. W. A., and D. L. Kramer. 1990. Territory size as a predictor or the upper limit to population density of juvenile salmonids in streams. Canadian Journal of Fisheries and Aquatic Sciences 47:1724–1737.

Grantham, T. E., D. A. Newburn, M. A. McCarthy, and A. M. Merenlender. 2012. The role of streamflow and land use in limiting oversummer survival of juvenile steelhead in California streams. Transactions of the American Fisheries Society 141:585–598.

Gresswell, R. E. 1999. Fire and aquatic ecosystems in forested biomes of North America. Transactions of the American Fisheries Society 128:193–221.

Grueber, C. E., S. Nakagawa, R. J. Laws, and I. G. Jamieson. 2011. Multimodel inference in ecology and evolution: challenges and solutions. Journal of evolutionary biology 24:699–711.

Guay, J. C., D. Boisclair, D. Rioux, M. Leclerc, M. Lapointe, and P. Legendre. 2000. Development and validation of numerical habitat models for juveniles of Atlantic salmon (*Salmo salar*). Canadian Journal of Fisheries and Aquatic Sciences 57:2065–2075.

Guisan, A., T. C. J. Edwards, and T. Hastie. 2002. Generalized linear and generalized additive models in studies of species distributions: setting the scene. Ecological Modelling 157:89–100.

Gustafson, R. G., R. S. Waples, J. M. Myers, L. A. Weitkamp, G. J. Bryant, O. W. Johnson, and J. J. Hard. 2007. Pacific salmon extinctions: quantifying lost and remaining diversity. Conservation Biology 21:1009–1020.

Hanson, P. C., T. B. Johnson, D. E. Schindler, and J. F. Kitchell. 1997. Fish Bioenergetics 3.0. Madison, WI.

Harvey, B. C., J. L. White, and R. J. Nakamoto. 2005. Habitat-specific biomass, survival, and growth of rainbow trout (*Oncorhynchus mykiss*) during summer in a small coastal stream. Canadian Journal of Fisheries and Aquatic Sciences 62:650–658.

Hayes, J. W., N. F. Hughes, and L. H. Kelly. 2007. Process-based modelling of invertebrate drift transport, net energy intake and reach carrying capacity for drift-feeding salmonids. Ecological Modelling 207:171–188.

Hayes, S. A., M. H. Bond, C. V Hanson, E. V Freund, J. J. Smith, E. C. Anderson, A. J. Ammann, and R. B. MacFarlane. 2008. Steelhead growth in a small Central California watershed: upstream and estuarine rearing patterns. Transactions of the American Fisheries Society 137:114–128.

Hayes, S. A., M. H. Bond, C. V Hanson, A. W. Jones, A. J. Ammann, J. A. Harding, A. L. Collins, J. Perez, and R. B. Macfarlane. 2011. Down, up, down and “smolting” twice? Seasonal movement patterns by juvenile steelhead (*Oncorhynchus mykiss*) in a coastal watershed with a bar closing estuary. Canadian Journal of Fisheries and Aquatic Sciences 68:1341–1350.

Hewlett, J. D., and C. James. 1982. Stream temperature under an inadequate buffer strip in the southeast Piedmont. Water Resources Bulletin 18:983–988.

Hidalgo, H. G., T. Das, M. D. Dettinger, D. R. Cayan, D. W. Pierce, T. P. Barnett, G. Bala, A. Mirin, a. W. Wood, C. Bonfils, B. D. Santer, and T. Nozawa. 2009. Detection and attribution of streamflow timing changes to climate change in the Western United States. Journal of Climate 22:3838–3855.

Hill, J., and G. D. Grossman. 1993. An energetic model of microhabitat use for Rainbow Trout and Rosyside Dace. Ecology 74:685–698.

Hinch, S. G., and E. G. Martins. 2011. A review of potential climate change effects on survival of Fraser River sockeye salmon and an analysis of interannual trends in en route loss and pre-spawn mortality. Cohen Commission Tech. Rept. 9: Page 134. Vancouver, BC.

Hitt, N. P. 2003. Immediate effects of wildfire on stream temperature. Journal of Freshwater Ecology 18:171–173.

Hobbs, R. J., and L. F. Huenneke. 1992. Disturbance, diversity, and invasion: implications for conservation. Conservation Biology 6:324–337.

Holsinger, L., R. E. Keane, D. J. Isaak, L. Eby, and M. K. Young. 2014. Relative effects of climate change and wildfires on stream temperatures: a simulation modeling approach in a Rocky Mountain watershed. Climatic Change 124:191–206.

Hurvich, C. M., and C. Tsai. 1989. Regression and time series model selection in small samples. Biometrika 76:297–307.

Hutchinson, G. E. 1965. The ecological theater and the evolutionary play. Yale University Press, New Haven, Connecticut.

Hynes, H. B. N. 1975. The stream and its valley. Verhandlungen der Internationalen Vereinigung für Theoretische und Angewandte Limnologie 19:1–15.

Im, D., H. Kang, K.-H. Kim, and S.-U. Choi. 2011. Changes of river morphology and physical fish habitat following weir removal. Ecological Engineering 37:883–892.

Inoue, M., S. Sakamoto, and S. Kikuchi. 2013. Terrestrial prey inputs to streams bordered by deciduous broadleaved forests, conifer plantations and clear-cut sites in southwestern Japan: effects on the abundance of red-spotted masu salmon. Ecology of Freshwater Fish 22:335–347.

Isaak, D. J., C. H. Luce, B. E. Rieman, D. E. Nagel, E. E. Peterson, D. L. Horan, S. Parkes, and G. L. Chandler. 2010. Effects of climate change and wildfire on stream temperatures and salmonid thermal habitat in a mountain river network. Ecological Applications 20:1350–71.

Jackson, B. K., S. M. P. Sullivan, and R. L. Malison. 2012. Wildfire severity mediates fluxes of plant material and terrestrial invertebrates to mountain streams. Forest Ecology and Management 278:27–34.

Janisch, J. E., S. M. Wondzell, and W. J. Ehinger. 2012. Headwater stream temperature: interpreting response after logging, with and without riparian buffers, Washington, USA. Forest Ecology and Management 270:302–313.

Jiang, Y., Q. Zhuang, and D. Mandallaz. 2012. Modeling Large Fire Frequency and Burned Area in Canadian Terrestrial Ecosystems with Poisson Models. Environmental Modeling & Assessment 17:483–493.

Johnson, S. L., and J. a. Jones. 2000. Stream temperature responses to forest harvest and debris flows in western Cascades, Oregon. Canadian Journal of Fisheries and Aquatic Sciences 57:30–39.

Jost, L. 2007. Partitioning diversity into independent alpha and beta components. Ecology 88:2427–2439.

Jowett, I. G., and A. J. H. Davey. 2007. A comparison of composite habitat suitability indices and generalized additive models of invertebrate abundance and fish presence–habitat availability. Transactions of the American Fisheries Society 136:428–444.

Kaushal, S. S., G. E. Likens, N. A. Jaworski, M. L. Pace, A. M. Sides, D. Seekell, K. T. Belt, D. H. Secor, and R. L. Wingate. 2010. Rising stream and river temperatures in the United States. Frontiers in Ecology and the Environment 8:461–466.

Kawaguchi, Y., and S. Nakano. 2001. Contribution of terrestrial invertebrates to the annual resource budget for salmonids in forest and grassland reaches of a headwater stream. Freshwater Biology 46:303–316.

Kawaguchi, Y., Y. Taniguchi, and S. Nakano. 2003. Terrestrial invertebrate inputs determine the local abundance of stream fishes in a forested stream. Ecology 84:701–708.

Keeley, E. R. 2001. Demographic responses to food and space competition. Ecology 82:1247–1259.

Kiffney, P. M., J. S. Richardson, and J. P. Bull. 2003. Responses of periphyton and insects to experimental manipulation of riparian buffer width along forest streams. Journal of Applied Ecology 40:1060–1076.

Knapp, R. A., and H. K. Preisler. 1999. Is it possible to predict habitat use by spawning salmonids? A test using California golden trout (*Oncorhynchus mykiss aguabonita*). Canadian Journal of Fisheries and Aquatic Sciences 56:1576–1584.

Koetsier, P., Q. Tuckett, and J. White. 2007. Present effects of past wildfires on the diets of stream fish. Western North American Naturalist 67:429–438.

Kynard, B., M. Horgan, M. Kieffer, and D. Seibel. 2000. Habitats used by Shortnose Sturgeon in two Massachusetts rivers, with notes on estuarine Atlantic Sturgeon: a hierarchical approach. Transactions of the American Fisheries Society 129:487–503.

Labonne, J., S. Allouche, and P. Gaudin. 2003. Use of a generalised linear model to test habitat preferences: the example of *Zingel asper*, an endemic endangered percid of the River Rho. Freshwater Biology 48:687–697.

Lake, P. S. 2000. Disturbance, patchiness, and diversity in streams. Journal of the North American Benthological Society 19:573–592.

Lancaster, J., and S. Waldron. 2001. Stable isotope values of lotic invertebrates: sources of variation, experimental design, and statistical interpretation. Limnology and Oceanography 46:723–730.

Larson, L. L., and S. L. Larson. 1996. Riparian shade and stream temperature: a perspective. Rangelands 18:149–152.

Leclerc, M., A. Saint-Hilaire, and J. Bechara. 2003. State-of-the-art and perspectives of habitat modelling for determining conservation flows. Canadian Water Resources Journal 28:135–151.

Lee, J. H., J. T. Kil, and S. Jeong. 2010. Evaluation of physical fish habitat quality enhancement designs in urban streams using a 2D hydrodynamic model. Ecological Engineering 36:1251–1259.

Ligon, F. K., W. E. Dietrich, and W. J. Trush. 1995. Downstream ecological effects of dams. BioScience 45:183–192.

Lytle, D. a, and N. L. Poff. 2004. Adaptation to natural flow regimes. Trends in ecology & evolution 19:94–100.

Lytle, D. A. 2002. Flash floods and aquatic insect life-history evolution: evaluation of multiple models. Ecology 83:370–385.

Macdonald, J. S., D. a. Patterson, M. J. Hague, and I. C. Guthrie. 2010. Modeling the influence of environmental factors on spawning migration mortality for Sockeye Salmon fisheries management in the Fraser River, British Columbia. Transactions of the American Fisheries Society 139:768–782.

MacDonald, R. J., S. Boon, J. M. Byrne, M. D. Robinson, and J. B. Rasmussen. 2014. Potential future climate effects on mountain hydrology, stream temperature, and

native salmonid life history. Canadian Journal of Fisheries and Aquatic Sciences 71:189–202.

Mahlum, S. K., L. A. Eby, M. K. Young, C. G. Clancy, and M. Jakober. 2011. Effects of wildfire on stream temperatures in the Bitterroot River Basin, Montana. International Journal of Wildland Fire 20:240–247.

Malcolm, I. a., A. F. Youngson, and C. Soulsby. 2003. Survival of salmonid eggs in a degraded gravel-bed stream: effects of groundwater-surface water interactions. River Research and Applications 19:303–316.

Malison, R. L., and C. V. Baxter. 2010a. The fire pulse: wildfire stimulates flux of aquatic prey to terrestrial habitats driving increases in riparian consumers. Canadian Journal of Fisheries and Aquatic Sciences 67:570–579.

Malison, R. L., and C. V. Baxter. 2010b. Effects of wildfire of varying severity on benthic stream insect assemblages and emergence. Journal of the North American Benthological Society 29:1324–1338.

Mallet, J. P., N. Lamouroux, P. Sagnes, and H. Persat. 2000. Habitat preferences of European grayling in a medium size stream, the Ain River, France. Journal of Fish Biology 56:1312–1326.

Manel, S., H. C. Williams, and S. J. Ormerod. 2001. Evaluating presence-absence models in ecology: the need to account for prevalence. Journal of Applied Ecology 38:921–931.

Mantua, N., I. Tohver, and A. Hamlet. 2010. Climate change impacts on streamflow extremes and summertime stream temperature and their possible consequences for freshwater salmon habitat in Washington State. Climatic Change 102:187–223.

Martínez del Rio, C., N. Wolf, S. a Carleton, and L. Z. Gannes. 2009. Isotopic ecology ten years after a call for more laboratory experiments. Biological Reviews 84:91–111.

Martins, E. G., S. G. Hinch, D. a. Patterson, M. J. Hague, S. J. Cooke, K. M. Miller, M. F. Lapointe, K. K. English, and A. P. Farrell. 2011. Effects of river temperature and climate warming on stock-specific survival of adult migrating Fraser River sockeye salmon (*Oncorhynchus nerka*). Global Change Biology 17:99–114.

Mathur, D., W. H. Bason, E. J. J. Purdy, and C. A. Silver. 1985. A critique of the Instream Flow Incremental Methodology. Canadian Journal of Fisheries and Aquatic Sciences 42:825–831.

McCutchan, J. H. J., W. M. J. Lewis, C. Kendall, and C. C. Mcgrath. 2003. Variation in trophic shift for stable isotope ratios of carbon, nitrogen, and sulfur. Oikos 102:378–390.

McElravy, E. P., G. A. Lamberti, and V. H. Resh. 1989. Year-to-year variation in the aquatic macroinvertebrate fauna of a northern California stream. Journal of the North American Benthological Society 8:51–63.

McEwan, D. R. 2001. Central Valley steelhead. Pages 1–44 *in* R. L. Brown, editor. Contributions to the biology of Central Valley salmonids. California Department of Fish and Wildlife, Fish Bulletin 179.1, Sacramento, CA.

McLean, D. G., M. Church, and B. Tassone. 1999. Sediment transport along lower Fraser River 1. Measurements and hydraulic computations. Water Resources Research 35:2533–2548.

Meehl, G. A., T. F. Stocker, W. D. Collins, P. Friedlingstein, A. T. Gaye, J. M. Gregory, A. Kitoh, R. Knutti, J. M. Murphy, A. Noda, S. C. B. Raper, I. G. Watterson, A. J. Weaver, and Z.-C. Zhao. 2007. Global climate projections. In: climate change 2007: the physical science basis. Contribution of working group I to the fourth assessment report of the intergovernmental panel on climate change. (S. Solomon, D. Qin, M. Manning, Z. Chen, M. Marquis, K. B. Averyt, M. Tignor, and H. L. Miller, Eds.). Cambridge University Press, Cambridge, United Kingdom and New York, NY, USA.

Meissner, K., and T. Muotka. 2006. The role of trout in stream food webs: integrating evidence from field surveys and experiments. Journal of Animal Ecology 75:421–433.

Miller, D., C. Luce, and L. Benda. 2003. Time, space, and episodicity of physical disturbance in streams. Forest Ecology and Management 178:121–140.

Minshall, G. W. 1967. Role of allochthonous detritus in the trophic structure of a woodland springbrook community. Ecology 48:139–149.

Minshall, G. W. 2001. Water quality, substratum and biotic responses of five central Idaho (USA) streams during the first year following the Mortar Creek fire. International Journal of Wildland Fire 10:185–199.

Minshall, G. W. 2003. Responses of stream benthic macroinvertebrates to fire. Forest Ecology and Management 178:155–161.

Minshall, G. W., J. T. Brock, and J. D. Varley. 1989. Wildfires and Yellowstone's stream ecosystems. BioScience 39:707–715.

Minshall, G. W., C. T. Robinson, and D. E. Lawrence. 1997. Postfire responses of lotic ecosystems in Yellowstone National Park, U.S.A. Canadian Journal of Fisheries and Aquatic Sciences 54:2509–2525.

Mitchell, T. D., and P. D. Jones. 2005. An improved method of constructing a database of monthly climate observations and associated high-resolution grids. International Journal of Climatology 25:693–712.

MoE, B. 2008. Comprehensive review of Fraser River at Hope flood hydrology and flows scoping study - final report.

Mohseni, O., and H. G. Stefan. 1999. Stream temperature/air temperature relationship: a physical interpretation. Journal of Hydrology 218:128–141.

Montgomery, D. R., and J. M. Buffington. 1997. Channel-reach morphology in mountain drainage basins. Geological Society of America Bulletin 109:596–611.

Moore, J. W., D. B. Herbst, W. N. Heady, and S. M. Carlson. 2012. Stream community and ecosystem responses to the boom and bust of an invading snail. Biological Invasions 14:2435–2446.

Moore, J. W., and B. X. Semmens. 2008. Incorporating uncertainty and prior information into stable isotope mixing models. Ecology letters 11:470–80.

Moore, R. D., D. L. Spittlehouse, and A. Story. 2005. Riparian microclimate and stream temperature responses to forest harvesting: a review. Journal of the American Water Resources Association 41:813–834.

Morrison, J., M. C. Quick, and M. G. G. Foreman. 2002. Climate change in the Fraser River watershed: flow and temperature projections. Journal of Hydrology 263:230–244.

Mouton, A. M., B. De Baets, and P. L. M. Goethals. 2010. Ecological relevance of performance criteria for species distribution models. Ecological Modelling 221:1995–2002.

Moyel, P. B. 2002. Inland fishes of California, revised and expanded. University of California Press, Berkeley, California, USA.

Myers, J. M., R. G. Kope, G. J. Bryant, D. Teel, L. J. Lierheimer, T. C. Wainwright, W. S. Grant, F. W. Waknitz, K. Neely, S. T. Lindley, and W. R. S. 1998. Status review of Chinook salmon from Washington, Idaho, Oregon, and California. United States Department of Commerce. National Oceanic Atmospheric Administration Technical. Memo NMFS-NWFSC-35.

Myrick, C. A., and J. J. J. Cech. 2000. Temperature influences on California rainbow trout physiological performance. Fish Physiology and Biochemistry 22:245–254.

Naiman, R. J., and D. Henri. 1997. The ecology of interfaces: riparian zones. Annual Review of Ecology and Systematics 28:621–658.

Nakano, S., H. Miyasaka, and N. Kuhara. 1999. Terrestrial-aquatic linkages: riparian arthropod inputs alter trophic cascades in a stream food web. Ecology 80:2435–2441.

Nakano, S., and M. Murakami. 2001. Reciprocal subsidies: dynamic interdependence between terrestrial and aquatic food webs. Proceedings of the National Academy of Sciences 98:166–170.

Nehlsen, W., J. E. Williams, and J. A. Lichatowich. 1991. Pacific salmon at the crossroads: stocks at risk from California, Oregon, Idaho, and Washington. Fisheries:4–21.

Nelson, K. C., and M. A. Palmer. 2007. Stream temperature surges under urbanization and climate change: data, models, and responses. Journal of the American Water Resources Association 43:440–452.

Nilsson, C., C. A. Reidy, M. Dynesius, and C. Revenga. 2005. Fragmentation and flow regulation of the world's large river systems. Science 308:405–8.

Ormerod, S. J., M. Dobson, a. G. Hildrew, and C. R. Townsend. 2010. Multiple stressors in freshwater ecosystems. Freshwater Biology 55:1–4.

Ozaki, N., T. Fukushima, H. Harasawa, T. Kojiri, K. Kawashima, and M. Ono. 2003. Statistical analyses on the effects of air temperature fluctuations on river water qualities. Hydrological Processes 17:2837–2853.

Paetzold, A., C. J. Schubert, and K. Tockner. 2005. Aquatic terrestrial linkages along a braided-river: riparian arthropods feeding on aquatic insects. Ecosystems 8:748–759.

Parnell, A. C., R. Inger, S. Bearhop, and A. L. Jackson. 2010. Source partitioning using stable isotopes: coping with too much variation. PLoS ONE 5:e9672.

Parnell, A. C., D. L. Phillips, S. Bearhop, B. X. Semmens, E. J. Ward, J. W. Moore, A. L. Jackson, J. Grey, D. J. Kelly, and R. Inger. 2013. Bayesian stable isotope mixing models. Environmetrics:387–399.

Peeters, E. T. H. M., and J. J. P. Gardeniers. 1998. Logistic regression as a tool for defining habitat requirements of two common gammarids. Freshwater Biology 39:605–615.

Peterson, E. E. 2013. STARS: spatial tools for the analysis of river systems - a tutorial. Page 43. Dutton Park, QLD.

Peterson, E. R., and J. M. Ver Hoef. 2010. A mixed-model moving-average approach to geostatistical modeling in stream networks. Ecology 91:644–651.

Petts, G. E. 2009. Instream flow science for sustainable river management. Journal of the American Water Resources Association 45:1071–1086.

Phillips, D. L., and J. W. Gregg. 2003. Source partitioning using stable isotopes: coping with too many sources. Oecologia 136:261–9.

Pickett, S. T. A., and P. S. White. 1985. The ecology of natural disturbance and patch dynamics. Pages 1–472. First edition. Academic Press, San Diego, California.

Poff, N. L., J. D. Allan, M. B. Bain, J. R. Karr, K. L. Prestegaard, B. D. Richter, R. E. Sparks, and J. C. Stromberg. 1997. The natural flow regime. BioScience 47:769–784.

Poff, N. L., J. D. Allan, M. a. Palmer, D. D. Hart, B. D. Richter, A. H. Arthington, K. H. Rogers, J. L. Meyer, and J. a. Stanford. 2003. River flows and water wars: emerging science for environmental decision making. Frontiers in Ecology and the Environment 1:298–306.

Poff, N. L., J. D. Olden, D. M. Merritt, and D. M. Pepin. 2007. Homogenization of regional river dynamics by dams and global biodiversity implications. Proceedings of the National Academy of Sciences 104:5732–7.

Poff, N. L., and J. V. Ward. 1990. Physical habitat template of lotic systems: Recovery in the context of historical pattern of spatiotemporal heterogeneity. Environmental Management 14:629–645.

Poff, N. L., and J. K. H. Zimmerman. 2010. Ecological responses to altered flow regimes: a literature review to inform the science and management of environmental flows. Freshwater Biology 55:194–205.

Polis, G. a., W. B. Anderson, and R. D. Holt. 1997. Toward an integration of landscape and food web ecology: the dynamics of spatially subsidized food webs. Annual Review of Ecology and Systematics 28:289–316.

Pollock, M. M., T. J. Beechie, M. Liermann, and R. E. Bigley. 2009. Stream temperature relationships to forest harvest in western Washington. Journal of the American Water Resources Association 45:141–156.

Power, M. E., J. R. Holomuzki, and R. L. Lowe. 2013. Food webs in Mediterranean rivers. Hydrobiologia 719:119–136.

Power, M. E., M. S. Parker, and W. E. Dietrich. 2008. Seasonal reassembly of a river food web: floods, droughts, and impacts of fish. Ecological Monographs 78:263–282.

Pringle, C. M. 1997. Exploring how disturbance is transmitted upstream: going against the flow. Journal of the North American Benthological Society 16:425–438.

R Development Core Team. 2013. R: A language and environment for statistical computing. R Foundation for Statistical Computing, Vienna, Austria.

Ramchunder, S. J., L. E. Brown, and J. Holden. 2013. Rotational vegetation burning effects on peatland stream ecosystems. Journal of Applied Ecology 50:636–648.

Regonda, S. K., and B. Rajagopalan. 2005. Seasonal cycle shifts in hydroclimatology over the Western United States. Journal of Climate 18:372–384.

Resh, V. H., A. V Brown, A. P. Covich, M. E. Gurtz, H. W. Li, G. W. Minshall, S. R. Reice, A. L. Sheldon, J. B. Wallace, and R. C. Wissman. 1988. The role of disturbance in stream ecology. Journal of the North American Benthological Society 7:433–455.

Richter, B. D., R. Mathews, D. L. Harrison, and R. Wigington. 2003. Ecologically sustainable water management: managing river flows for ecological integrity. Ecological Applications 13:206–224.

Rieman, B., and J. Clayton. 1997. Wildfire and native fish: issues of forest health and conservation of sensitive species. Fisheries 22:6–15.

Rieman, B., D. Lee, D. Burns, R. Gresswell, M. Young, R. Stowell, J. Rinne, and P. Howell. 2003. Status of native fishes in the western United States and issues for fire and fuels management. Forest Ecology and Management 178:197–211.

Royer, T. V, and G. W. Minshall. 1997. Temperature patterns in small streams following wildfire. Archiv fur Hydrobiologie 140:237–242.

Rundio, D. E., and S. T. Lindley. 2008. Seasonal patterns of terrestrial and aquatic prey abundance and use by *Oncorhynchus mykiss* in a California coastal basin with a Mediterranean climate. Transactions of the American Fisheries Society 137:467–480.

Running, S. W. 2006. Climate change. Is global warming causing more, larger wildfires? Science 313:927–928.

Saito, L., W. W. Miller, D. W. Johnson, R. G. Qualls, L. Provencher, E. Carroll, and P. Szameitat. 2000. Fire effects on stable isotopes in a Sierran forested watershed. Journal of environmental quality 36:91–100.

Sály, P., T. Erős, P. Takács, A. Specziár, I. Kiss, and P. Bíró. 2009. Assemblage level monitoring of stream fishes: the relative efficiency of single-pass vs. double-pass electrofishing. Fisheries Research 99:226–233.

Sanzone, D. M., J. L. Meyer, E. Marti, E. P. Gardiner, J. L. Tank, and N. B. Grimm. 2003. Carbon and nitrogen transfer from a desert stream to riparian predators. Oecologia 134:238–50.

Schelker, J., L. Kuglerová, K. Eklöf, K. Bishop, and H. Laudon. 2013. Hydrological effects of clear-cutting in a boreal forest – snowpack dynamics, snowmelt and streamflow responses. Journal of Hydrology 484:105–114.

Schindler, D. W. 2001. The cumulative effects of climate warming and other human stresses on Canadian freshwaters in the new millennium. Canadian Journal of Fisheries and Aquatic Sciences 58:18–29.

Schmidt, S. N., J. D. Olden, C. T. Solomon, and M. J. Vander Zanden. 2007. Quantitative approaches to the analysis of stable isotope food web data. Ecology 88:2793–802.

Sear, D. A. 1995. Morphological and sedimentological changes in a gravel-bed river following 12 years of flow regulation for hydropower. Regulated Rivers: Research & Management 10:247–264.

Semmens, B. X., E. J. Ward, J. W. Moore, and C. T. Darimont. 2009. Quantifying inter- and intra-population niche variability using hierarchical Bayesian stable isotope mixing models. PLoS ONE 4:e6187.

Sepulveda, A. J., W. H. Lowe, and P. P. Marra. 2012. Using stable isotopes to test for trophic niche partitioning: a case study with stream salamanders and fish. Freshwater Biology 57:1399–1409.

Servizi, J. A., and J. O. T. Jensen. 1977. Resistance of adult sockeye salmon to acute thermal shock. International Pacific Salmon Fisheries Commission Progress Report No. 34:1–11.

Sestrich, C. M., T. E. McMahon, and M. K. Young. 2011. Influence of fire on native and nonnative salmonid populations and habitat in a Western Montana basin. Transactions of the American Fisheries Society 140:136–146.

Sloat, M. R., and A. K. Osterback. 2013. Maximum stream temperature and the occurrence, abundance, and behavior of steelhead trout (*Oncorhynchus mykiss*) in a southern California stream. Canadian Journal of Fisheries and Aquatic Sciences 70:64–73.

Smith, J. J., and H. W. Li. 1983. Energetic factors influencing foraging tactics of juvenile steelhead trout, *Salmo gairdneri*. Pages 173–180 *in* D. L. G. Noakes, D. G. Lindquist, G. S. Helfman, and J. A. Ward, editors. Predators and prey in fishes. Springer Netherlands.

Smith, K. 1981. The prediction of river water temperatures. Hydrological Sciences Bulletin 26:19–32.

Smith, K., and M. E. Lavis. 1975. Environmental influences on the temperature of a small upland stream. Oikos 26:228–236.

Smith, L. N. 2006. Stratigraphic evidence for multiple drainings of glacial Lake Missoula along the Clark Fork River, Montana, USA. Quaternary Research 66:311–322.

Sogard, S. M., J. E. Merz, W. H. Satterthwaite, M. P. Beakes, D. R. Swank, E. M. Collins, R. G. Titus, and M. Mangel. 2012. Contrasts in habitat characteristics and life history patterns of *Oncorhynchus mykiss* in California's Central Coast and Central Valley. Transactions of the American Fisheries Society 141:747–760.

Sogard, S. M., T. H. Williams, and H. Fish. 2009. Seasonal patterns of abundance, growth, and site fidelity of juvenile steelhead in a small coastal California stream. Transactions of the American Fisheries Society 138:549–563.

Sommer, T. R., M. L. Nobriga, W. C. Harrell, W. Batham, and W. J. Kimmerer. 2001. Floodplain rearing of juvenile chinook salmon: evidence of enhanced growth and survival. Canadian Journal of Fisheries and Aquatic Sciences 58:325–333.

Spencer, C. N., K. O. Gabel, and F. R. Hauer. 2003. Wildfire effects on stream food webs and nutrient dynamics in Glacier National Park, USA. Forest Ecology and Management 178:141–153.

Stalkner, C. B., B. L. Lamb, J. Henriksen, K. D. Bovee, and J. Bartholow. 1995. The instream flow incremental methodology: a primer for IFIM. Washington, DC: U.S. Geological Survey Biological Report 29. 45 p.

Stefan, H. G., and E. B. Preud'homme. 1993. Stream temperature estimation from air temperature. Water Resources Bulletin 29:27–45.

Steffler, P., and J. Blackburn. 2002. River 2D: two-dimensional depth averaged model of river hydrodynamics and fish habitat. Introduction to depth averaged modeling and user's manual. University of Alberta, Edmonton, Alberta.

Stewart, I. T., D. R. Cayan, and M. D. Dettinger. 2004. Changes in snowmelt runoff timing in western North America under a "business as usual" climate change scenario. Climatic Change 62:217–232.

Stock, B. C., and B. X. Semmens. 2013. MixSIAR GUI User Manual, version 1.0.

Strayer, D. L., R. E. Beighley, L. C. Thompson, S. Brooks, C. Nilsson, G. Pinay, and R. J. Naiman. 2003. Effects of land cover on stream ecosystems: roles of empirical models and scaling Issues. Ecosystems 6:407–423.

Theobald, D. M., J. B. Norman, E. Peterson, S. Ferraz, A. Wade, and M. R. Sherburne. 2006. Functional Linkage of Water basins and Streams (FLoWS) v1 user's guide: ArcGIS tools for network-based analysis. Page 43. Fort Collins, CO.

Thompson, S. M., and P. L. Campbell. 1979. Hydraulics of a large channel paved with boulders. Journal of Hydraulic Research 17:341–354.

Thorp, J. H., and A. P. Covich. 2009. Ecology and classification of North American freshwater invertebrates. Pages 1–48. Second edition. Academic Press, San Diego.

Tomanova, S., E. Goitia, and J. Helešic. 2006. Trophic levels and functional feeding groups of macroinvertebrates in neotropical streams. Hydrobiologia 556:251–264.

Townsend, C. R. 1989. The patch dynamics concept of stream community ecology. Journal of North American Benthological Society 8:36–50.

Townsend, C. R., S. Dolédec, R. Norris, K. Peacock, and C. Arbuckle. 2003. The influence of scale and geography on relationships between stream community composition and landscape variables: description and prediction. Freshwater Biology 48:768–785.

Turner, M. G., and W. H. Romme. 1994. Landscape dynamics in crown fire ecosystems. Landscape Ecology 9:59–77.

USFWS. 1981. Standards for the development of habitat suitability models. 103 ESM. Division of Ecological Services, Department of the Interior, Washington, DC.

Vadas, R. L. J., and D. J. Orth. 2001. Formulation of habitat suitability models for stream fish guilds: do the standard methods work? Transactions of the American Fisheries Society 130:217–235.

Vanderklift, M. a, and S. Ponsard. 2003. Sources of variation in consumer-diet delta 15N enrichment: a meta-analysis. Oecologia 136:169–82.

Vannote, R. L., G. W. Minshall, K. W. Cummins, J. R. Sedell, and C. E. Cushing. 1980. The river continuum concept. Canadian Journal of Fisheries and Aquatic Sciences 37:130–137.

Venditti, J. G., and M. Church. (n.d.). Morphology and controls on the position of a gravel-sand transition: Fraser River, British Columbia. Journal of Geophysical Research: Earth Surface.

Ventura, M., and E. Jeppesen. 2009. Effects of fixation on freshwater invertebrate carbon and nitrogen isotope composition and its arithmetic correction. Hydrobiologia 632:297–308.

Ver Hoef, J. M., and E. E. Peterson. 2010. A moving average approach for spatial statistical models of stream networks. Journal of the American Statistical Association 105:6–18.

Ver Hoef, J. M., E. E. Peterson, D. Clifford, and R. Shah. 2012. SSN: an R package for spatial statistical modeling on stream networks. Available at: http://cran.r-project.org/web/packages/SSN/vignettes/SSN.pdf.

Verkaik, I., M. Rieradevall, S. D. Cooper, J. M. Melack, T. L. Dudley, and N. Prat. 2013a. Fire as a disturbance in Mediterranean climate streams. Hydrobiologia 719:353–382.

Verkaik, I., M. Vila-Escalé, M. Rieradevall, and N. Prat. 2013b. Seasonal drought plays a stronger role than wildfire in shaping macroinvertebrate communities of Mediterranean streams. International Review of Hydrobiology 98:271–283.

Vismara, R., A. Azzellino, R. Bosi, G. Crosa, and G. Gentili. 2001. Habitat suitability curves for Brown Trout (*Salmo trutta fario* L.) in the River Adda, northern Italy: comparing univariate and multivariate approaches. Regulated Rivers: Research & Management 17:37–50.

Waddle, T. J. 2001. PHABSIM for Windows: User's Manual and Exercises: Page 288. Fort Collins, CO.

Waitt, R. B. 1985. Case for periodic colossal jökulhlaups from Pleistocene glacial Lake Missoula. Geological Society of America Bulletin 96:1271–1286.

Wan, S., D. Hui, and Y. Luo. 2001. Fire effects on nitrogen pools and dynamics in terrestrial ecosystems: a meta-analysis. Ecological Applications 11:1349–1365.

Wang, T., a. Hamann, D. L. Spittlehouse, and S. N. Aitken. 2006. Development of scale-free climate data for Western Canada for use in resource management. International Journal of Climatology 26:383–397.

Wang, T., A. Hamann, D. L. Spittlehouse, and T. Q. Murdock. 2012. ClimateWNA—high-resolution spatial climate data for Western North America. Journal of Applied Meteorology and Climatology 51:16–29.

Waples, R. S., G. R. Pess, and T. Beechie. 2008. Evolutionary history of Pacific salmon in dynamic environments. Evolutionary Applications 1:189–206.

Ward, J. V, and J. A. Stanford. 1995. The serial discontinuity concept: extending the model to floodplain rivers. Regulated Rivers: Research & Management 10:159–168.

Webb, B. W., P. D. Clack, and D. E. Walling. 2003. Water-air temperature relationships in a Devon river system and the role of flow. Hydrological Processes 17:3069–3084.

Webb, B. W., D. M. Hannah, R. D. Moore, L. E. Brown, and F. Nobilis. 2008. Recent advances in stream and river temperature research. Hydrological Processes 22:902–918.

Webb, B. W., and F. Nobilis. 2007. Long-term changes in river temperature and the influence of climatic and hydrological factors. Hydrological Sciences Journal 52:74–85.

Wenger, S. J., D. J. Isaak, C. H. Luce, H. M. Neville, K. D. Fausch, J. B. Dunham, D. C. Dauwalter, M. K. Young, M. M. Elsner, B. E. Rieman, A. F. Hamlet, and J. E. Williams. 2011. Flow regime, temperature, and biotic interactions drive differential declines of trout species under climate change. Proceedings of the National Academy of Sciences 108:14175–14180.

Westerling, A. L., H. G. Hidalgo, D. R. Cayan, and T. W. Swetnam. 2006. Warming and earlier spring increase western U.S. forest wildfire activity. Science 313:940–943.

Wiens, J. A. 1989. Spatial scaling in Ecology. Functional Ecology 3:385–397.

Williams, J. G. 2001. Chinook salmon in the Lower American River, California's largest urban stream. Pages 1–38 *in* R. L. Brown, editor. Contributions to the biology of Central Valley salmonids. California Department of Fish and Wildlife, Fish Bulletin 179.2, Sacramento, CA.

Wipfli, M. S. 1997. Terrestrial invertebrates as salmonid prey and nitrogen sources in streams: contrasting old-growth and young-growth riparian forests in southeastern Alaska, U.S.A. Canadian Journal of Fisheries and Aquatic Sciences 54:1259–1269.

Wipfli, M. S., and C. V. Baxter. 2010. Linking ecosystems, food webs, and fish production: subsidies in salmonid watersheds. Fisheries 35:373–387.

Woodland, R. J., P. Magnan, H. Glémet, M. a Rodríguez, and G. Cabana. 2012a. Variability and directionality of temporal changes in $\delta^{13}C$ and $\delta^{15}N$ of aquatic invertebrate primary consumers. Oecologia 169:199–209.

Woodland, R. J., M. a Rodríguez, P. Magnan, H. Glémet, and G. Cabana. 2012b. Incorporating temporally dynamic baselines in isotopic mixing models. Ecology 93:131–44.

Yoshiyama, R. M., E. R. Gerstung, F. W. Fisher, and P. B. Moyle. 2001. Historical and present distribution of Chinook salmon in the Central Valley drainage of California. Pages 71–176 *in* R. L. Brown, editor. Contributions to the biology of

Central Valley salmonids. California Department of Fish and Wildlife, Fish Bulletin 179.1, Sacramento, CA.

Zar, J. H. 1999. Biostatistical analysis. Fourth edition. Princeton Hall PTR, New Jersey.